

# **MEASUREMENT OF EXCESS MOLAR ENTHALPIES OF BINARY AND TERNARY SYSTEMS INVOLVING HYDROCARBONS AND ETHERS**

A thesis submitted to the College of Graduate Studies and Research in partial fulfillment of the requirements for the degree of Master of Science in the Department of Chemical and Biological Engineering

University of Saskatchewan  
Saskatoon

By

Manjunathan Ulaganathan

©Copyright Manjunathan Ulaganathan, May 2014, All right reserved.

## **PERMISSION TO USE**

In presenting this thesis in partial fulfillment of the requirements for a Postgraduate degree from the University of Saskatchewan, I agree that the Libraries of this University may make it freely available for inspection. I further agree that permission for copying of this thesis/dissertation in any manner, in whole or in part, for scholarly purposes may be granted by the professor or professors who supervised my thesis work or, in their absence, by the Head of the Department or the Dean of the College in which my thesis work was done. It is understood that any copying or publication or use of this thesis or parts thereof for financial gain shall not be allowed without my written permission. It is also understood that due recognition shall be given to me and to the University of Saskatchewan in any scholarly use which may be made of any material in my thesis.

Requests for permission to copy or to make other use of material in this thesis in whole or part should be addressed to:

Head

Department of Chemical and Biological Engineering

University of Saskatchewan

57 Campus Drive

Saskatoon, Saskatchewan S7N 5A9

Canada.

## ABSTRACT

The study of excess thermodynamic properties of liquid mixtures is very important for designing the thermal separation processes, developing solution theory models and to have a better understanding of molecular structure and interactions involved in the fluid mixtures. In particular, heat of mixing or excess molar enthalpy data of binary and ternary fluid mixtures have great industrial and theoretical significance. In this connection, the experimental excess molar enthalpies for seventeen binary and nine ternary systems involving hydrocarbons, ethers and alcohol have been measured at 298.15K and atmospheric conditions for a wide range of composition by means of a flow microcalorimeter (LKB 10700-1)

The binary experimental excess molar enthalpy values are correlated by means of the Redlich-Kister polynomial equations and the Liebermann - Fried solution theory model. The ternary excess molar enthalpy values are represented by means of the Tsao-Smith equation with an added ternary term and the Liebermann-Fried model was used to predict ternary excess molar enthalpy values.

The Liebermann-Fried solution theory model was able to closely represent the experimental excess enthalpy data for most of the binary and ternary systems with reasonable accuracy. The correlated and predicted excess molar enthalpy data for the ternary systems are plotted in Roozeboom diagrams

## **ACKNOWLEDGEMENT**

First and foremost I like to thank my advisor, Dr. Ding-Yu Peng, head of the Chemical and Biological Engineering department, for his continued guidance, support and patience from the day I started working in the Applied Thermodynamics Laboratory. Dr. Peng inspired my interest to study thermodynamics, and taught me many valuable lessons in life. He often said "know your responsibilities, be honest to yourself and others". I will forever try to follow his advice.

I would also like to thank my thesis advisory committee members Dr. Aaron Phoenix and Dr. Venkatesh Meda for their guidance and support; Rlee Prokopishyn for his technical expertise with the instruments in the lab. Thanks to Dragan Cekic for all the help with the Chemical Engineering store; Richard Blondin and Heli Eunike for providing great assistance in the analytical lab.

Finally I would like to thank my Mom, Dad, Namachu anna, Dharani anni and all my relatives. A special thanks to my Uncle Dr. Meganathan and Chandru, aunt Vijayanthi and Chithra for their continued support and motivation. Thanks to my friends Swami, Krishna, Bala, Basheer Bhai, Rangu, Ram, Rajesh, Karadi, Annaveri, Jack, Sid, Naveen, Kurt and Amir for their help and support throughout the journey. A special mention to Dr. Sheldon Cooper, Dr. Alan Harper and Battlefield 3 developers, who kept me entertained during the rough times.

# TABLE OF CONTENTS

PERMISSION TO USE.....	i
ABSTRACT.....	ii
ACKNOWLEDGEMENT.....	iii
TABLE OF CONTENTS.....	iv
LIST OF TABLES.....	vii
LIST OF FIGURES.....	x
LIST OF ABBREVIATIONS.....	xv
NOMENCLATURE.....	xvi
<b>1.0 INTRODUCTION.....</b>	<b>1</b>
1.1 Objectives .....	2
1.2 An overview of the thesis .....	3
1.3 Importance of the study .....	3
1.3.1 Excess Thermodynamic Properties.....	3
1.3.2 Excess molar enthalpy .....	4
1.4 System studied .....	5
<b>2.0 LITERATURE REVIEW .....</b>	<b>10</b>
2.1 Methods of measuring excess molar enthalpy values.....	10
2.1.1 Calorimetric methods.....	10
2.1.2 Types of calorimeters.....	11
2.2 Flow calorimeters.....	13

2.3 Correlation and prediction methods.....	14
2.3.1 Empirical methods .....	15
2.3.2 Solution theory models .....	16
<b>3.0 MATERIALS AND METHODS .....</b>	<b>20</b>
3.1 Materials .....	20
3.1.1 Degassing the chemicals .....	21
3.2 Flow microcalorimeter.....	23
3.2.1 Calorimeter construction and modifications.....	24
3.2.2 Calorimeter Calibration .....	30
3.2.3 Verification of the calorimeter.....	32
3.3 Calorimeter operational procedure .....	34
3.3.1 Binary system.....	34
3.3.2 Ternary system.....	36
<b>4.0 RESULTS AND DISCUSSION .....</b>	<b>39</b>
4.1 Experimental excess molar enthalpy .....	39
4.2 Representation of binary excess molar enthalpy .....	44
4.2.1 Correlation by means of Redlich - Kister polynomial equation .....	44
4.2.2 Correlation by means of Liebermann-Fried model.....	51
4.3 Representation of ternary excess molar enthalpy values .....	59

4.3.1 Correlation of experimental data by Tsao and Smith equation.....	60
4.3.2 Prediction of experimental data by Liebermann - Fried solution theory model .....	90
<b>5.0 CONCLUSIONS AND RECOMMENDATIONS.....</b>	<b>92</b>
5.1 Conclusions.....	92
5.2 Recommendations.....	93
<b>6.0 REFERENCES.....</b>	<b>94</b>
<b>Appendix A .....</b>	<b>104</b>
A1 Pump constant calculation .....	105
<b>Appendix B .....</b>	<b>111</b>
B1 Heats of mixing calculations .....	112
B2 Weight corrections for buoyancy effect of air .....	125
<b>Appendix C .....</b>	<b>128</b>
C1 Statistics of data correlation .....	129
C2 Representation of ternary excess molar enthalpy using the Liebermann-Fried model. .	132
<b>Appendix D.....</b>	<b>150</b>
D1 Calibration and Mixing run procedure.....	151

## LIST OF TABLES

Table 1.1	Lists of binary systems	8
Table 1.2	Lists of ternary systems	9
Table 3.1	Source, purity and densities of the chemicals at 298.15 K	20
Table 3.2	Modifications of the calorimeter	29
Table 4.1	List of binary systems studied in the research work	39
Table 4.2	Experimental molefraction $x_i$ and excess molar enthalpy values $H_{m,ij}^E$ (J/mol) at 298.15K for the binary systems	40
Table 4.3	Experimental molefraction $x_i$ and excess molar enthalpy values $H_{m,ij}^E$ (J/mol) at 298.15K for the binary systems	41
Table 4.4	Experimental molefraction $x_i$ and excess molar enthalpy values $H_{m,ij}^E$ (J/mol) at 298.15K for the binary systems	42
Table 4.5	Experimental molefraction $x_i$ and excess molar enthalpy values $H_{m,ij}^E$ (J/mol) at 298.15K for the binary systems	43
Table 4.6	Coefficients $h_k$ of the Redlich Kister polynomial equation calculated for the binary systems and the standard error 's'	45
Table 4.7	Physical properties of the components used in the Liebermann-Fried model	53
Table 4.8	Binary interaction parameters and standard deviation of the Liebermann-Fried model	54
Table 4.9	Studied ternary systems	59
Table 4.10	Equation 4.6 fitting parameters $c_i$ and standard deviation s for the ternary systems listed in table 4.6	61
Table 4.11	Experimental excess molar enthalpies $H_{m,1+23}^E$ (J/mol) and the calculated values of $H_{m,123}^E$ (J/mol) for the $x_1$ 2-MTHF + $x_2$ EBz + $(1 - x_1 - x_2)$ <i>p</i> -Xylene ternary system at 298.15K	63

Table 4.12	Experimental excess molar enthalpies $H_{m,1+23}^E$ (J/mol) and the calculated values of $H_{m,1+23}^E$ (J/mol) for the $x_1$ 2-MTHF + $x_2$ EBz + $1 - x_1 - x_2$ Mesitylene ternary system at 298.15K	66
Table 4.13	Experimental excess molar enthalpies $H_{m,1+23}^E$ (J/mol) and the calculated values of $H_{m,1+23}^E$ (J/mol) for the $x_1$ 2-ME + $x_2$ EBz + $1 - x_1 - x_2$ Mesitylene ternary system at 298.15K	69
Table 4.14	Experimental excess molar enthalpies $H_{m,1+23}^E$ (J/mol) and the calculated values of $H_{m,123}^E$ (J/mol) for the $x_1$ 2-ME $x_2$ + 2-MTHF + $1 - x_1 - x_2$ <i>p</i> -Xylene ternary system at 298.15K	72
Table 4.15	Experimental excess molar enthalpies $H_{m,1+23}^E$ (J/mol) and the calculated values of $H_{m,123}^E$ (J/mol) for the $x_1$ 1-Butanol + $x_2$ Mesitylene + $1 - x_1 - x_2$ <i>p</i> -Xylene ternary system at 298.15K	75
Table 4.16	Experimental excess molar enthalpies $H_{m,1+23}^E$ (J/mol) and the calculated values of $H_{m,123}^E$ (J/mol) for the $x_1$ 1-Butanol + $x_2$ DNBE + $1 - x_1 - x_2$ Mesitylene ternary system at 298.15K	78
Table 4.17	Experimental excess molar enthalpies $H_{m,1+23}^E$ (J/mol) and the calculated values of $H_{m,123}^E$ (J/mol) for the $x_1$ 1-Butanol + $x_2$ 2-MTHF + $1 - x_1 - x_2$ EBz ternary system at 298.15K	81
Table 4.18	Experimental excess molar enthalpies $H_{m,1+23}^E$ (J/mol) and the calculated values of $H_{m,123}^E$ (J/mol) for the $x_1$ DNBE + $x_2$ 2-MTHF + $1 - x_1 - x_2$ EBz ternary system at 298.15K	84
Table 4.19	Experimental excess molar enthalpies $H_{m,1+23}^E$ (J/mol) and the calculated values of $H_{m,123}^E$ (J/mol) for the $x_1$ DNBE + $x_2$ 2-MTHF + $1 - x_1 - x_2$ EBz ternary system at 298.15K	87
Table 4.20	Standard deviation 's' for the ternary enthalpy values predicted by the Liebermann-Fried model.	90
Table A1.1	Pump A calibration results	106
Table A1.2	Pump B calibration results	108
Table A1.3	Pump Constant $K_p$ comparison	110
Table B1.1	Pure component properties	112

Table B1.2	Calibration results of DNBE in pump A	112
Table B1.3	Calibration results of 2-MTHF in pump B	114
Table B1.4	Experimental data of the DNBE (1) + 2-MTHF binary system	116
Table B2.1	Ambient conditions and pure component properties for preparing EBz (1) + <i>p</i> -Xylene (2) mixture of molefraction $x_1 \approx 0.2500$	126
Table B2.2	Summary of weighing	126
Table C1.1	Summary of F statistical test	131
Table D1.1	Motor speed settings for different molefraction of 1-Butanol (1) + <i>p</i> -Xylene (2) mixing run	162

## LIST OF FIGURES

Figure 3.1	(Hassan, 2010) Schematic diagram of Vacuum pump degassing method	22
Figure 3.2	Modified from (Hassan, 2010), schematic representation of LKB flow microcalorimeter (10700-1)	24
Figure 3.3	Schematic diagram of the calorimeter unit, (Hassan, 2010)	25
Figure 3.4	Schematic diagram of pump control system	27
Figure 3.5	Calibration circuit diagram, (Hassan, 2010)	31
Figure 3.6	Deviations of the excess molar enthalpy at 298.15K for Ethanol (1) + n-Hexane (2) plotted against molefraction $x_1$ .	33
Figure 4.1	Excess molar enthalpies, $H_{m,ij}^E$ for the binary systems presented in Table 4.2 at 298.15K	46
Figure 4.2	Excess molar enthalpies, $H_{m,ij}^E$ for the binary systems at presented in Table 4.3 at 298.15 K.	47
Figure 4.3	Excess molar enthalpies, $H_{m,ij}^E$ for the binary systems presented in Table 4.4 at 298.15 K.	48
Figure 4.4	Excess molar enthalpies, $H_{m,ij}^E$ or the binary systems presented in Table 4.5 at 298.15 K.	49
Figure 4.5	Excess molar enthalpies, $H_{m,ij}^E$ representation by the Liebermann-Fried model for the binary systems presented in Table 4.2 at 298.15 K	55
Figure 4.6	Excess molar enthalpies, $H_{m,ij}^E$ representation by the Liebermann-Fried model for the binary systems presented in Table 4.3 at 298.15 K	56
Figure 4.8	Excess molar enthalpies, $H_{m,ij}^E$ representation by the Liebermann-Fried model for the binary systems presented in Table 4.5 at 298.15K	58
Figure 4.9	Excess molar enthalpies, $H_{m,1+23}^E$ for the ternary system $x_1$ 2-MTHF + $x_2$ EBz + $1 - x_1 - x_2$ p-Xylene at 298.15 K.	64

Figure 4.10	Constant enthalpy contours, $H_{m,123}^E$ (J/mol) at 298.15 K for the $x_1$ 2-MTHF + $x_2$ EBz + 1 - $x_1 - x_2$ <i>p</i> -Xylene, calculated from the representation of the experimental results using the equation 2.3 and 2.4	65
Figure 4.11	Excess molar enthalpies, $H_{m,1+23}^E$ for the ternary system $x_1$ 2-MTHF + $x_2$ EBz + 1 - $x_1 - x_2$ Mesitylene at 298.15 K	67
Figure 4.12	Constant enthalpy contours, $H_{m,123}^E$ (J/mol) at 298.15 K for the $x_1$ 2-MTHF + $x_2$ EBz + 1 - $x_1 - x_2$ Mesitylene, calculated from the representation of the experimental results using the equation 2.3 and 2.4	68
Figure 4.13	Excess molar enthalpies, $H_{m,1+23}^E$ for the ternary system $x_1$ 2-ME + $x_2$ EBz + 1 - $x_1 - x_2$ Mesitylene at 298.15 K	70
Figure 4.14	Constant enthalpy contours, $H_{m,123}^E$ (J/mol) at 298.15 K for the $x_1$ 2-ME + $x_2$ EBz + 1 - $x_1 - x_2$ Mesitylene, calculated from the representation of the experimental results using the equation 2.3 and 2.4	71
Figure 4.15	Excess molar enthalpies $H_{m,1+23}^E$ for the ternary system $x_1$ 2-ME + $x_2$ 2-MTHF + 1 - $x_1 - x_2$ <i>p</i> -Xylene at 298.15 K	73
Figure 4.16	Constant enthalpy contours, $H_{m,123}^E$ (J/mol) at 298.15 K for the $x_1$ 2-ME + $x_2$ 2-MTHF + 1 - $x_1 - x_2$ <i>p</i> -Xylene, calculated from the representation of the experimental results using the equation 2.3 and 2.4.	73
Figure 4.17	Excess molar enthalpies, $H_{m,1+23}^E$ for the ternary system $x_1$ 1-Butanol + $x_2$ Mesitylene + 1 - $x_1 - x_2$ <i>p</i> -Xylene at 298.15 K	76
Figure 4.19	Excess molar enthalpies, $H_{m,1+23}^E$ for the ternary system $x_1$ 1-Butanol + $x_2$ DNBE + 1 - $x_1 - x_2$ Mesitylene at 298.15 K	79
Figure 4.20	Constant enthalpy contours, $H_{m,123}^E$ (J/mol) at 298.15 K for the $x_1$ 1-Butanol + $x_2$ DNBE + 1 - $x_1 - x_2$ Mesitylene, calculated from the representation of the experimental results using the equation 2.3 and 2.4	80
Figure 4.21	Excess molar enthalpies, $H_{m,1+23}^E$ for the ternary system $x_1$ 1-Butanol + $x_2$ 2-MTHF + 1 - $x_1 - x_2$ EBz at 298.15 K.	82

Figure 4.22	Constant enthalpy contours, $H_{m,123}^E$ (J/mol) at 298.15 K for the $x_1$ 1-Butanol + $x_2$ 2-MTHF + $1 - x_1 - x_2$ EBz, calculated from the representation of the experimental results using the equation 2.3 and 2.4	83
Figure 4.23	Excess molar enthalpies, $H_{m,1+23}^E$ for the ternary system $x_1$ DNBE + $x_2$ 2-MTHF + $1 - x_1 - x_2$ EBz at 298.15 K	85
Figure 4.24	Constant enthalpy contours, $H_{m,123}^E$ (J/mol) at 298.15 K for the $x_1$ DNBE + $x_2$ 2-MTHF + $1 - x_1 - x_2$ EBz, calculated from the representation of the experimental results using the equation 2.3 and 2.4	86
Figure 4.25	Excess molar enthalpies, $H_{m,1+23}^E$ for the ternary system $x_1$ DNBE + $x_2$ Mesitylene + $1 - x_1 - x_2$ <i>p</i> -Xylene at 298.15 K	88
Figure 4.26	Constant enthalpy contours, $H_{m,123}^E$ (J/mol) at 298.15 K for the $x_1$ DNBE + $x_2$ Mesitylene + $1 - x_1 - x_2$ <i>p</i> -Xylene, calculated from the representation of the experimental results using the equation 2.3 and 2.4	89
Figure A1.1	Pump A calibration plot. Volumetric flow rate Q against motor speed R	107
Figure A1.2	Pump B calibration plot. Volumetric flow rate Q against motor speed R.	109
Figure B1.1	Calibration curve for DNBE in pump A	113
Figure B1.2	Calibration curve for 2-MTHF in pump B	115
Figure C2.1	Excess molar enthalpies, $H_{m,1+23}^E$ for the ternary system $x_1$ 2-MTHF + $x_2$ EBz + $1 - x_1 - x_2$ <i>p</i> -Xylene at 298.15 K. (Liebermann-Fried model representation)	132
Figure C2.2	Constant enthalpy contours, $H_{m,123}^E$ (J/mol) at 298.15 K for the $x_1$ 2-MTHF + $x_2$ EBz + $1 - x_1 - x_2$ <i>p</i> -Xylene, calculated from the representation of the experimental results using the Liebermann-Fried model.	133

Figure C2.3	Excess molar enthalpies, $H_{m,1+23}^E$ for the ternary system $x_1$ 2-MTHF + $x_2$ EBz + 1 – $x_1$ – $x_2$ Mesitylene at 298.15 K. (Liebermann-Fried model representation)	134
Figure C2.4	Constant enthalpy contours, $H_{m,123}^E$ (J/mol) at 298.15 K for the $x_1$ 2-MTHF + $x_2$ EBz + 1 – $x_1$ – $x_2$ Mesitylene, calculated from the representation of the experimental results using the Liebermann-Fried model.	135
Figure C2.5	Excess molar enthalpies, $H_{m,1+23}^E$ for the ternary system $x_1$ 2-ME + $x_2$ EBz + 1 – $x_1$ – $x_2$ Mesitylene at 298.15 K. (Liebermann-Fried model representation)	136
Figure C2.6	Constant enthalpy contours, $H_{m,123}^E$ (J/mol) at 298.15 K for the $x_1$ 2-ME + $x_2$ EBz + 1 – $x_1$ – $x_2$ Mesitylene, calculated from the representation of the experimental results using the Liebermann-Fried model	137
Figure C2.7	Excess molar enthalpies, $H_{m,1+23}^E$ for the ternary system $x_1$ 2-ME + $x_2$ 2-MTHF + 1 – $x_1$ – $x_2$ <i>p</i> -Xylene at 298.15 K. (Liebermann-Fried model representation)	138
Figure C2.8	Constant enthalpy contours, $H_{m,123}^E$ (J/mol) at 298.15 K for the $x_1$ 2-ME + $x_2$ 2-MTHF + 1 – $x_1$ – $x_2$ <i>p</i> -Xylene, calculated from the representation of the experimental results using the Liebermann-Fried model.	139
Figure C2.9	Excess molar enthalpies, $H_{m,1+23}^E$ for the ternary system $x_1$ 1-Butanol + $x_2$ Mesitylene + 1 – $x_1$ – $x_2$ <i>p</i> -Xylene at 298.15 K. (Liebermann-Fried model representation)	140
Figure C2.10	Constant enthalpy contours, $H_{m,123}^E$ (J/mol) at 298.15 K for the $x_1$ 1-Butanol + $x_2$ Mesitylene + 1 – $x_1$ – $x_2$ <i>p</i> -Xylene, calculated from the representation of the experimental results using the Liebermann-Fried model	141
Figure C2.11	Excess molar enthalpies, $H_{m,1+23}^E$ for the ternary system $x_1$ 1-Butanol + $x_2$ DNBE + 1 – $x_1$ – $x_2$ Mesitylene at 298.15 K. (Liebermann-Fried model representation)	142

Figure C2.12	Constant enthalpy contours, $H_{m,123}^E$ (J/mol) at 298.15 K for the $x_1$ 1-Butanol + $x_2$ DNBE + $1 - x_1 - x_2$ Mesitylene, calculated from the representation of the experimental results using the Liebermann-Fried model.	143
Figure C2.13	Excess molar enthalpies, $H_{m,1+23}^E$ for the ternary system $x_1$ 1-Butanol + $x_2$ 2-MTHF + $1 - x_1 - x_2$ EBz at 298.15 K. (Liebermann-Fried model representation)	144
Figure C2.14	Constant enthalpy contours, $H_{m,123}^E$ (J/mol) at 298.15 K for the $x_1$ 1-Butanol + $x_2$ 2-MTHF + $1 - x_1 - x_2$ EBz, calculated from the representation of the experimental results using the Liebermann-Fried model.	145
Figure C2.15	Excess molar enthalpies, $H_{m,1+23}^E$ for the ternary system $x_1$ DNBE + $x_2$ 2-MTHF + $1 - x_1 - x_2$ EBz at 298.15 K. (Liebermann-Fried model representation)	146
Figure C2.16	Constant enthalpy contours, $H_{m,123}^E$ (J/mol) at 298.15 K for the $x_1$ DNBE + $x_2$ 2-MTHF + $1 - x_1 - x_2$ EBz, calculated from the representation of the experimental results using the Liebermann-Fried model.	147
Figure C2.17	Excess molar enthalpies, $H_{m,1+23}^E$ for the ternary system $x_1$ DNBE + $x_2$ Mesitylene + $1 - x_1 - x_2$ <i>p</i> -Xylene at 298.15 K. (Liebermann-Fried model representation)	148
Figure C2.18	Constant enthalpy contours, $H_{m,123}^E$ (J/mol) at 298.15 K for the $x_1$ 1-Butanol + $x_2$ Mesitylene + $1 - x_1 - x_2$ <i>p</i> -Xylene, calculated from the representation of the experimental results using the Liebermann-Fried model.	149
Figure D1.1	Flow control valve	152
Figure D1.2	Glass syringe connected to pump B outlet tube	153
Figure D1.3	Calorimeter software	154
Figure D1.4	Motor gear position	158

## LIST OF ABBREVIATIONS

2-MTHF	2-Methyltetrahydrofuran
2-ME	2-Methoxyethanol
CEPA	Canadian Environmental Protection Agency
DNBE	Di- <i>n</i> -butyl ether
DSC	Differential Scanning Calorimeter
EBZ	Ethylbenzene
MTBE	Methyl Tertiary Butyl Ether
NRTL	Non Random Two liquids
PFG	Precision frequency generator
UNQUAC	Universal Quasi Chemical

## NOMENCLATURE

### ALPHABETS

		Unit
A	Liebermann-Fried model parameter	
c	Ternary parameter	
E	Voltage reading	volt (v)
F	F statistical test parameter	
$f$	Molar flow rate	mol/sec
G	Gibbs free energy	J/mol
G	Motor gear ratio	
H	Excess molar enthalpy	J/mol
$h$	Redlich - Kister polynomial coefficient	
$I$	Current	ampere (A)
I	Expression used in equation 4	
K	Pump calibration constant	cm <sup>3</sup> /sec
M	Molecular weight	g/mol
m	mass of substance	gram (g)
$N$	Number of components	
$n$	Number of data points	
P	Pressure	kPa
$p$	Parameter number	
$Q$	Volumetric flow rate	cm <sup>3</sup> /sec
R	Universal gas constant	J/mol K
$r$	Electrical resistance	ohm ( $\Omega$ )

$S$	Entropy	J/mol K
$s$	Standard error	
$T$	Temperature	Kelvin (K)
$t$	Temperature	°C
$V$	Volume	cm <sup>3</sup>
$x$	Apparent molefraction component	

## GREEK LETTERS

$\alpha$	Isobaric thermal expansivity	K <sup>-1</sup>
$\gamma$	Activity coeeficient	
$\varepsilon$	Calibration constant	J/v/s
$\phi$	Volume fraction	
$\rho$	Density	g/cm <sup>3</sup>
$R$	Pump controller reading	counts/sec
$\nu, l$	Degrees of freedom	

## SUPERSCRIPTS

0	Ideal/Baseline	
E	Excess function	

## SUBSCIPTS

1,2	Pump indices	
$i,j,k,p,q$	Component indices	

A,B	Pump notation
<i>cal</i>	Calculated values
<i>exp</i>	Experimental data
<i>H</i>	Humidity
<i>k</i>	Parameter indices
M	Mixture
<i>m</i>	Molar property
<i>p</i>	Pump
P	Isobaric properties

## **1.0 INTRODUCTION**

Declining petroleum resources and increased energy usage and environmental deterioration forced the nations to make the petroleum refining process efficient, economical, and environment friendly. During the period from 1915 to the late 1970's tetraethyllead was extensively used for its excellent anti-knocking properties which resulted in dramatic improvement engine efficiency and life. But research conducted through 1960 to 1970 revealed that using tetraethyllead in gasoline increased the blood lead level, which reflected a detrimental effect on human health and therefore use of tetraethyllead as a gasoline additive was banned all over the world. The gasoline regulations (*CEPA*, 1990) restricts the use of leaded gasoline in commercial vehicles in Canada

Phasing out lead as an additive reduced the gasoline's octane number had affected the performance of automobiles that were dependent on high-octane fuels. In order to increase the fuels' octane ratings, fuel suppliers have used oxygenates namely alcohol and ethers, as fuel additives. Among the oxygenates, methyl tertiary butyl ether (MTBE) showed a superior performance as an octane enhancer and greatly reduced the emission of atmospheric pollutants like carbon monoxide (CO) and volatile organic compounds from the vehicle exhaust. Due to its low cost, its ease of production, and the favorable transfer and blending characteristics, MTBE was produced and used worldwide as oxygenated gasoline additive since 1973 (30 million tons/year in 1995) (Ancillotti and Fattore, 1998).

In early 2000s, studies revealed that in many places in the United States MTBE caused serious health issues including the risk of cancer on long term exposure (Davis and Farland, 2001). Thereafter, research work focused on finding safe, efficient and economical ether and alcohols to blend with gasoline was triggered, and the studies of thermodynamic properties of mixtures involving hydrocarbons, ethers and alcohol turn out to be essential in design and operation of separation equipment.

Thermodynamic properties of mixtures involving hydrocarbons, ethers and alcohols are of fundamental importance in petroleum based applications such as modeling and design of heat exchangers, reactors and fluid-phase separation equipment. Thermodynamic data for representative mixtures are useful as the experimentally obtained information will help us to understand the molecular interactions occurring between the constituent species in liquid mixtures and to test and validate thermodynamic models.

## **1.1 Objectives**

The study reported in this thesis is a continuation of the research work conducted in the Applied Thermodynamics Laboratory in the Department of Chemical and Biological Engineering at the University of Saskatchewan. Hassan (2010) has measured the excess molar enthalpy of 10 binary and six ternary systems involving hydrocarbons, ethers and alcohols. The main objectives of my research work are

- (1) To measure the enthalpy of mixing for selected binary and ternary systems at fixed pressure and temperature and
- (2) To determine the optimal parameter values for use with selected empirical models to represent the experimental excess molar enthalpy data for binary and ternary systems

In this thesis, the experimental work on the excess molar enthalpy of 16 binary systems and 9 ternary systems involving hydrocarbon and ethers is described. The measured excess molar enthalpy values of the binary systems are correlated by means of the Redlich – Kister polynomial equation and the Liebermann-Fried solution theory model, respectively. In addition, a description of the application of the Tsao-Smith model and the Liebermann – Fried solution theory to the experimental results obtained for the ternary systems is also presented.

## **1.2 An overview of the thesis**

A literature review is presented in Chapter 2, which serves to describe the methods for measuring the excess molar enthalpy values and the correlation and prediction methods for representing the experimental excess molar values.

In Chapter 3 the details of the equipment used, material properties and the experimental procedures followed in the course of the study will be discussed. In Chapter 4 the experimental results and discussion are presented.

Chapter 5 concludes the thesis with recommendations for future work.

## **1.3 Importance of the study**

### **1.3.1 Excess Thermodynamic Properties**

An excess property of a solution can be best expressed as the difference between the actual property values of a solution and the value it would have as an ideal solution at the same composition, temperature and pressure Smith *et al.* (2005). Mathematically it can be written as

$$M^E = M - M^{id} \tag{1.1}$$

Where  $M^E$  is the excess property of the solution and  $M$  is the actual property value of the solution and  $M^{id}$  is the property value as an ideal solution, there are many excess properties of which following are the most widely studied, which are excess molar enthalpy  $H_m^E$ , excess molar volume  $V_m^E$ , Excess molar Gibbs energy  $G_m^E$ , and excess molar entropy  $S_m^E$ . At constant temperature, pressure excess molar volume and excess molar enthalpy is zero an ideal solution.

$$\Delta H_{mix}^{id} = 0 \quad (1.2)$$

$$\Delta V_{mix}^{id} = 0 \quad (1.3)$$

Whereas change in Gibbs energy and Entropy for an ideal solution mixture is non-zero and expressed as

$$\Delta G_{mix}^{id} = RT \sum x_i \ln x_i \quad (1.4)$$

$$\Delta S_{mix}^{id} = -R \sum x_i \ln x_i \quad (1.5)$$

The intermolecular forces resulting from the interaction of various species when forming a liquid mixture are related to the excess thermodynamic properties of the system. Studying thermodynamic excess properties such as excess molar enthalpy and excess molar volume provide knowledge about intermolecular forces and molecular interactions in a liquid mixture.

### 1.3.2 Excess molar enthalpy

The excess molar enthalpy data are the most often measured excess thermodynamic property since it is relatively easy to obtain and the data can be used to calculate other excess thermodynamic properties, vapor-liquid equilibrium values and are the observables to determine

the intermolecular forces. Heat of mixing is a very essential property in separation processes and also it determines the variation of activity coefficient with temperature. Activity coefficient is a very critical parameter considered in the design of chemical processes which involves phase separation.

$$H_m^E = -RT^2 \left[ \frac{\partial(G_m^E)}{\partial T} \right]_{P,x} = -RT^2 \sum_i x_i \left[ \frac{\partial(\ln \gamma_i)}{\partial T} \right]_{P,x} \quad (1.6)$$

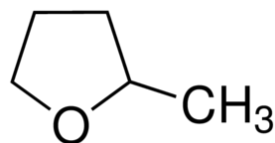
(Zudkevitch, 1978) explained the importance of the heat of mixing values in his review, in which he reported that a substantial 30% production decline was encountered with unacceptable product purity during the distillation of cyclohexanone and cyclohexanol. The reason for the anomaly in the distillation process was due to omitting the heat of mixing values from the calculation, this example emphasize the significance of heat of mixing data in separation process.

#### 1.4 System studied

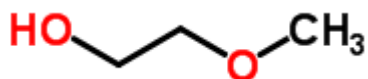
In this research work a special attention was paid in choosing the chemicals to study, Marsh *et al.* (1999) in their paper listed the works of various researchers on thermophysical properties of binary and ternary mixtures involving oxygenates and hydrocarbons. Upon reviewing Marsh *et al.* (1999) paper it was observed that the thermophysical properties of many potential binary and ternary systems involving hydrocarbons and ethers needs to be studied. Based on Marsh *et al.* review seven chemical species were chosen for the study and they are listed as follows

### Chemical name and their structural formula

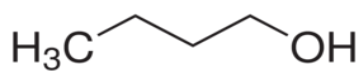
1) 2-Methyltetrahydrofuran (2-MTHF)



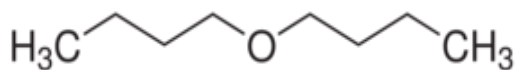
2) 2-Methoxyethanol (2-ME)



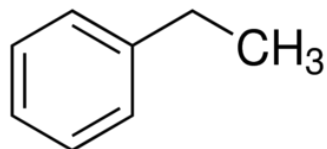
3) 1-Butanol



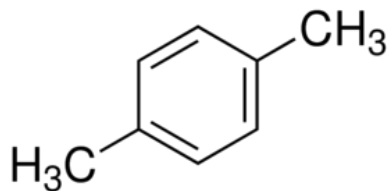
4) Di-n-Butyl ether (DNBE)



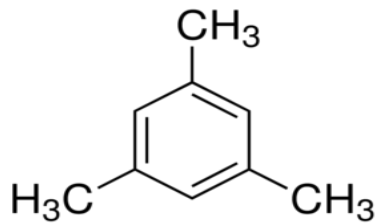
5) Ethylbenzene (EBz)



6) *p*-Xylene



7) Mesitylene (1,3,5-Trimethylbenzene)



With the selected seven chemicals, excess molar enthalpy for 21 binary systems and 35 ternary systems can be studied. Among the 21 binary systems, five binary systems have been already studied by different authors and they are

Kammerer and Lichtenthaler (1998) reported the experimental excess molar enthalpy values for (1-Butanol + DNBE) binary system, Giner *et al.* (2003) reported excess molar enthalpy for (2-MTHF + 1-Butanol) binary system. Cobos *et al.* (1988) measured excess molar enthalpy values for (1-Butanol + 2-ME) binary system, Hsu and Lawrence Clever (1975) reported (Mesitylene + *p*-Xylene) binary excess molar enthalpy values and Tanaka and Benson (1976) published the excess molar enthalpy value for (EBz + *p*-Xylene) binary system.

Since five out of 21 binary systems have already been studied the remaining 16 binary systems are studied in this research work and they are listed as follows.

**Table 1.1.** Lists of binary systems

S.No	Binary system	
1	2-MTHF	Ethylbenzene
2		Mesitylene
3		<i>p</i> -Xylene
4		2-ME
5		DNBE
6		1-Butanol
7	2-ME	Ethylbenzene
8		Mesitylene
9		<i>p</i> -Xylene
10	1-Butanol	Ethylbenzene
11		Mesitylene
12		<i>p</i> -Xylene
13	DNBE	Ethylbenzene
14		Mesitylene
15		<i>p</i> -Xylene
16	Ethylbenzene	Mesitylene

Among the possible 35 ternary systems nine ternary system have been chosen for this study, because measuring experimental excess molar enthalpy for all the 35 systems will require a large amount of time and materials so we limited our focus to study only nine ternary systems and the studied ternary systems are listed as follows.

**Table 1.2.** Lists of ternary systems

<b>Ternary System</b>	<b>Component 1</b>	<b>Component 2</b>	<b>Component 3</b>
<b>1</b>	2-MTHF	EBz	<i>p</i> -Xylene
<b>2</b>	2-MTHF	EBz	Mesitylene
<b>3</b>	2-ME	EBz	Mesitylene
<b>4</b>	2-ME	2-MTHF	<i>p</i> -Xylene
<b>5</b>	1-Butanol	Mesitylene	<i>p</i> -Xylene
<b>6</b>	1-Butanol	Mesitylene	DNBE
<b>7</b>	1-Butanol	2-MTHF	EBz
<b>8</b>	DNBE	2-MTHF	EBz
<b>9</b>	DNBE	Mesitylene	<i>p</i> -Xylene

## 2.0 LITERATURE REVIEW

This chapter covers the different calorimetric approach for measuring excess molar enthalpy values and discusses the different correlation and prediction methods for representing the experimental excess molar enthalpy values.

### 2.1 Methods of measuring excess molar enthalpy values

Heat of mixing values can be calculated from using other excess thermodynamic properties such as excess Gibbs energy, Gibbs-Helmholtz equation (equation 2.1) relates the excess molar enthalpy and excess Gibbs energy.

$$H_m^E = -T^2 \left\{ \frac{\partial \left( \frac{G_m^E}{T} \right)}{\partial T} \right\}_p \quad (2.1)$$

In order to calculate the excess molar enthalpy from the equation 2.1 temperature derivatives of the excess Gibbs energy is required. But for most systems the excess molar Gibbs energy and excess molar enthalpy is available only at specific temperatures so calculating excess properties from equation 2.1 is generally not considered. Thus calorimetric measurement is the most reliable technique in determining the excess molar enthalpy values.

#### 2.1.1 Calorimetric methods

Any change in the state of a system is accompanied with either loss or gain of energy. Measuring and studying the energy difference of a system is a source of information for understanding molecular interactions and molecular structure. Calorimetric method is undoubtedly the most prevailing and technologically advanced procedure for measuring the

excess molar enthalpy of liquid mixtures. In their paper Ott and Sipowska (1996) extensively covered the different types of calorimeter used for measuring the excess molar enthalpies of non-electrolyte solutions. Calorimetric attempts to measure the excess molar enthalpy values dates back more than a century. Researchers like Clarke (1905), Bose (1907), Baud (1915) reported heats of mixing values for alcohol-water mixtures, hydrocarbon with halogenated mixtures and aromatic with aliphatic hydrocarbon mixtures. In 1921 Hirobe (1925) published excess molar enthalpies for 51 binary mixtures using a sophisticated isothermal calorimeter and the deviation of some of the data published by Hirobe are within few percent of the results obtained with the best modern calorimeters.

### **2.1.2 Types of calorimeters**

Different types of calorimeters have been developed and used successfully for measuring excess molar enthalpy values based on different operating conditions. Hassan (2010) in his thesis described three different kinds of calorimeters operated under normal temperature and pressure to measure excess molar enthalpy values. They are

- 1) Isothermal Titration Calorimeter
- 2) Differential Scanning calorimeter
- 3) Flow calorimeter

#### **Isothermal Titration Calorimeter**

Isothermal titration calorimeters are built on the same conduction principle as flow calorimeters and the principle involved is that a fixed quantity of component 1 is placed inside a

mixing cell and component 2 is injected into the mixing cell either continuously or in fixed volumes. The prototype of the isothermal titration calorimeter was first designed and developed by Christensen *et al.* (1968) and Wadso (1968), further modification of the titration calorimeter by Holt and Smith (1974) and Rodríguez de Rivera *et al.* (2009) improved the accuracy of the results. These calorimeters are widely used for studying the bio-molecular interactions studies but its application in measuring the excess molar enthalpy values is less pronounced. Liao *et al.* (2009a, 2009b, 2012) used isothermal titration for measuring binary excess molar enthalpies of various mixtures involving hydrocarbons, ether, alcohol and acids and reported higher accurate results.

### **Differential Scanning Calorimeter (DSC)**

The Differential scanning calorimeter is a versatile instrument for direct assessment of change in heat energy of a system. DCS is measure of change of difference in the heat flow rate to the sample and to a reference sample while they are subjected to a controlled temperature program Höhne *et al.* (2003). The DSC measures the excessive heat quantity released or absorbed by a sample on the basis of temperature difference between the sample and a reference material Gill *et al.* (2010). Differential scanning calorimeter is commonly used for biochemical reactions, and also for thermal transition and reactions, crystallization, oxidation, fusion, heat of reaction and heat capacity measurements. Even though the DSC are not widely used for heat of mixing measurements Jablonski *et al.* (2003) showed that the DSC are a potential tool for heat of mixing measurements.

## 2.2 Flow calorimeters

In recent years flow calorimetry has been the preferred method for researchers to measure the heat effects during mixing process. Flow calorimeters have distinct advantages over batch and isothermal displacement calorimeters, for example when relative volatiles are involved, formation of vapor-phase is a serious problem and leads to large errors in batch calorimeter. Flow calorimeters can be used to measure

- i. Excess molar enthalpy values under wide range of pressure and temperature conditions, for both gas and liquid components
- ii. Studies involving corrosive and reactive chemicals where the batch and isothermal displacement calorimeter cannot be used.

In flow calorimeter two different working fluids mix in a mixing cell at steady state with fixed flow rates. The flow rates can be adjusted to measure heat of mixing values at wide range of composition with high precision. Monk and Wadsö (1968) designed and tested the prototype of the flow reaction calorimeter and showed the advantages of using flow calorimeter over batch calorimeter. Flow calorimeters of different types have been successfully designed and used by many researchers for measuring excess molar enthalpy values at various pressure and temperature conditions, namely Picker (1974), Wormald and colleagues, Elliott and Wormald, (1976), Wormald *et al.* (1977), and Christensen and co-workers Christensen *et al.* (1976).

Tanaka *et al.* (1975) modified the design of Monk and Wadso's flow calorimeter and measured the excess molar enthalpy values for non-electrolytes with higher accuracy. Later

Kimura *et al.* (1983) reported a 0.5% increased accuracy in his work by modifying the operating techniques of the flow calorimeter.

One of the few setbacks of flow calorimeter is it requires large amount of chemicals to measure the excess molar enthalpy values so for measurements involving rare and expensive components calorimeters are not the best choice. Regardless of the drawback flow calorimeter's numerous successful measurements ensured a prominent position in the scientific community to justify its usage. Choosing the right calorimeter depends on the requirements of the specific research field, if the measurement especially involves heat of mixing values for multicomponent systems a flow calorimeter would be the right choice, while a batch calorimeter would be much suitable for measurements involving chemical reactions and biological processes.

### **2.3 Correlation and prediction methods**

The synthesis of chemical compounds, design of separation process, solvent selection and ideal operating conditions needs a reliable knowledge of phase equilibrium behavior of a fluid mixture as a function of temperature, pressure and composition. A thermodynamic model describes the real fluid mixture behavior using the existing experimental data and pure component properties.

Correlation and prediction methods are always an interesting topic among researchers in the experimental thermodynamics field, with the scope of avoiding time consumption and difficulties encountered in the experimental measurement of excess enthalpies especially for the multicomponent mixtures. Among the correlation and prediction methods some of them are mathematical expressions and some of them are theoretical models.

### 2.3.1 Empirical methods

Empirical expressions are the mathematical models which are very useful and convenient for data correlation. These models have parameters in their formula which is fitted to the experimental data, the best fit of parameters and quality of the representation was judged by the standard deviation. The empirical expressions have limitations, for example the model with highest number of adjustable parameters doesn't necessarily means it is the excellent representation of the experimental data.

#### 2.3.1.1 The Redlich - Kister polynomial equation

Redlich and Kister described an expression which is the most widely used polynomial equation to represent binary excess molar enthalpy data. The other notable mathematical models used for representing experimental excess molar enthalpies are the expressions given by Brandreth *et al.* (1966), Mrazek and Van Ness (1961), Rogalski and Malanowski (1977) SSF equation and Wilson's equation. Prchal *et al.* (1982) reviewed the mathematical models used for representing the binary experimental excess molar enthalpy values and in their paper they found that the Redlich-Kister model best describes the binary experimental heat of mixing values. Redlich-Kister assumed a particular form of enthalpy values ( $H^E$ ) as a function of mole fraction ( $x_i$ ) with one or more adjustable parameters and the parameters are chosen by the method of least square to minimize the error in ( $H^E$ ).

Ternary excess molar enthalpy data can be represented through empirical expressions, one of the widely used empirical equations for representing ternary excess molar enthalpy with high accuracy is the one proposed by Tsao and Smith (1953) with an added ternary term defined by

Morris *et al.* (1975) The Redlich - Kister expression and the Tsao and Smith expression for representing the binary and ternary experimental excess molar enthalpy values are discussed in detail in chapter 4.

### 2.3.2 Solution theory models

An interesting approach to represent excess enthalpy values is by means of local composition models like the Wilson equation (Wilson, 1964) , the NRTL equation (Renon and Prausnitz, 1968), and the UNIQUAC model (Abrams and Prausnitz, 1975) and other solution theory models such as the Flory theory Flory (1965) Abe and Flory (1965) and the Liebermann-Fried model Liebermann and Fried (1972a,b). Even though the solution theory models are still at semi-empirical to empirical stage, it correlates and predict binary and multicomponent excess molar enthalpy values with reliable accuracy and the solution theory models are widely used with one or more parameters fitted to the experimental data.

The model proposed by Van Laar in 1906 is based on inserting the van der Waals equation into the thermal equation of state for a proposed thermodynamically reversible mixing process. The assumptions used involved that, for a binary mixture consisting of two species of similar size and same energies of interaction, the molecules of each species are uniformly distributed throughout the mixture and that the van der Waals equation of state is applicable to both of the pure liquids and the resulting liquid mixture.

At a given temperature and pressure  $S^E = V^E = 0$  and

$$G^E = U^E + PV^E - TS^E = U^E$$

The solution theory assumes that mixture interactions were independent of each other and quadratic mixing rules would provide reasonable approximations. The regular solution models are based on random mixing of molecules but the mixing of molecules is not really random due to the intermolecular forces. This drawback of the regular solution models was later overcome by Wilson model based on the local composition concept.

### **Models based on the Local composition concept**

Wilson in 1964 came up with his much acclaimed Gibbs free energy equation based on the local composition model in which he explained that mixing of molecules are not completely random and explained that specific molecular interactions are due to intermolecular forces between the molecules. Wilson model is capable of representing the behavior of multicomponent system using only the binary system parameters. A drawback of the Wilson model is that it cannot handle liquid - liquid immiscibility.

Other widely known models which are based on local composition concept are the NRTL (Non Random Two Liquids) proposed by Renon and Prausnitz in 1968 and the UNIQUAC (Universal Quasi Chemical) model proposed by Abrams and Prausnitz in 1975. The NRTL was proven to predict and correlate experimental data with high accuracy. NRTL can be used to predict and correlate enthalpy data for liquid-liquid immiscible systems unlike Wilson's model. The original NRTL model has been modified by many authors and was used to predict excess properties for electrolytes, polar and non-polar systems.

Universal Quasi-Chemical or UNIQUAC model was developed by Abrams and Prausnitz (1975) in their model they adopted the two-liquid model and the local composition model. They

assumed that the activity coefficient expression consists of two parts, the combinatorial part which is due to the size difference and shape of the molecules, and the residual part which is due to the energetic interactions. UNIQUAC can be applied to multicomponent mixtures in terms of binary parameters, liquid-liquid equilibrium, and representation of systems with widely different molecular sizes.

Based on the partition functions Flory derived a liquid equation of state which relates to the excess functions of the mixture. The Flory theory was developed for the correlation of thermodynamic properties of long chain liquid molecules and liquid mixtures, then later modified from its original form and applied to calculate one excess thermodynamic property from other excess thermodynamic property and also to calculate excess properties of systems involving small non-polar molecules. The Flory theory is widely praised for its simplicity in determining the model parameters from the physical properties of the pure components like isobaric expansivity  $\alpha_p$ , isothermal compressibility  $\kappa_T$  and the interchange energy parameter  $X_{i,j}$  which is calculated by regression of the experimental values.

#### **2.3.2.1 Liebermann - Fried model**

Liebermann and Fried Gibbs free energy model has two parts, one part represents the contribution due to the intermolecular forces and the other part reflects the contribution due to the difference in the size of the molecules. Wang and Lu (2000) used the Liebermann-Fried Gibbs energy model and successfully predicted the isobaric VLE values for Methyl *tert* butyl ether - alkanes system using excess enthalpy data determined at a different temperature. Peng *et al.* (2001) used the Liebermann-Fried model to correlate the excess enthalpy values of

hydrocarbon + ether binary systems and used the parameters obtained from that correlation to predict the excess enthalpies and VLE values for several multicomponent systems. Wang *et al.* (2005) used the excess molar enthalpy values for 123 binary mixtures at 298.15K from the literature and calculated the Liebermann-Fried binary interaction parameters for those 123 mixtures. Using those parameters the VLE values for the respective binary systems with reasonable accuracy was reported. Detailed explanation of the Liebermann-Fried model is discussed in chapter 4.

### 3.0 MATERIALS AND METHODS

#### 3.1 Materials

For this research work a total of nine chemicals were used and their properties are listed in Table 3.1. All the chemicals are stored in Type 4A molecular sieve beds (The molecular sieves are dried in an oven maintained at 100°C for at least 24 hours prior to storing the chemicals) and later they are degassed using a vacuum pump set up.

**Table 3.1. Source, purity and densities of the chemicals at 298.15 K**

Chemical	Source	Purity	Density (g/cm <sup>3</sup> )	
			Measured	Literature
Ethanol	Alcohol Inc	>99%	0.785063	0.78560 <sup>[a]</sup>
n-Hexane	Sigma Aldrich	>99%	0.655305	0.65512 <sup>[a]</sup>
2-MTHF	Sigma Aldrich	>99%	0.847982	0.84810 <sup>[b]</sup>
2-ME	Sigma Aldrich	>99%	0.960064	0.96011 <sup>[c]</sup>
1-Butanol	Sigma Aldrich	>99%	0.805740	0.80580 <sup>[d]</sup>
DNBE	Sigma Aldrich	>99%	0.763705	0.76394 <sup>[e]</sup>
EBz	Sigma Aldrich	>99%	0.862598	0.86252 <sup>[f]</sup>
Mesitylene	Sigma Aldrich	>99%	0.861146	0.86110 <sup>[g]</sup>
<i>p</i> -Xylene	Sigma Aldrich	>99%	0.856574	0.85660 <sup>[g]</sup>

(a) Wang *et al.* (1992); (b) Wang *et al.* (2006); (c) Peng *et al.* (1998); (d) Polák *et al.* (1970); (e)

Peng *et al.* (2002); (f) George and Sastry (2003); (g) Nayak *et al.* (2002)

The densities of the chemicals are measured by means of an Anton-Paar density meter (Model DMA-5000M) and the uncertainties of the measured density and temperature are

$\pm 0.000005 \text{ g/cm}^3$  and  $\pm 0.001^\circ\text{C}$ , respectively. These uncertainty values are provided by the density meter manufacturer.

### 3.1.1 Degassing the chemicals

The removal of dissolved gases from aqueous phase is an important process in many applications and it is carried out by different techniques namely pressure reduction, heating, membrane degasification and Inert gas substitution. Gas removal from liquids is very vital for carrying out excess molar enthalpy measurements. In particular using the degassed pure liquids helped to prevent the bubble formation in the mixing cell Tanaka *et al.* (1975). In this study all the pure component liquids are degassed using a vacuum pump setup figure 3.1.

A conical flask (a) with the pure component liquid and a magnetic bar (c) is placed on a magnetic stirrer (b) which agitates the liquid. The outlet of the flask was connected to a vacuum pump (f) through a three way valve (e), when the vacuum pump is turned on it creates a negative pressure inside the system which in turn evacuates the dissolved gas in the liquid. The agitation helps in removing the gas at a faster rate and the loss of pure component as vapor was prevented by condensing the vapor, the condensation was achieved by using a vapor trap (d) placed inside an ice bath. The degassing process was carried out until the bubbles stops appearing from the pure component liquid and the process take about five to ten minutes for each pure component.

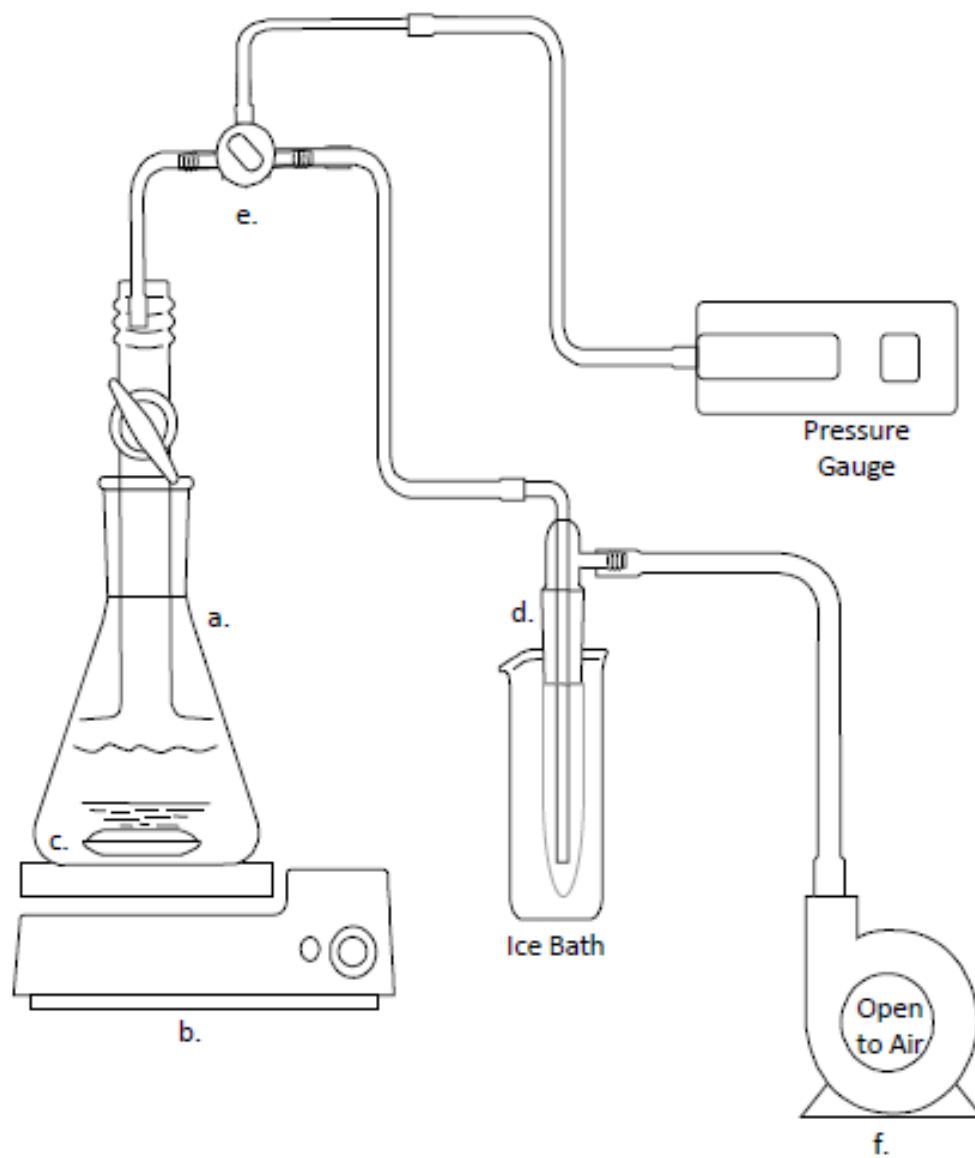


**Figure 3.1 Hassan (2010) Schematic diagram of Vacuum pump degassing method**

a. Sample flask; b. Magnetic stirrer; c. Magnetic bar; d. Vacuum Trap; e. 3-Way valve;

Vacuum pump

### 3.2 Flow microcalorimeter

An LKB 10700-1 flow microcalorimeter is used in this research work and the prototype of this calorimeter is the one which Monk and Wadsö (1968) used for determining the heat of dilution of aqueous electrolyte. Harsted and Thomsen (1974) reviewed the calorimeter prototype and made some modifications to the Monk and Wadsö (1968) model and achieved more accurate results. Later Tanaka *et al.* (1975) made several changes in the operating techniques which are as follows

- i. Degassing the chemicals,
- ii. Modification of the auxiliary parts namely using large cooling coils for an improved air bath temperature control.
- iii. Digitalized measurement of the thermopile response and calibration heater circuit current and a modified pump construction for satisfactory flow system.

Kimura *et al.* (1983) achieved more accurate excess molar enthalpy measurements with further modifications in the calorimeter operating techniques.

### 3.2.1 Calorimeter construction and modifications.

The figure below is the schematic representation of the LKB-Flow microcalorimeter (Model 10700-1)

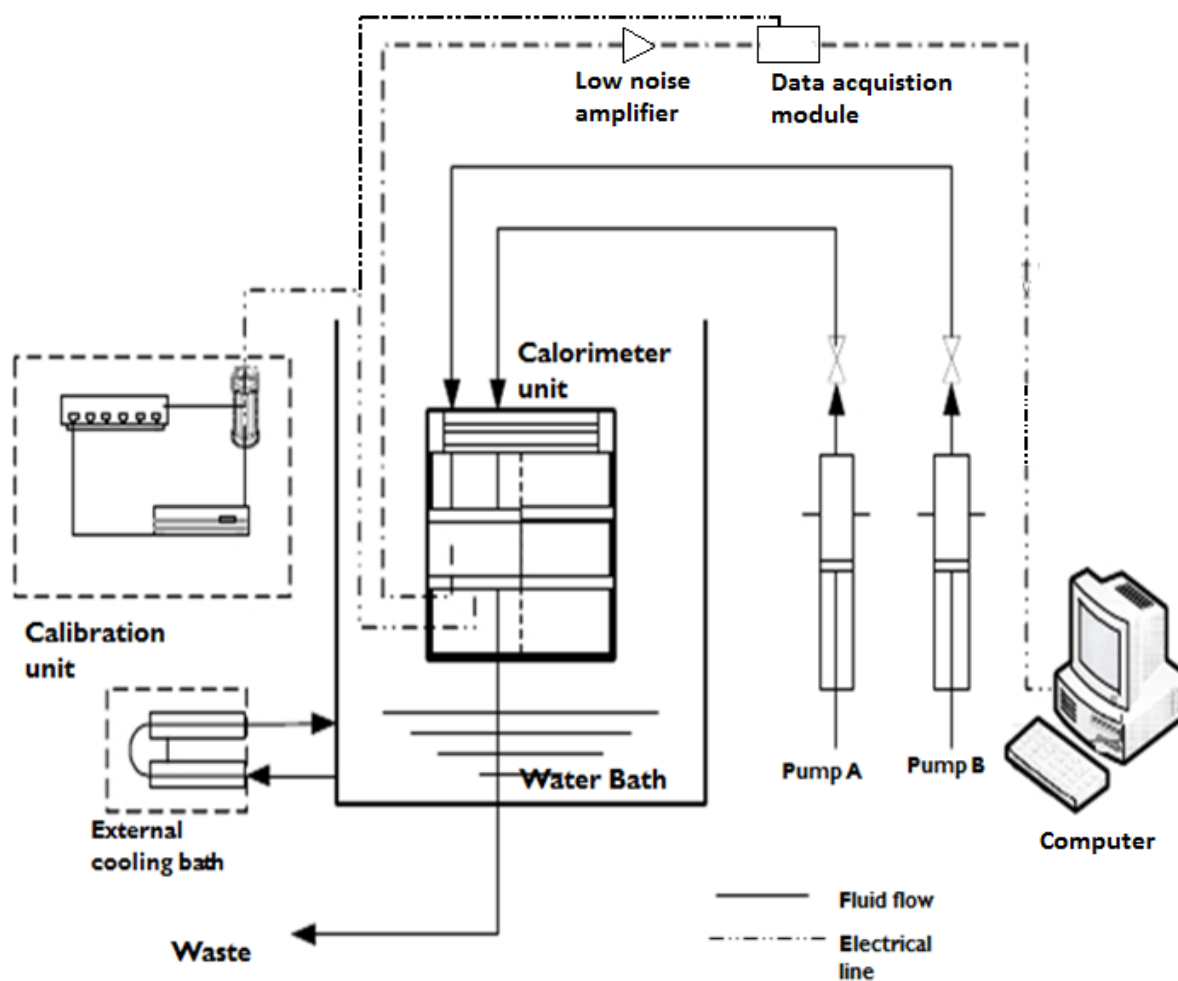


**Figure 3.2.** Modified from Hassan (2010), schematic representation of LKB flow microcalorimeter (10700-1)

The calorimeter unit (Figure 3.3) consists of two compartments: one is a mixing cell and another is a reference cell. The cells are enclosed in a heat sink and sandwiched between two thermopiles (thermocouples connected in series), the thermopiles are placed in a close contact with the mixing cell and a calorimeter calibration heater circuit is connected to this unit. The calibration heater circuit consists of a DC power supply along with a standard resistance ( $10\ \Omega$ ) connected to the calibration heater.

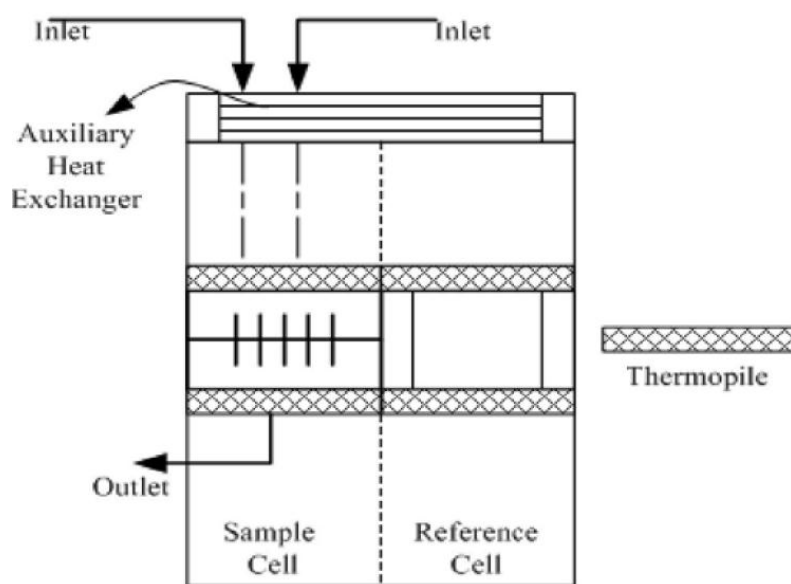


**Figure 3.3.** Schematic diagram of the calorimeter unit, (Hassan, 2010)

The calorimeter is placed in a constant temperature water bath, whose temperature is controlled by a heater (PF Hetotherm) and a coolant (VWR temperature controller) unit. The temperature of the water bath is maintained at  $\pm 0.005\ ^\circ\text{C}$  and it is monitored by a thermometer (HP, Model-2804A).

## Syringe pump and motor controller

The chemicals flow through the Teflon tubing at specified flow rate into the calorimeter cell by means of two precision positive displacement syringe pumps. The pump consists of a stainless steel piston (1.59cm OD) which pushes the working fluids through a kovar glass syringe surrounded by a water jacketed glass cylinder (1.90cm ID). The piston is moved by a precision screw which is rotated by a three stage planetary gearbox (99.705:1) connected to a stepper motor. The stepper motor controls the movement of the pistons through precision screws

The variable speed DC motor used by Tanaka *et al.* (1975) were replaced with a regulating stepper motor (Phidgets Inc 3319 nema 17) which is driven by Applied Motion products with STR2 driver set to 5000 pulses per revolution. A microprocessor and a precision frequency generator are used to apply an adjustable frequency to the driver set in order to control the motor speed. The pulses per second applied to the driver are measured by a separate circuit and displayed in counts per second, 10 second average and total counts.

The number of counts of the motor shaft is measured by means of a highly advanced internal encoder built inside the motor, and the uncertainty of the motor speed control is  $\pm 0.5$  count/sec. There are two sets of buttons to control the motor speed: one set is to increase/decrease the motor speed by 100 counts and the second set is used to fine tuning. By adjusting the speed of the individual pumps, mixing at variable compositions can be accomplished. The other auxiliary parts include a refrigerated circulating bath for water bath temperature control.

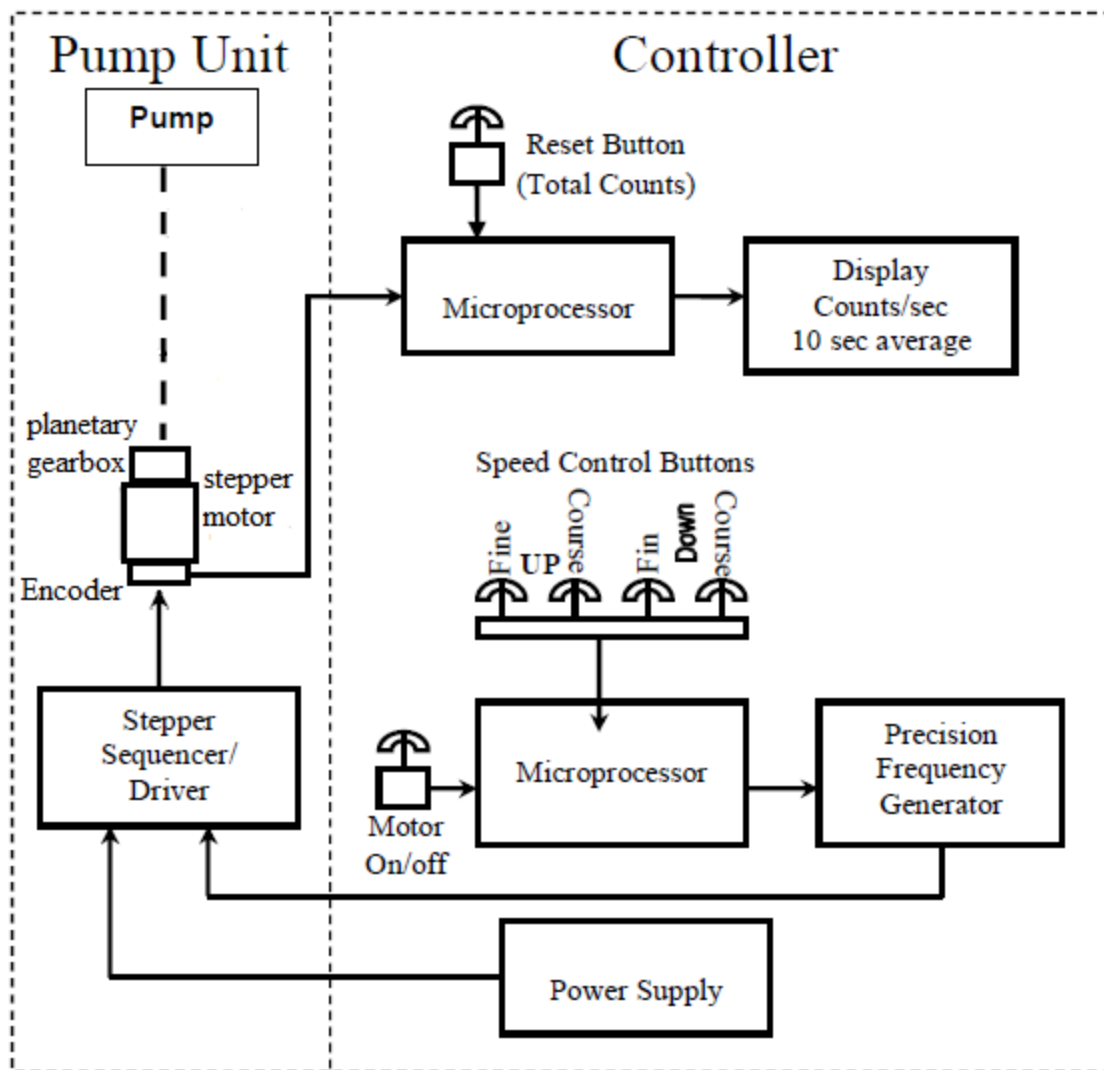


**Figure 3.4.** Schematic diagram of pump control system (Courtesy: Rlee Prokopishyn)

#### Mixing of fluids and data acquisition

The working fluids are initially degassed by means of vacuum pump system in order to avoid gas bubble formation during the mixing run. The fluids are conveyed into the mixing cell at specific flow rate by means of the pumps running at specific speed. Before reaching the

mixing cell the fluids are brought to the working temperature through the temperature control system consisting of heat exchangers. Heat arising from the mixing of the fluids is transported from the mixing cell to the surrounding thermopile by heat conduction. The thermopile reflects this temperature as electrical signals and these signals are processed by a data acquisition system which consists of an amplifier, a digital signal converter (National instruments USB 6008 acquisition model) and a computer software (National instrument labview 8.5.1 software). The electrical signals are amplified by the amplifier, the amplifier does a differential amplification up to 2500 times and the amplified signals are fed into a Digital signal converter which converts the amplified signal into a digital signal and finally the digitalized signal is fed into the computer. Through the software, this digitalized signal is observed as the real time thermopile voltage and it is recorded at fixed intervals and an average of 100 data points was taken as the final voltage of the mixture  $E_M(Q)$ .

The following table shows a brief summary of the modifications that have been done on the calorimeter.

**Table 3.2.** Modifications of the calorimeter

	<b>Tanaka et al</b>	<b>Nazmul</b>	<b>Present work</b>
<b>Motor</b>	Variable speed DC motor	Stepper motor	Stepper motor
	(Bodine Electric, Type NSH-12)	Lin Engineering Model WO-4118S-01	Phidgets Inc 3319 Nema 17
<b>Motor speed measurement</b>	120 equally photo masked sector passing through photo sensor	180 photo masked sector	Inbuilt internal encoder
<b>Motor speed control</b>	Feedback circuit system	Microprocessor controlled	Microprocessor controlled
<b>Data acquisition system</b>	1) Keithly 150B amplifier	1) NUDAM, ND-6011 amplifier	1) 804208 low noise amplifier
	2) Texas Instruments, servo/riter II recorder	2) NUDAM, ND-650 digital signal converter	2) National instruments USB 6008 acquisition model
	3) Digital measurements 2001 voltmeter		
<b>Motor speed Uncertainty</b>	$\pm 3.0$ counts/s	$\pm 1.0$ counts/s	$\pm 0.5$ counts/s

### 3.2.2 Calorimeter Calibration

Calibration is essential for all the type of calorimeters which are used to measure the excess molar enthalpy values. The calibration step must be performed prior to the mixing run and the calibration constants should be calculated. The calibration constants relate the thermoelectric output and the heat effect associated with it when there is no mixing of fluids inside the mixing cell. It is carried out for individual liquids flowing from each pump into the mixing cell. The calibration is done by two ways: chemical and electrical. Chemical calibration method was prone to sensitivity variation Rodríguez de Rivera and Socorro (2007) so in this study the electrical calibration method was practiced. The working fluids are pumped at specific flow rate and the average baseline voltage  $E_Q^o$  is recorded, now the calibration heater is turned on and the baseline voltage changes and the average value of the baseline voltage  $E_Q$  are recorded.

The calibration unit (Figure 3.4) consists of a constant DC voltage power supply (Trygon PLS 50-1), a calorimeter heater  $r_s$  (10.0  $\Omega$ ), and a calorimeter heater  $r_c$  (49.52  $\Omega$ ) all connected in series connection. The potential across the resistance and the current passing through the heater are measured and recorded through the National instrument labview 8.5.1 software.

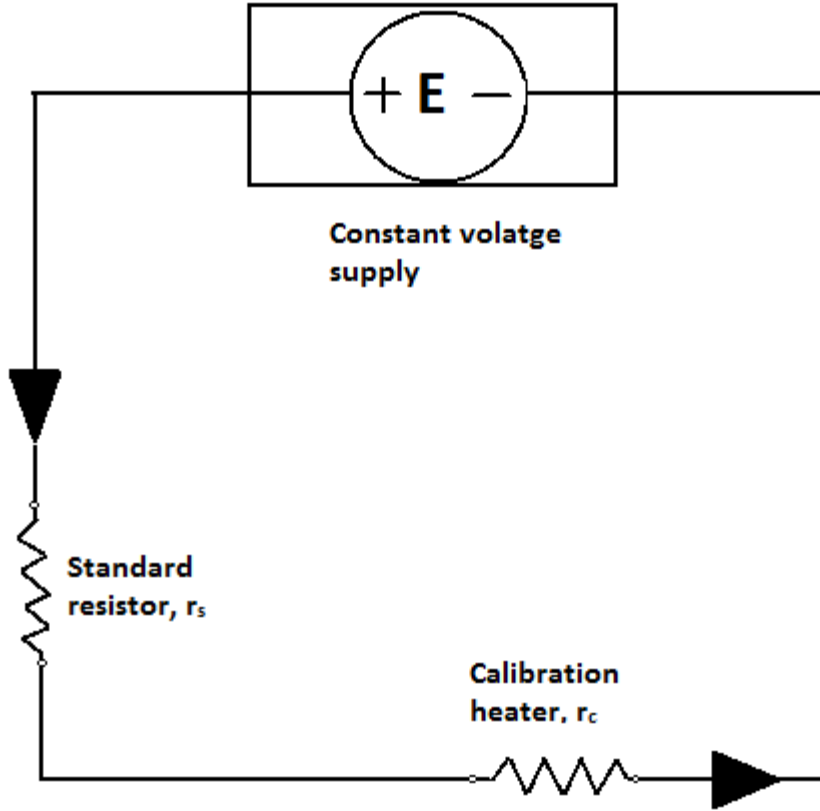


**Figure 3.5.** Calibration circuit diagram, (Hassan, 2010)

The calibration constant  $\varepsilon$  is then calculated from the equation

$$\varepsilon = \frac{I^2 r_c}{E_Q^0 - E_Q} \quad (3.1)$$

where  $I$  is the current flowing through the heater,  $r_c$  is the resistance of the heater. A graph is plotted between the  $\varepsilon$  and the motor speed  $R$  (counts/sec) and from the plot an expression for calibration constant in relation with motor speed  $R$  (counts/sec) is obtained. This is of the form

$$\varepsilon = k_0 + k_1 R \quad (3.2)$$

Where  $k_0$  and  $k_1$  are constants for the given liquid

### 3.2.3 Verification of the calorimeter

The calorimeter verification step is essential because it ensures that the calorimeter is reliable for making excess molar enthalpy measurements. Any experimentally measured  $H^E$  will have uncertainty which has the source, mainly from the calorimeter and the impurities of the chemicals used for the study. In order to avoid any uncertainty caused by the calorimeter, the calorimeter verification step is carried out. In this research work we measured the excess molar enthalpy values of Ethanol (1) + n-Hexane (2) binary system at 298.15K and compared our results with the other researchers who measured excess molar enthalpy of the same binary system at same conditions. For this purpose we compared our results with O'Shea and Stokes, (1986) who measured the heat of mixing of Ethanol + n-Hexane system and published the most complete set of data and it is taken as main reference system. However the obtained result was also compared with the data from Wang *et al.* (1992), Mato *et al.* (2006) and Hassan (2010).

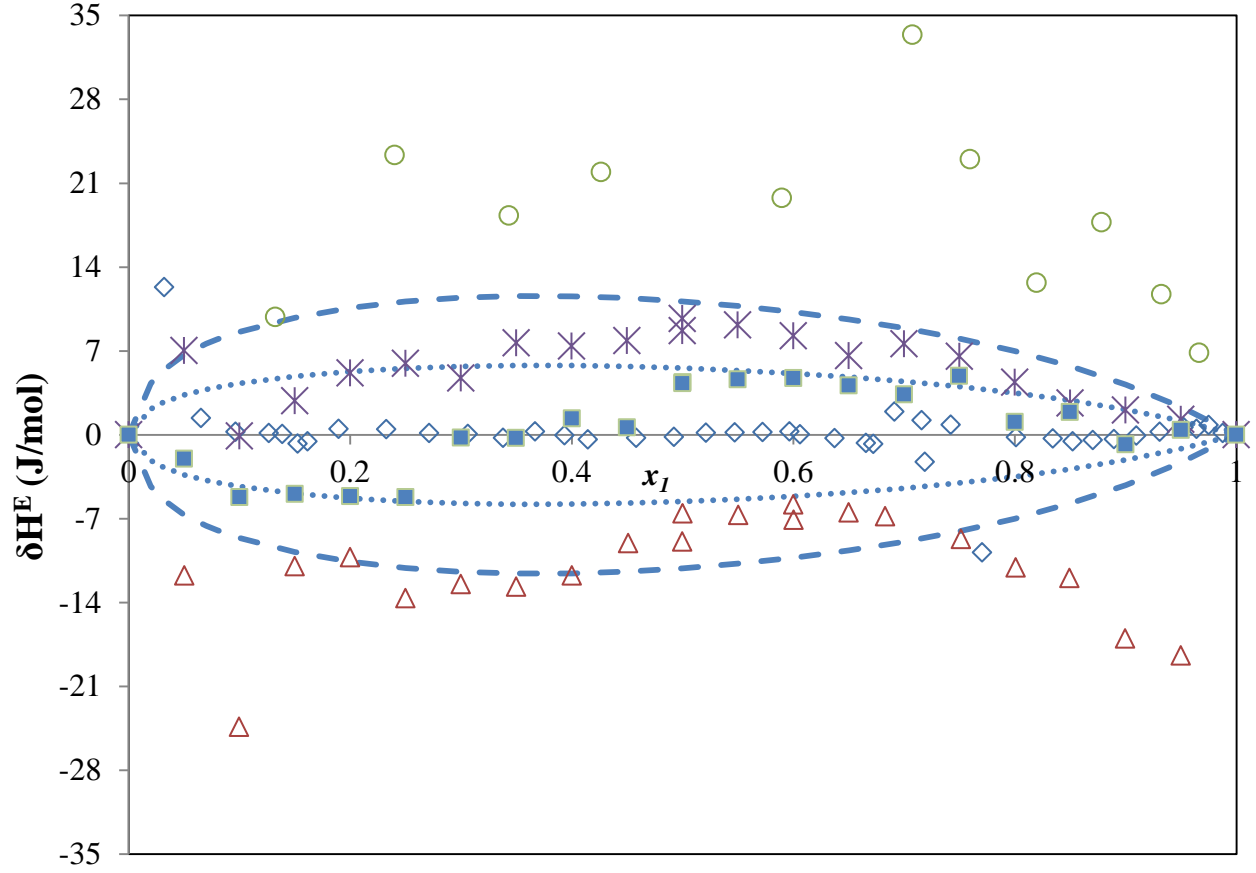


**Figure 3.6.** Deviations of the excess molar enthalpy at 298.15K for  $x_1$  ethanol (1) +  $x_2$  n-Hexane (2) plotted against molefraction  $x_1$ . Experimental results: \*, Present work;  $\diamond$ , O'Shea and Stokes;  $\Delta$ , Wang *et al*;  $\circ$ , Mato *et al*;  $\blacksquare$ , Hassan; Curves: ..... ,  $\pm 1\%$  and - - - - ,  $\pm 2\%$  from equation 3.3

$$H_m^E / (J \cdot mol^{-1}) = x_1(1 - x_1) \{1 + 0.96(2x_1 - 1)\}^{-1} \{2227.55(2x_1 - 1) + 1472.22(2x_1 - 1)^2 + 470.59(2x_1 - 1)^3 + 641.92(2x_1 - 1)^4 + 212.41(2x_1 - 1)^5\} \quad (3.3)$$

The deviation of the experimental results from the smoothed results of O'Shea and Stokes are plotted. The figure 3.6 shows that the average deviation of the present data is  $\pm 1.5\%$  from the enthalpy calculated using the O'Shea and Stokes correlation.

### **3.3 Calorimeter operational procedure**

#### **3.3.1 Binary system**

Before the start of any calibration or mixing run, the water bath is maintained at  $25.000 \pm 0.005^\circ\text{C}$  for at least 24 hours. For a binary mixing run, the degassed component liquids are pumped into the calorimeter mixing cell at specific flow rate by means of pump A and pump B. The combined flow rate of the pumps gives a total displacement of  $0.005 \text{ cm}^3/\text{sec}$ . By adjusting the motor speed of the pumps, desired mole fraction of the mixtures can be achieved.

The mixing run for both binary and ternary mixtures are always started at equimolar molefraction (i.e.  $x_1 = 0.5$ ) and completed at  $x_1 = 0.05$  and then the second half of the measurements was started at  $x_1 = 0.5$  and ended by measuring the enthalpy for the molefraction  $x_1 = 0.95$ . The excess molar enthalpy value for the molefraction  $x_1 = 0.5$  was measured twice just to make sure the repeatability of the experiment. The thermopile voltage for every individual experimental point is the average value calculated from 100 data points recorded over a period of time. The calibration and mixing run procedure is explained in detail in Appendix D

The thermopile voltage reading for the pure component liquids (i.e.  $x_1 = 1.0$  and  $x_1 = 0.0$ ) are taken as the baseline voltage  $E_1^0(Q_1)$  and  $E_2^0(Q_2)$ . The baseline voltage for the mixture was given by the equation by Tanaka *et al.* (1975)

$$E_M^0(q) = \phi_1 E_1^0(Q) + \phi_2 E_2^0(Q) \quad (3.4)$$

where  $\phi_i = \frac{Q_i}{\sum_j Q_j}$  and it is the volume fraction of the component  $i$

The excess molar enthalpy values are calculated from the thermopile voltage using the following equation given by Tanaka *et al.* (1975)

$$H_m^E = \frac{\varepsilon_M [E_M(Q) - E_M^0(Q)]}{(Q_1/V_{m1} + Q_2/V_{m2})(Q_1 + Q_2)} \quad (3.5)$$

where  $V_{m_i}$  represents the molar volume of the pure component  $i$  and  $E_m(Q)$  is the observed thermopile voltage for the specific mixing run composition..

In the equation 3.5 ' $\varepsilon_M$ ' refers to the mixture calibration constant and it is calculated from the calibration constant  $\varepsilon_i$  and flow rates of the pure components and the expression for mixture calibration constant is given as follows

$$\varepsilon_M / (J.V^{-1}cm^3) = Q_1 \varepsilon_1 + Q_2 \varepsilon_2 \quad (3.6)$$

The procedure followed in calculating the excess molar enthalpy for the binary mixtures is explained in detail in Appendix B

### 3.3.2 Ternary system

Before measuring the ternary excess molar enthalpy, all three binary excess molar enthalpy values involving the constituent species are measured first. i.e., component 1 + (component 2 and 3), and component 2 + component 3 and the experimental values are fitted with the Redlich-Kister polynomial equation. Three separate binary liquid mixtures with fixed composition are prepared using component 2 and 3, such that the molefraction ratio of the prepared mixtures are  $x_2/x_3 = (0.25/0.75), (0.5/0.5), (0.75/0.25)$  respectively, and these mixtures are termed as pseudo-pure component. The excess molar enthalpy  $H_{m,1+23}^E$  are measured by mixing component 1 with the three pseudo-pure components separately, since the resulting mixture from mixing component 1 + component (2+3) are not pure components, they are called pseudo-binary mixtures. Measurement of  $H_{m,1+23}^E$  is same as the measurement of binary excess molar enthalpy, component 1 is taken in pump A and the pseudo-pure liquid is taken in pump B and the procedure for the calculation of excess molar enthalpy is same as that of binary system.

Ternary excess molar enthalpy  $H_{m,123}^E$  was calculated from the excess molar enthalpy values of the pseudo-binary mixture, using the following equation.

$$H_{m,123}^E = H_{m,1+23}^E + (1 - x_1)H_{m,23}^E \quad (3.7)$$

In the above equation  $H_{m,23}^E$  is the excess molar enthalpy of the specific binary mixture and  $x_1$  being the molefraction of component 1.

## Pseudo-Binary mixture preparation

Preparation of pseudo-pure component requires accurate weight measurements of pure components. To make accurate weight measurements Mettler H315 precision balance was used in this study, the balance has a 1000g weight range and 0.1mg precision range. For preparing the mixture pure dehydrated and degassed component 2 and 3 was taken. A pre-calculated amount of component 2 was measured and taken in a flask, and then a pre-calculated amount of component 3 was measured and poured into the same flask. A magnetic bar is slipped into the flask and placed on a magnetic stirrer and the liquid mixture is stirred for complete mixing of the components.

Prior to mixture preparation, the temperature and humidity values of the room were noted in order to do the weight correction due to buoyancy.

## Pre-estimation of weights

Before the pseudo-pure component was prepared, calculations were made in order to prepare pseudo-pure mixture of desired composition and quantity. Using the density of the pure liquids and their molecular weights, it is possible to calculate the molefraction of the final mixture and the quantity using the following equation.

$$\text{molefraction } x_1 = \frac{n_1}{n_1+n_2} \quad \text{and } x_2 = \frac{n_2}{n_1+n_2} \quad (3.8)$$

where  $n_1$  and  $n_2$  are the number of moles of component 1 and 2 respectively and

$$n_1 = \frac{\frac{m_1}{M_1}}{\left(\frac{m_1}{M_1} + \frac{m_2}{M_2}\right)} \text{ and } n_2 = \frac{\frac{m_2}{M_2}}{\left(\frac{m_1}{M_1} + \frac{m_2}{M_2}\right)} \quad (3.9)$$

where  $m_i$  and  $M_i$  are the estimated mass and molecular weight of the component  $i$ , and the mass of the compounds can be expressed as

$$m_i = \rho_i V_i \quad (3.10)$$

where  $\rho_i$  and  $V_i$  are the density and volume of the component  $i$

Using the excel solver function, the mass of the component 1 and 2 was calculated for preparing a mixture of specific composition.

### **Weight Correction**

When weight measurements are carried out on any analytical balance, the object for which the weight measured encounters the buoyancy effect of the surrounding air Bauer (1959). Therefore the weight measurements should be adjusted for the buoyancy effect in order to avoid error caused by the buoyancy effect of the air, Bauer (1959) explained a method for correcting the weights measured in a fluid environment to vacuum condition. The molefraction and molecular weight of the mixtures are calculated after correcting the weights to vacuum. The details of the Bauer's method and a sample calculation are given in Appendix B2.

## 4.0 RESULTS AND DISCUSSION

In this chapter the experimental excess molar enthalpy values of the 15 binary systems and 9 ternary systems are presented and discussed. The correlation of experimental results with the Redlich-Kister polynomial equation, the Liebermann-Fried model and the Tsao-Smith equation are also presented and discussed.

### 4.1 Experimental excess molar enthalpy

Table 4.1 shows the 15 binary systems studied and table 4.2 to 4.3 shows the measured experimental excess molar enthalpy values.

**Table 4.1.** List of binary systems studied in the research work

S.No	Binary system	
1	2-MTHF	Ethylbenzene
2		Mesitylene
3		<i>p</i> -Xylene
4		2-ME
5		DNBE
6	2-ME	Ethylbenzene
7		Mesitylene
8		<i>p</i> -Xylene
9	1-Butanol	Ethylbenzene
10		Mesitylene
11		<i>p</i> -Xylene
12	DNBE	Ethylbenzene
13		Mesitylene
14		<i>p</i> -Xylene
15	Ethylbenzene	Mesitylene

**Table 4.2.** Experimental molefraction  $x_i$  and excess molar enthalpy values  $H_{m,i,j}^E$ (J/mol) at 298.15K for the binary systems

$x_i$	$H_{m,i,j}^E$	$x_i$	$H_{m,i,j}^E$	$x_i$	$H_{m,i,j}^E$	$x_i$	$H_{m,i,j}^E$
<b>2-MTHF (i) + EBz (j)</b>							
0.0500	-35.5	0.3002	-163.3	0.5001	-200.7	0.7500	-156.5
0.1000	-67.9	0.3499	-178.8	0.5502	-200.2	0.8000	-134.1
0.1500	-95.5	0.3999	-190.1	0.5998	-195.6	0.8497	-108.4
0.2004	-122.3	0.4499	-197.7	0.6502	-186.7	0.9000	-76.7
0.2501	-144.4	0.5001	-201.2	0.7001	-173.8	0.9502	-41.3
<b>2-MTHF (i) + <i>p</i>-Xylene (j)</b>							
0.0500	-38.7	0.2999	-173.5	0.4999	-209.5	0.7500	-159.4
0.1000	-72.9	0.3499	-188.8	0.5499	-207.9	0.8001	-135.9
0.1499	-103.7	0.3999	-199.9	0.5999	-202.2	0.8500	-109.1
0.2002	-131.1	0.4498	-206.8	0.6501	-192.5	0.9000	-77.0
0.2501	-154.5	0.5001	-209.5	0.7000	-178.0	0.9500	-40.4
<b>2-MTHF (i) + Mesitylene (j)</b>							
0.0500	2.5	0.3000	15.8	0.5001	23.8	0.7501	22.9
0.1000	5.3	0.3502	18.1	0.5500	24.8	0.8001	20.6
0.1500	7.8	0.4001	20.2	0.6002	25.1	0.8500	17.2
0.1999	10.1	0.4502	21.9	0.6499	25.0	0.9000	12.8
0.2498	13.2	0.5001	23.4	0.6999	24.3	0.9500	7.2
<b>2-ME (i) + 2-MTHF (j)</b>							
0.0500	117.6	0.3001	416.9	0.5001	448.7	0.7499	312.9
0.1000	212.3	0.3499	442.1	0.5501	436.3	0.8000	259.1
0.1500	285.9	0.3999	451.6	0.6002	414.2	0.8499	205.8
0.2000	343.8	0.4501	454.7	0.6501	386.1	0.9000	143.4
0.2500	392.9	0.5001	450.8	0.6999	351.5	0.9500	74.5

**Table 4.3.** Experimental molefraction  $x_i$  and excess molar enthalpy values  $H_{m,i,j}^E$ (J/mol) at 298.15K for the binary systems

$x_i$	$H_{m,i,j}^E$	$x_i$	$H_{m,i,j}^E$	$x_i$	$H_{m,i,j}^E$	$x_i$	$H_{m,i,j}^E$
<b>2-ME (i) + <i>p</i>-Xylene (j)</b>							
0.0500	392.4	0.3000	784.0	0.5000	719.7	0.7500	447.9
0.1000	570.8	0.3500	785.2	0.5500	681.3	0.8000	372.3
0.1500	669.4	0.4000	773.6	0.6000	635.9	0.8500	288.0
0.2000	734.7	0.4500	750.7	0.6500	579.4	0.9000	197.8
0.2500	770.0	0.5000	712.0	0.7000	518.9	0.9500	101.5
<b>2-ME (i) + EBz (j)</b>							
0.0500	382.7	0.3001	757.3	0.5000	695.9	0.7500	433.8
0.1000	555.4	0.3500	758.3	0.5500	658.7	0.8000	359.8
0.1500	651.6	0.3999	748.2	0.6003	612.7	0.8501	280.2
0.1999	709.5	0.4499	727.8	0.6500	560.9	0.9000	192.2
0.2498	741.4	0.5000	699.4	0.6999	500.7	0.9500	99.9
<b>2-ME (i) + Mesitylene (j)</b>							
0.0500	436.0	0.2998	945.7	0.5000	938.1	0.7500	655.6
0.1000	641.2	0.3498	963.5	0.5498	904.5	0.8000	559.9
0.1500	772.9	0.4003	964.2	0.5999	857.4	0.8501	449.5
0.2001	856.9	0.4499	953.4	0.6498	799.5	0.9000	321.3
0.2500	914.4	0.5000	935.5	0.7000	734.3	0.9500	173.1
<b>EBz (i) + Mesitylene (j)</b>							
0.0500	29.0	0.3001	131.5	0.5000	159.2	0.7498	122.3
0.1000	55.4	0.3502	143.3	0.5500	158.1	0.7999	104.8
0.1500	79.0	0.3999	151.5	0.5999	154.1	0.8500	83.8
0.1999	98.9	0.4500	157.1	0.6498	146.8	0.9000	59.2
0.2501	116.8	0.5000	159.9	0.7000	136.3	0.9500	30.6

**Table 4.4.** Experimental molefraction  $x_i$  and excess molar enthalpy values  $H_{m_{i,j}}^E$ (J/mol) at 298.15K for the binary systems

$x_i$	$H_{m_{i,j}}^E$	$x_i$	$H_{m_{i,j}}^E$	$x_i$	$H_{m_{i,j}}^E$	$x_i$	$H_{m_{i,j}}^E$
<b>1-Butanol (i) + <i>p</i>-Xylene (j)</b>							
0.0500	538.3	0.3000	1012.2	0.5000	919.4	0.7500	518.5
0.1000	745.7	0.3500	1016.1	0.5500	860.3	0.8000	414.2
0.1500	866.4	0.4000	999.0	0.6000	789.3	0.8500	312.4
0.2000	940.8	0.4500	966.6	0.6500	704.9	0.9000	192.8
0.2500	989.3	0.5000	920.5	0.7000	616.2	0.9500	73.5
<b>1-Butanol (i) + Mesitylene (j)</b>							
0.0500	554.8	0.3000	1073.1	0.5000	1004.5	0.7500	611.0
0.1000	773.8	0.3500	1082.3	0.5500	949.9	0.8000	503.0
0.1500	905.1	0.4000	1073.1	0.6000	882.0	0.8500	385.9
0.2000	987.2	0.4500	1047.4	0.6500	803.5	0.9000	246.1
0.2500	1041.7	0.5000	1007.8	0.7000	711.2	0.9500	101.6
<b>1-Butanol (i) + EBz (j)</b>							
0.0500	547.6	0.3000	1052.1	0.5000	968.0	0.7500	558.8
0.1000	761.6	0.3500	1058.0	0.5500	908.3	0.8000	451.6
0.1500	889.3	0.4000	1045.7	0.6000	838.0	0.8500	339.9
0.2000	970.6	0.4500	1016.3	0.6500	755.7	0.9000	197.7
0.2500	1024.0	0.5000	969.3	0.7000	661.9	0.9500	78.9
<b>DNBE (i) + Mesitylene (j)</b>							
0.0500	4.9	0.3000	26.1	0.5000	35.8	0.7500	30.3
0.1000	9.4	0.3500	29.2	0.5500	36.3	0.8000	26.4
0.1500	13.7	0.4000	32.2	0.6000	36.1	0.8500	21.5
0.2000	18.3	0.4500	34.3	0.6500	34.9	0.9000	15.2
0.2500	22.2	0.5000	35.5	0.7000	33.1	0.9500	10.0

**Table 4.5.** Experimental molefraction  $x_i$  and excess molar enthalpy values  $H_{m,i,j}^E$ (J/mol) at 298.15K for the binary systems

$x_i$	$H_{m,i,j}^E$	$x_i$	$H_{m,i,j}^E$	$x_i$	$H_{m,i,j}^E$	$x_i$	$H_{m,i,j}^E$
<b>DNBE (i) + <i>p</i>-Xylene (j)</b>							
0.0500	-7.8	0.3000	-31.5	0.5000	-34.1	0.7500	-23.1
0.1000	-14.7	0.3500	-33.4	0.5500	-33.2	0.8000	-18.6
0.1500	-20.0	0.4000	-34.3	0.6000	-31.3	0.8500	-13.8
0.2000	-25.0	0.4500	-34.7	0.6500	-29.2	0.9000	-8.7
0.2500	-28.8	0.5000	-34.4	0.7000	-26.3	0.9500	-3.9
<b>DNBE (i) + 2-MTHF (j)</b>							
0.0500	38.2	0.3000	155.4	0.5000	172.8	0.7500	120.2
0.1000	71.3	0.3500	165.8	0.5500	169.4	0.8000	99.5
0.1500	99.0	0.4000	171.8	0.6000	163.9	0.8500	75.2
0.2000	122.2	0.4500	174.7	0.6500	150.5	0.9000	48.9
0.2500	140.2	0.5000	174.3	0.7000	137.7	0.9500	20.9
<b>DNBE (i) + EBz (j)</b>							
0.0500	23.1	0.3000	87.7	0.5000	92.9	0.7500	61.0
0.1000	42.2	0.3500	92.2	0.5500	89.5	0.8000	49.2
0.1500	58.2	0.4000	94.5	0.6000	84.8	0.8500	36.7
0.2000	71.0	0.4500	95.1	0.6500	77.4	0.9000	22.4
0.2500	80.8	0.5000	92.9	0.7000	69.6	0.9500	8.7

## 4.2 Representation of binary excess molar enthalpy

The experimental excess molar enthalpy values measured for the 15 binary systems are correlated using the Redlich - Kister polynomial equation and predicted using the Liebermann - Fried solution theory model.

### 4.2.1 Correlation by means of Redlich - Kister polynomial equation

The experimental excess molar enthalpy is fitted to Redlich - Kister (RK) polynomial equation (eqn 4.1) by means of unweighted least square method and the equation has the expression

$$H_m^E / (J \cdot mol^{-1}) = x_1(1 - x_1) \sum_{k=1}^p h_k (1 - 2x_1)^{k-1} \quad (4.1)$$

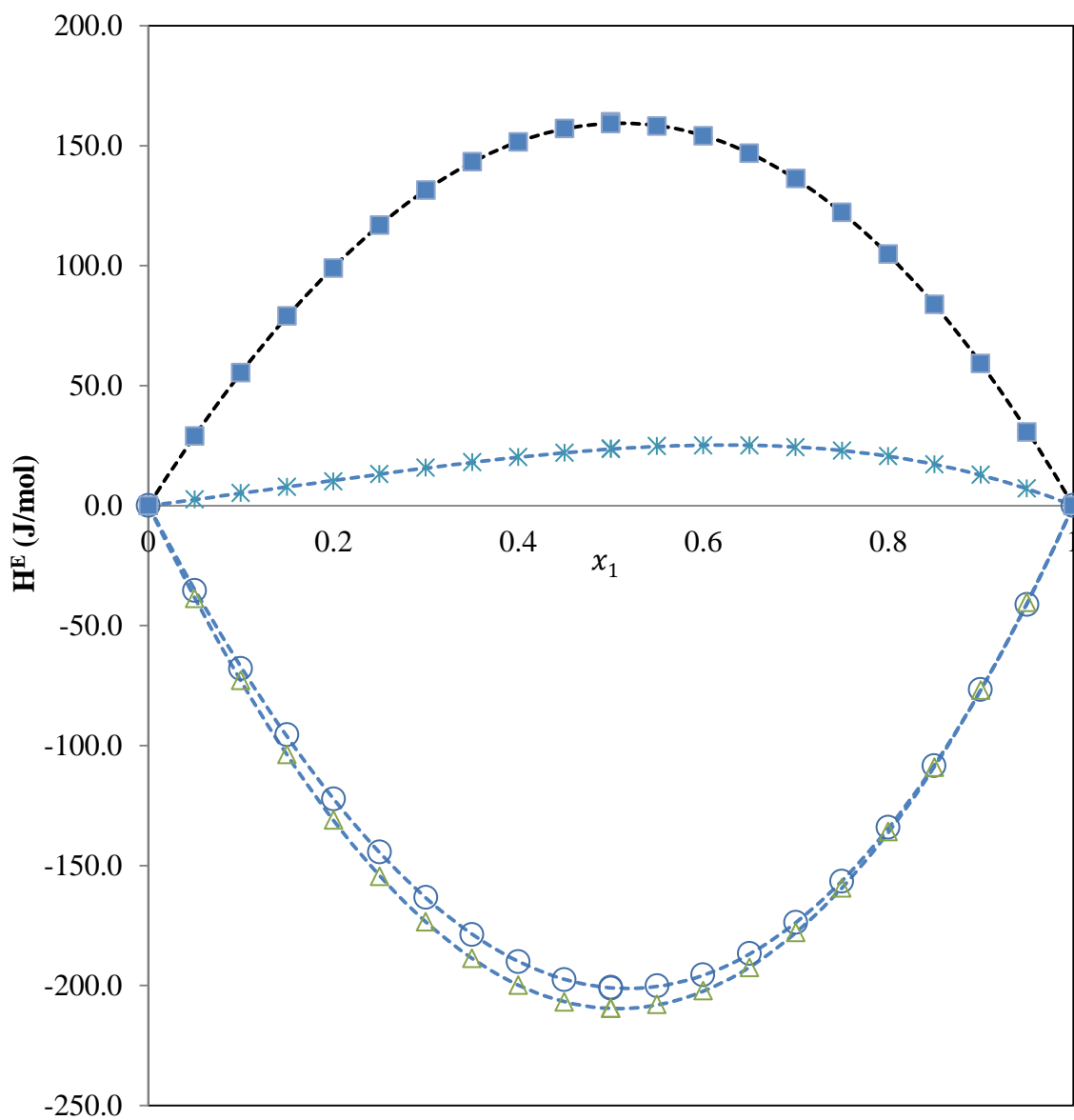
where, coefficient  $h_k$  is the adjustable parameter and it is determined by minimization of the standard deviation 's' of the estimates.

$$\text{Standard deviation } s = \sqrt{\frac{\sum_{r=1}^n (H_{exp,r}^E - H_{cal,r}^E)^2}{(n-p)}} \quad (4.2)$$

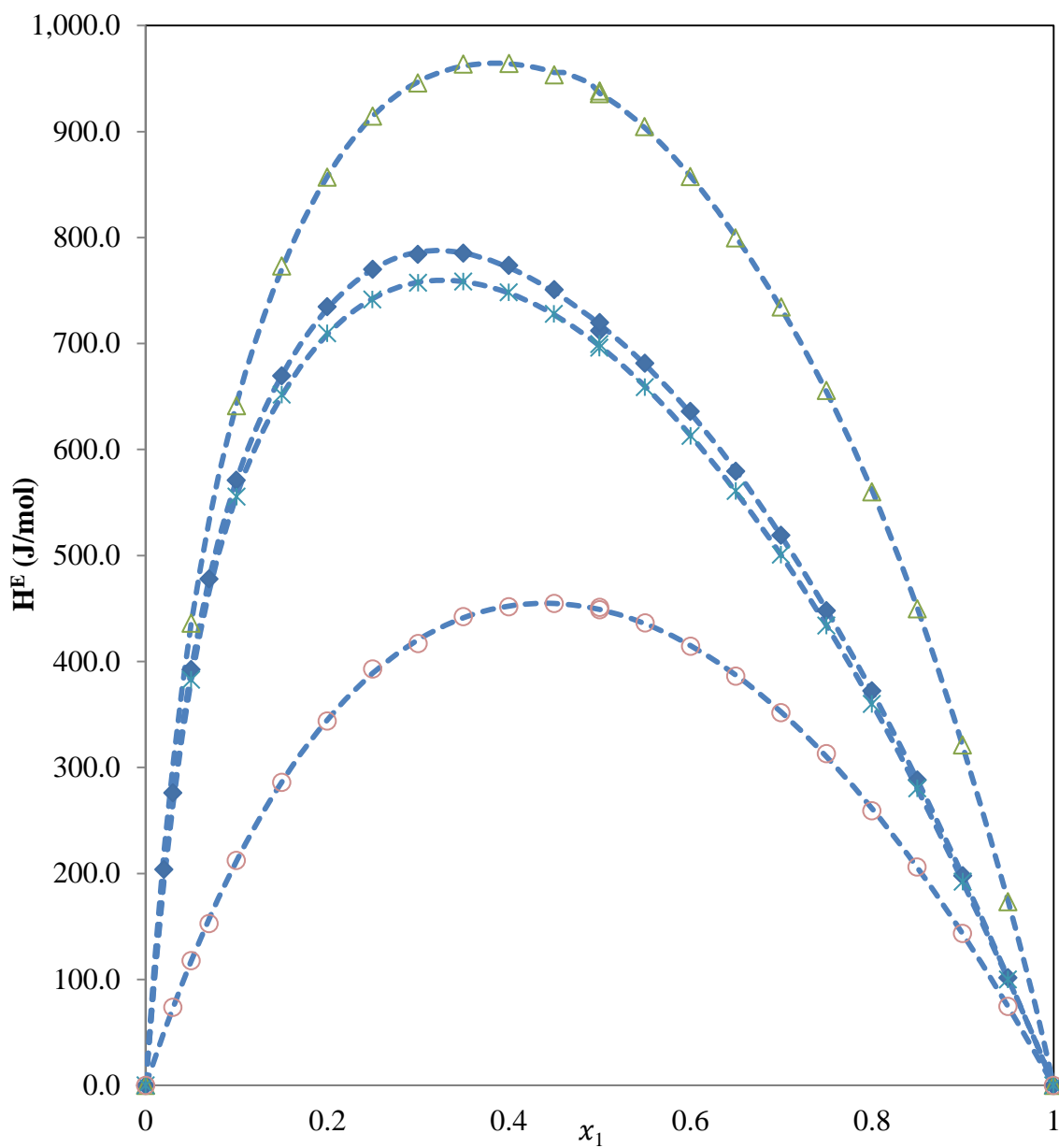
Where  $H_{exp}^E$  and  $H_{cal}^E$  is the experimental and calculated excess molar enthalpy value respectively and  $n$  is the number of data points and  $p$  is the number of parameters used in the polynomial. The total number of parameters corresponding to the best fit is determined by means of 'F' test. The details of F-test and a sample calculation are explained in Appendix C1. Table 4.6 shows summary of the fitting with the total number of parameters and the standard error for all the binary system.

**Table 4.6.** Coefficients  $h_k$  of the Redlich Kister polynomial equation calculated for the binary systems and the standard error 's'

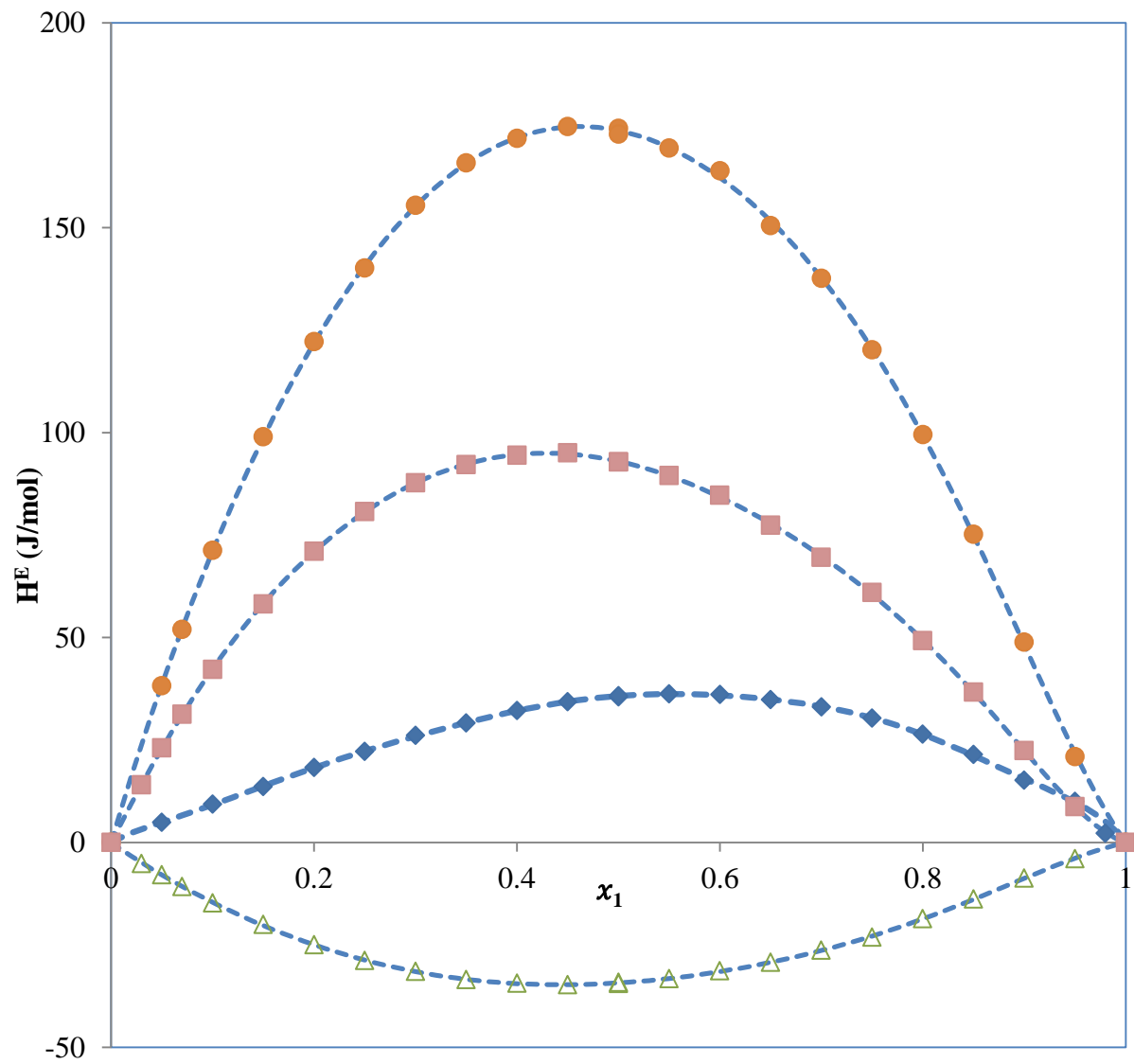
Component		$h_1$	$h_2$	$h_3$	$h_4$	$h_5$	$h_6$	$h_7$	$h_8$	$h_9$	$h_{10}$	$s$ J/mol
1	2											
2-MTHF	EBz	-803.65	59.67	4.97	12.35	-	-	-	-	-	-	0.38
2-MTHF	<i>p</i> -Xylene	-838.19	26.72	7.78	-	-	-	-	-	-	-	0.20
2-MTHF	Mesitylene	94.16	-52.47	7.82	-	-	-	-	-	-	-	0.15
2-ME	2-MTHF	1796.16	382.91	272.53	148.05	-	-	-	-	-	-	1.80
2-ME	<i>p</i> -Xylene	2872.36	1367.39	1408.97	1641.71	277.37	-1956.21	-103.13	3730.21	2449.78	-	2.40
2-ME	EBz	2790.7	1350.67	1057.72	1195.21	1604.89	-768.85	-2042.33	2790.28	3394.36	-	1.20
2-ME	Mesitylene	3743.98	1038.43	1160.81	1753.06	3662.42	-2478.46	-6770.85	4189.82	6788.19	-	1.81
EBz	Mesitylene	637.21	-27.59	-	-	-	-	-	-	-	-	0.29
1-Butanol	<i>p</i> -Xylene	3681.44	2152.02	961.51	990.14	1841.66	2894.36	-2033.86	-6537.55	4273.76	9429.40	1.90
1-Butanol	Mesitylene	4025.57	1950.53	1070.32	872.34	2407.86	3037.62	-3064.38	-6174.51	4754.26	9127.98	2.00
1-Butanol	EBz	3879.45	2072.87	878.87	2083.99	3150.09	-3988.52	-5812.00	8157.50	6953.59	-	3.50
DNBE	Mesitylene	142.95	-37.16	-39.00	-67.00	248.45	220.63	-655.24	-207.64	534.01	-	0.20
DNBE	<i>p</i> -Xylene	-136.98	-30.87	-9.72	7.16	33.05	-34.52	-	-	-	-	0.14
DNBE	2-MTHF	694.79	102.52	42.36	-18.18	-142.86	165.70	-	-	-	-	0.73
DNBE	EBz	372.03	109.29	19.23	-42.28	28.52	137.78	-136.79	-	-	-	0.26



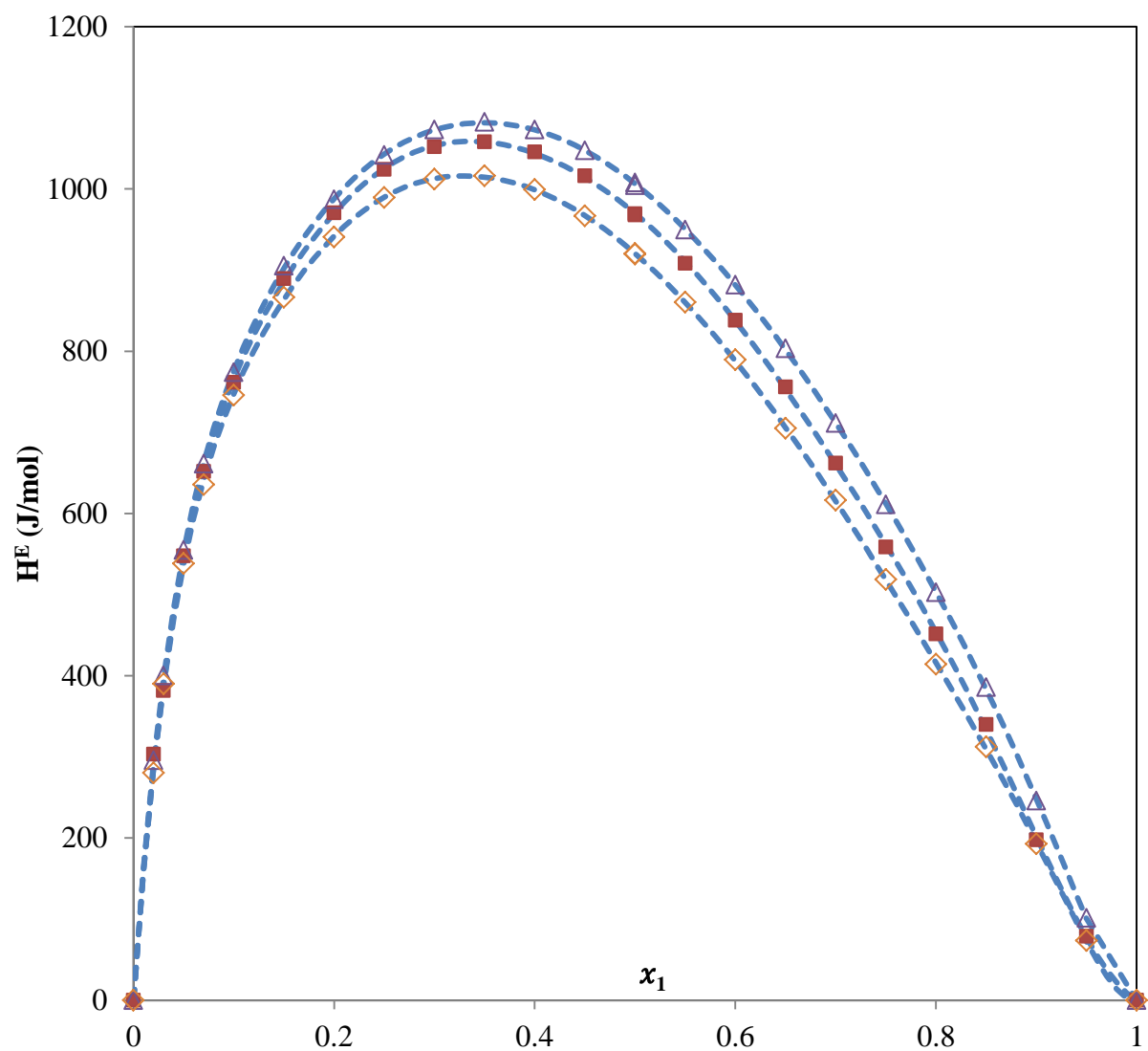
Excess molar enthalpies  $H_{m,ij}^E$  for the binary systems at 298.15K. Experimental results: ■,  $x_1$  EBZ +  $(1 - x_1)$  Mesitylene; \*,  $x_1$  2-MTHF +  $(1 - x_1)$  Mesitylene; ○,  $x_1$  2-MTHF +  $(1 - x_1)$  EBz; △,  $x_1$  2-MTHF +  $(1 - x_1)$  *p*-Xylene: Curves: ..... , calculated by the Redlich - Kister polynomial equation



Excess molar enthalpies  $H_{m,ij}^E$  for the binary systems at 298.15K. Experimental results:  $\Delta$ ,  $x_1$  2-ME + Mesitylene ( $1 - x_1$ );  $\blacklozenge$ ,  $x_1$  2-ME + ( $1 - x_1$ ) *p*-Xylene; \*,  $x_1$  2-ME + ( $1 - x_1$ ) EBz;  $\circ$ ,  $x_1$  2-ME + ( $1 - x_1$ ) 2-MTHF; Curves: ..... , calculated by the Redlich - Kister polynomial equation



Excess molar enthalpies  $H_{m,ij}^E$  for the binary systems at 298.15K. Experimental results:  $\circ$ ,  $x_1$  DNBE + 2-MTHF ( $1 - x_1$ );  $\blacksquare$ ,  $x_1$  DNBE + ( $1 - x_1$ ) EBZ;  $\blacklozenge$ ,  $x_1$  DNBE + ( $1 - x_1$ ) Mesitylene;  $\triangle$ ,  $x_1$  DNBE + ( $1 - x_1$ ) *p*-Xylene: Curves: ..... , calculated by the Redlich - Kister polynomial equation



Excess molar enthalpies  $H_{m,ij}^E$  for the binary systems at 298.15K. Experimental results:  $\Delta$ ,  $x_1$  1-Butanol + Mesitylene ( $1 - x_1$ );  $\blacksquare$ ,  $x_1$  1-Butanol + ( $1 - x_1$ ) EBz;  $\diamond$ ,  $x_1$  1-Butanol + ( $1 - x_1$ ) *p*-Xylene: Curves: ..... , calculated by the Redlich - Kister polynomial equation

The figures shows that, among the 15 binary systems studied, three binary systems showed exothermic mixing behavior i.e., mixing of components accompanied with the release of heat. The three binary systems which showed exothermic mixing behavior are 2-MTHF + (EBz and *p*-Xylene) and DNBE + *p*-Xylene.

The plot of  $H_m^E$  vs  $x_1$  gives a fairly symmetrical curve for 2-MTHF (1) + EBz (2) and 2-MTHF (1) + *p*-Xylene (2) binary systems and the maximum  $H_m^E$  values 200 J/mol and 210J/mol (approximately) occurs at equimolar composition for both systems. From the relatively low heat of mixing values of the above two systems, it is observed that there are only fewer hydrogen bond formation takes place between the unlike molecules and the interactions of unlike molecules are only moderately strong. In case of 2-MTHF (1) + Mesitylene (2) binary system the mixing process is endothermic and the low excess molar enthalpy value suggests that the interaction between Mesitylene and 2-MTHF molecules are weak in nature.

The plot between excess molar enthalpy  $H_m^E$  and molefraction  $x_1$  for the 1-Butanol binary systems, gives an unsymmetrical curve (figure 4.4), and the maximum  $H_m^E$  value of 1080 J/mol (approximately) is observed for the 1-Butanol (1) + Mesitylene (2) system at a molefraction of  $x_1 \approx 0.35$ . The large endothermic excess molar enthalpy values of the 1-butanol (1) + aromatic hydrocarbon binary systems indicates the need for high energy to break the hydrogen bonding between the 1-butanol molecules Francesconi and Comelli (1997). The energy required to break the hydrogen bonding is absorbed from the working fluids resulting in endothermic excess molar enthalpy values.

All the binary system involving 2-methoxyethanol have very high excess molar enthalpy values with endothermic mixing behavior, with 2-ME (1) + Mesitylene (2) being the system with highest value of  $H_m^E \approx 965.0$  J/mol at  $x_1 \approx 0.35$ . The high excess molar enthalpy values of the 2-methoxyethanol binary system can be attributed to the fact that high energy is needed to break the strong intermolecular bond between the -OH and -OCH<sub>3</sub> molecules Kinart *et al.* (2002).

The DNBE binary systems exhibits a different mixing pattern, it mixes endothermically with 2-MTHF, EBz and Mesitylene with relatively low excess molar enthalpy values, but it shows an exothermic mixing behavior with *p*-Xylene with very low excess molar enthalpy values. For the DNBE (1) + 2-MTHF (2) system, the maximum values of excess molar enthalpy is 174.7 J/mol at a molefraction of  $x_1 \approx 0.40$  and 95.1 J/mol for DNBE (1) + EBz (2) at a molefraction of  $x_1 \approx 0.45$ . For the other binary systems of DNBE the maximum values of excess molar enthalpies are significantly low. The EBz (1) and Mesitylene (2) mixing process is endothermic and the maximum excess molar enthalpy value is 160 J/mol and measured at equimolar composition.

#### **4.2.2 Correlation by means of Liebermann-Fried model**

Liebermann-Fried model has notable success in predicting the excess property values of mixtures. The method uses the pure component properties such as molar volume and isobaric thermal expansivity to calculate the binary interaction parameters through regression of excess molar enthalpy data, and these interaction parameters are used to predict the multicomponent excess molar enthalpy values. Peng *et al.* (2001) described the thermodynamic relation using the

Liebermann-Fried model to calculate the excess molar enthalpy values for multicomponent mixtures.

The General expression of the Liebermann-Fried model for N-component mixture is of the form

$$H_m^E = H(I) + H(V) \quad (4.3)$$

$$H(I) = RT^2 \sum_{j=1}^N \sum_{k=1}^N x_j x_k \left[ \frac{\frac{\delta A_{jk}}{\delta T} + \frac{\delta A_{kj}}{\delta T} - \ln(A_{jk} A_{kj})}{2(\sum_{p=1}^N x_p A_{jp})(\sum_{q=1}^N x_q A_{kq})} \left\{ \frac{\sum_{p=1}^N x_p \left( \frac{\delta A_{jp}}{\delta T} \right)}{\sum_{p=1}^N x_p A_{jp}} + \frac{\sum_{q=1}^N x_q \left( \frac{\delta A_{kq}}{\delta T} \right)}{\sum_{q=1}^N x_q A_{kq}} \right\} \right] \quad (4.4)$$

$$\text{where } \frac{1}{A_{jk}} \frac{\delta A_{jk}}{\delta T} = \left( \frac{2}{T} \right) \frac{\ln(A_{jk} A_{kj})}{\ln(A_{jk} A_{kj}) - 2} \quad (4.5)$$

and A is the binary interaction parameters, obtained by fitting the model to the experimental data of the binary system.

and

$$H(V) = RT^2 \frac{\sum_{j=1}^N \sum_{k=1}^N x_j x_k V_{m_k} [(\alpha_p)_k - (\alpha_p)_j]}{\sum_{k=1}^N x_k V_{m_k}} \quad (4.6)$$

where  $\alpha_p$ ,  $V_m$  are the isobaric thermal expansivity and molar volume of the pure component respectively.

$H(I)$  represents the non-ideal behavior of the mixtures due to the interaction between the molecules and  $H(V)$  represents the size of the molecules in the mixture.

For predicting the binary excess molar enthalpy the equation reduces to

$$H_m^E = \frac{2RTx_1x_2[\ln(A_{12}A_{21})]^2}{(x_1+x_2A_{12})(x_2+x_1A_{21})[2-(\ln(A_{12}A_{21}))]} \left[ \frac{x_2A_{12}}{x_1+x_2A_{12}} + \frac{x_1A_{21}}{x_2+x_1A_{21}} - \frac{2}{\ln(A_{12}A_{21})} \right] +$$

$$RT^2 \left[ \frac{x_1x_2(V_{m1}-V_{m2})(\alpha_{p1}-\alpha_{p2})}{x_1V_{m1}+x_2V_{m2}} \right] \quad (4.7)$$

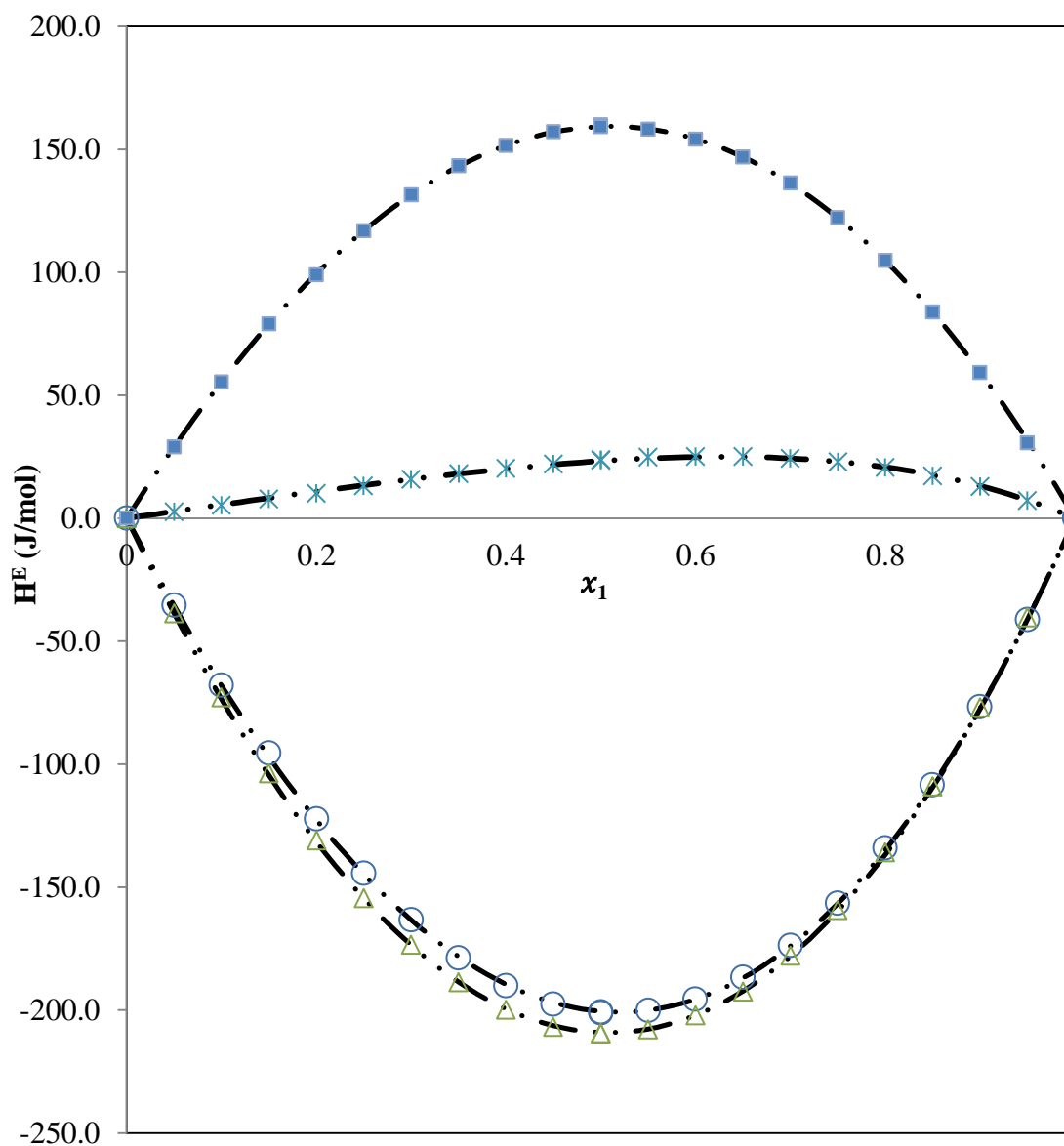
**Table 4.7.** Physical properties of the components used in the Liebermann-Fried model

Chemical name	Molar volume $\frac{V_{mi}}{\text{cm. mol}^{-3}}$	Isobaric thermal expansivity $\frac{\alpha_{pi}}{\text{K}^{-1}}$
2-MTHF	101.58	1.215 <sup>[a]</sup>
2-ME	79.26	0.956 <sup>[b]</sup>
1-Butanol	91.99	0.948 <sup>[c]</sup>
DNBE	170.52	1.126 <sup>[d]</sup>
EBz	123.08	1.019 <sup>[e]</sup>
<i>p</i> -Xylene	123.94	1.019 <sup>[e]</sup>
Mesitylene	139.57	0.940 <sup>[e]</sup>

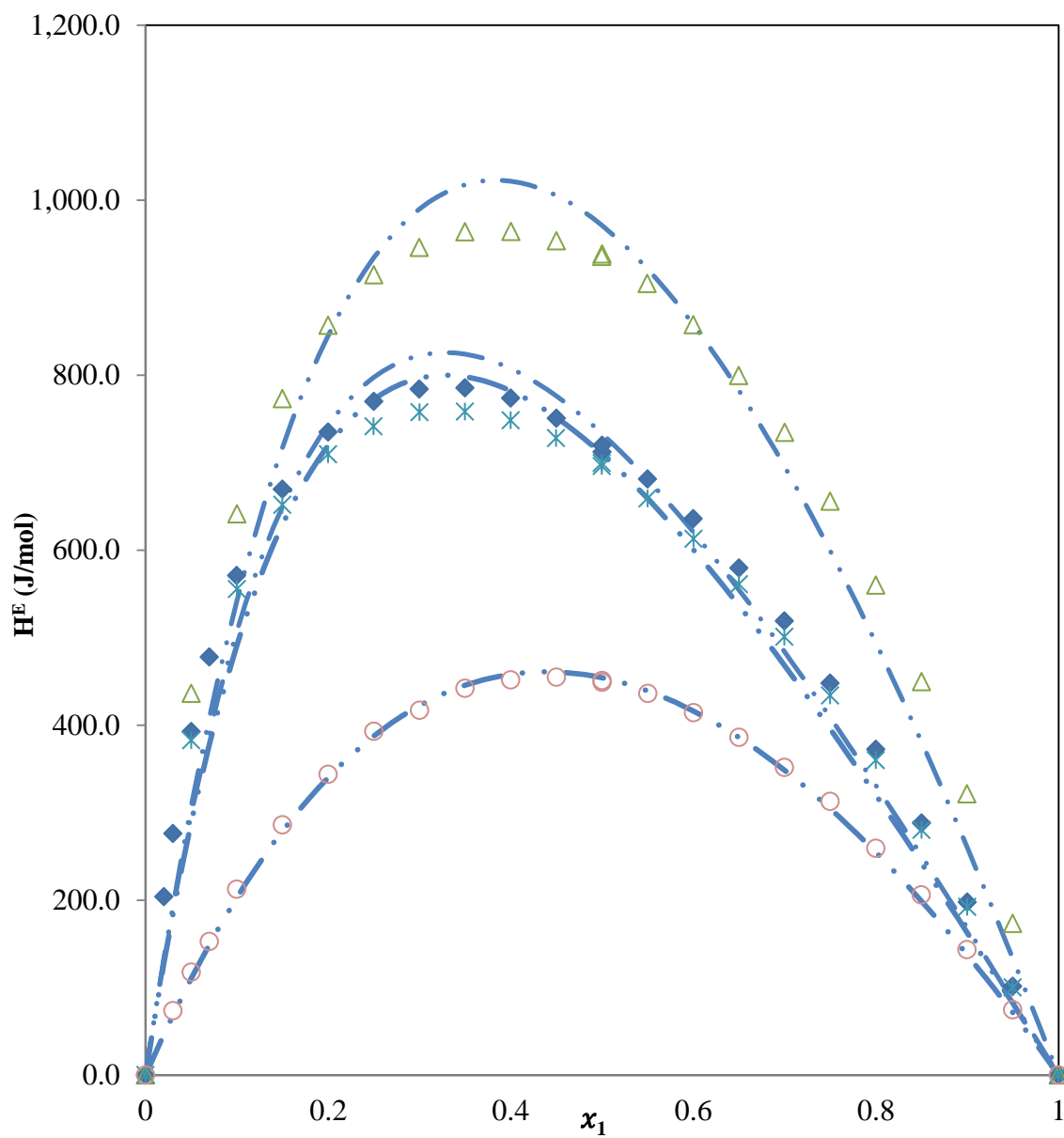
<sup>a</sup>Wang *et al.* (2001), <sup>b</sup>Nishimoto *et al.* (1997), <sup>c</sup>Cerdeiriña *et al.* (2001), <sup>d</sup>Hassan (2010), <sup>e</sup>Aicart *et al.* (1995)

**Table 4.8.** Binary interaction parameters and standard deviation of the Liebermann-Fried model

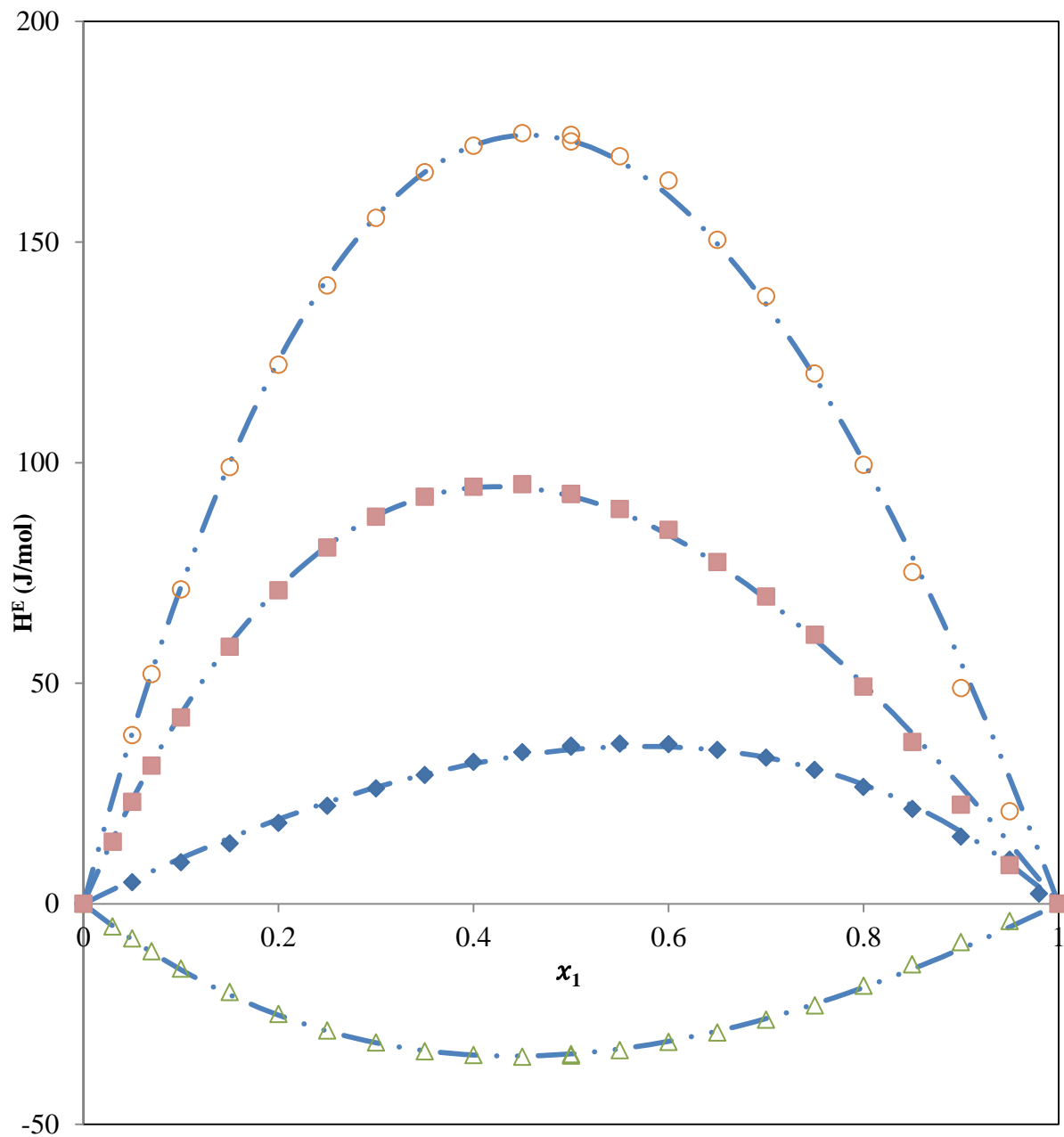
Binary system		Interaction parameters		Standard deviation $s$ $J.mol^{-1}$
$i$	$j$	$A_{ij}$	$A_{ji}$	
2-MTHF	Ethylbenzene	1.17861	1.00707	0.56
2-MTHF	Mesitylene	1.44968	0.66783	0.32
2-MTHF	<i>p</i> -Xylene	1.12651	1.0621	0.49
2-ME	2-MTHF	0.66207	1.10219	5.44
2-ME	Ethylbenzene	0.37599	1.58494	38.76
2-ME	Mesitylene	0.45314	1.1635	59.14
2-ME	<i>p</i> -Xylene	0.37348	1.57301	38.89
1-Butanol	Ethylbenzene	0.33219	1.52887	40.56
1-Butanol	Mesitylene	0.35082	1.42232	49.22
1-Butanol	<i>p</i> -Xylene	0.32184	1.61321	40.35
DNBE	Ethylbenzene	0.70566	1.32291	1.68
DNBE	2-MTHF	0.78282	1.11273	2.63
DNBE	Mesitylene	1.45088	0.67341	0.75
DNBE	<i>p</i> -Xylene	0.81068	1.27552	0.6
EBz	Mesitylene	0.98236	0.90051	0.31



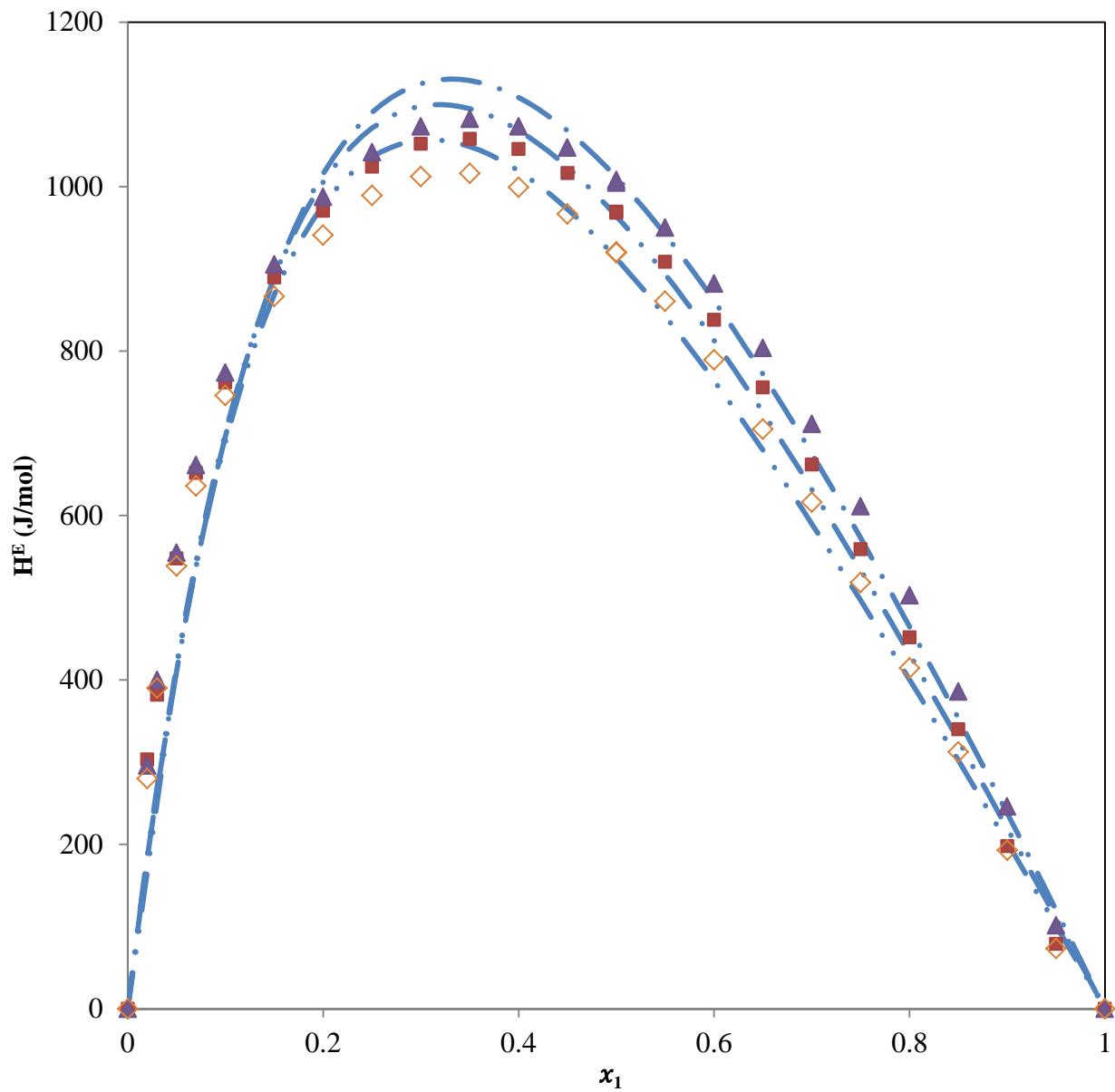
Excess molar enthalpies  $H_{m,ij}^E$  for the binary systems at 298.15K. Experimental results: ■,  $x_1$  EBZ +  $(1 - x_1)$  Mesitylene; \*,  $x_1$  2-MTHF +  $(1 - x_1)$  Mesitylene; ○,  $x_1$  2-MTHF +  $(1 - x_1)$  EBz; △,  $x_1$  2-MTHF +  $(1 - x_1)$  *p*-Xylene; Curves: — — — — —, calculated by the Liebermann-Fried model



Excess molar enthalpies  $H_{m,ij}^E$  for the binary systems at 298.15K. Experimental results:  $\Delta$ ,  $x_1$  2-ME + Mesitylene ( $1 - x_1$ );  $\blacklozenge$ ,  $x_1$  2-ME + ( $1 - x_1$ ) *p*-Xylene; \*,  $x_1$  2-ME + ( $1 - x_1$ ) EBz;  $\circ$ ,  $x_1$  2-ME + ( $1 - x_1$ ) 2-MTHF; Curves: ---, calculated by the Liebermann-Fried model



Excess molar enthalpies  $H_{m,ij}^E$  for the binary systems at 298.15K. Experimental results:  $\circ$ ,  $x_1$  DNBE + 2-MTHF ( $1 - x_1$ );  $\blacksquare$ ,  $x_1$  DNBE + ( $1 - x_1$ ) EBZ;  $\blacklozenge$ ,  $x_1$  DNBE + ( $1 - x_1$ ) Mesitylene;  $\triangle$ ,  $x_1$  DNBE + ( $1 - x_1$ ) *p*-Xylene: Curves: — — — — —, calculated by the Liebermann-Fried model.



Excess molar enthalpies  $H_{m,ij}^E$  for the binary systems at 298.15K. Experimental results:  $\Delta$ ,  $x_1$  1-Butanol + Mesitylene ( $1 - x_1$ );  $\blacksquare$ ,  $x_1$  1-Butanol + ( $1 - x_1$ ) EBz;  $\diamond$ ,  $x_1$  1-Butanol + ( $1 - x_1$ ) *p*-Xylene; Curves:  $-\cdots-$ , calculated by the Liebermann-Fried model

### 4.3 Representation of ternary excess molar enthalpy values

Table 4.9 shows the list of nine ternary systems studied in this work. The ternary excess molar enthalpy values are represented using the Tsao and Smith equation and predicted using the Liebermann-Fried model.

**Table 4.9.** Studied ternary systems

<b>Ternary System</b>	<b>Component 1</b>	<b>Component 2</b>	<b>Component 3</b>
<b>1</b>	2-MTHF	EBz	<i>p</i> -Xylene
<b>2</b>	2-MTHF	EBz	Mesitylene
<b>3</b>	2-ME	EBz	Mesitylene
<b>4</b>	2-ME	2-MTHF	<i>p</i> -Xylene
<b>5</b>	1-Butanol	Mesitylene	<i>p</i> -Xylene
<b>6</b>	1-Butanol	DNBE	Mesitylene
<b>7</b>	1-Butanol	2-MTHF	EBz
<b>8</b>	DNBE	2-MTHF	EBz
<b>9</b>	DNBE	Mesitylene	<i>p</i> -Xylene

#### 4.3.1 Correlation of experimental data by Tsao and Smith equation

The relation used to calculate the ternary excess molar enthalpy  $H_{m,123}^E$  is given as follows.

$$H_{m,123}^E = H_{m,1+23}^E + (1 - x_1)H_{m,23}^E \quad (4.8)$$

In the above equation  $H_{m,1+23}^E$  is the excess molar enthalpy value of the pseudo-binary mixture and is given by Tsao and Smith (1953) and  $H_{m,23}^E$  is the excess molar enthalpy of the specific binary mixture and  $x_1$  is the molefraction of component 1.

$$\text{and where } H_{m,1+23}^E = \left(\frac{x_2}{1-x_1}\right)H_{m,12}^E + \left(\frac{x_3}{1-x_1}\right)H_{m,13}^E + H_{m,T}^E \quad (4.9)$$

The ternary excess molar enthalpy is measured by mixing component 1 to the three pseudo-pure mixtures of specific compositions in three separate measurements.

$H_{m,T}^E$  is an added ternary term and it is given by

$$H_{m,T}^E = x_1x_2 \left(\frac{1-x_1-x_2}{1-x_1+x_2}\right) (c_0 + c_1x_1 + c_2x_2 + c_3x_1^2 + c_4x_1x_2 + \cdots) \quad (4.10)$$

The values of the parameter  $c_i$  are obtained by the least square analyses, where the equation 4.9 and 4.10 are fitted to the experimental values of the pseudo-binary mixtures

**Table 4.10.** Equation 4.10 fitting parameters  $c_i$  and standard deviation 's' for the ternary systems listed in table 4.6

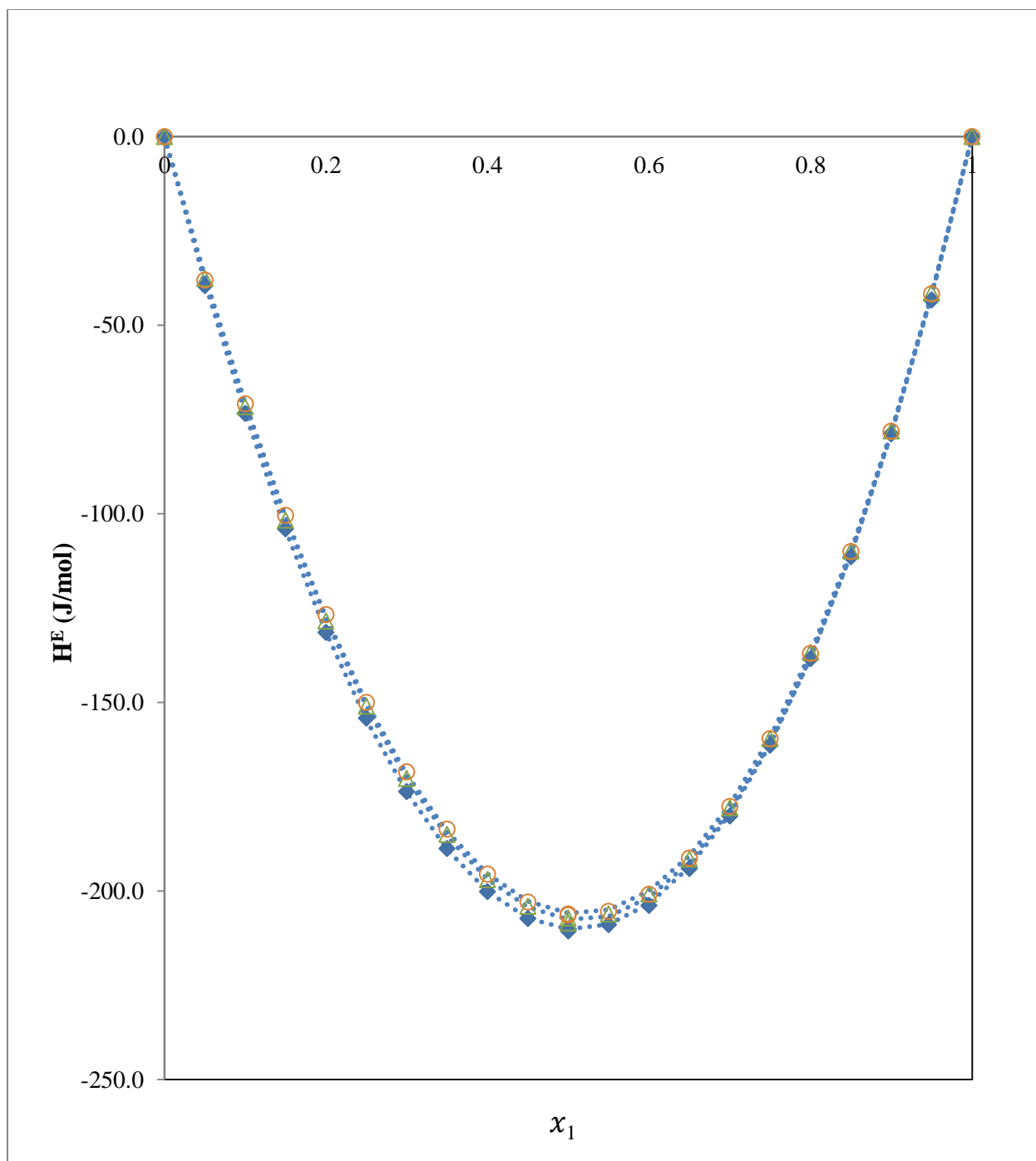
Coefficient $c_i$	Ternary 1	Ternary 2	Ternary 3	Ternary 4	Ternary 5	Ternary 6	Ternary 7	Ternary 8	Ternary 9
$c_0$	-535.2	-748.07	1517.1	-9249.5	6005.2	9687.3	-11493.1	493.7	-584.0
$c_1$	1125.6	1506.84	-4987.5	41141.4	-52041.5	-82469.3	50869.6	2711.7	934.7
$c_2$	1994.6	-251.62	-5060.5	4668.3	3938.6	-19171.7	-2819.4	2077.4	980.4
$c_3$	-741.1	-1830.32	5638.8	-64253.1	125006.7	208054.0	-81612.9	-6607.0	-593.9
$c_4$	-2093.7	-3220.12	4677.0	-3700.4	-12352.1	108548.6	-4996.3	-3805.6	-1063.0
$c_5$	-2157.9	-	5677.9	-3881.4	2681.7	45747.3	31313.9	186.1	-885.3
$c_6$	-	-	-2772.2	34960.9	-87882.3	-151146.2	42415.3	4717.0	-
$c_7$	-	-	-	-	-	-236717.8	-	8340.8	-
$\frac{S}{J.mol^{-1}}$	0.59	0.95	2.59	6.20	23.03	33.72	15.06	1.86	0.35

Table 4.10 summarizes the values of the coefficient  $c_i$  for the nine ternary systems, while fitting the experimental excess molar enthalpy data to the ternary system, the binary contribution term  $H_{m,ij}^E$  is calculated by means of Redlich-Kister equation with values of the coefficients given in the table 4.6. The ternary excess molar enthalpy value  $H_{m,123}^E$  and the excess molar enthalpy values of the pseudo-binary mixtures are reported in the table 4.11 to table 4.19 for the nine ternary systems. The ternary excess molar enthalpy values are then plotted in the Roozeboom diagram and it shows that there is no indication of an local maxima for all of the systems and the maximum value of  $H_{m,123}^E$  for all the ternary system are located at the edge of the plot for the constituent binary systems.

**Table 4.11.** Experimental excess molar enthalpies  $H_{m,1+23}^E$  (J/mol) and the calculated values of  $H_{m,123}^E$  (J/mol) for the  $x_1$ 2-MTHF +  $x_2$  EBz +  $(1 - x_1 - x_2)$  *p*-Xylene ternary system at 298.15K

$x_1$	$H_{m,1+23}^E$	$H_{m,123}^E$	$x_1$	$H_{m,1+23}^E$	$H_{m,123}^E$	$x_1$	$H_{m,1+23}^E$	$H_{m,123}^E$
$x_2/x_3 = 0.3334, H_{m,23}^E = -6.95$								
0.0500	-39.5	-45.1	0.4000	-200.2	-204.6	0.7000	-180.2	-180.8
0.1000	-73.4	-79.6	0.4500	-207.3	-211.2	0.7500	-161.4	-161.8
0.1500	-104.1	-110.3	0.5000	-210.1	-213.6	0.8000	-138.4	-138.4
0.2000	-131.5	-137.2	0.5000	-210.6	-213.6	0.8500	-111.4	-110.5
0.2500	-154.2	-160.0	0.5500	-208.9	-211.8	0.9000	-78.9	-78.2
0.3000	-173.7	-178.9	0.6000	-203.9	-205.8	0.9500	-43.3	-41.4
0.3500	-188.8	-193.8	0.6500	-194.0	-195.4			
$x_2/x_3 = 1.0002, H_{m,23}^E = -9.86$								
0.0500	-37.7	-45.2	0.4000	-197.0	-196.6	0.7000	-178.0	-177.0
0.1000	-71.6	-77.3	0.4500	-204.1	-203.5	0.7500	-159.7	-159.1
0.1500	-101.7	-106.1	0.5000	-208.5	-206.4	0.8000	-136.8	-136.7
0.2000	-128.4	-131.4	0.5000	-207.2	-206.4	0.8500	-109.9	-109.7
0.2500	-151.1	-153.2	0.5500	-206.1	-205.2	0.9000	-78.0	-78.0
0.3000	-170.2	-171.4	0.6000	-200.9	-200.0	0.9500	-41.4	-41.5
0.3500	-185.0	-185.9	0.6500	-191.6	-190.7			
$x_2/x_3 = 3.0057, H_{m,23}^E = -7.72$								
0.0500	-38.1	-44.0	0.4000	-195.6	-194.8	0.7000	-177.6	-174.8
0.1000	-70.9	-76.6	0.4500	-203.0	-201.3	0.7500	-159.6	-157.1
0.1500	-100.4	-105.6	0.5000	-206.4	-203.9	0.8000	-137.1	-135.1
0.2000	-126.7	-130.9	0.5000	-206.1	-203.9	0.8500	-110.0	-108.6
0.2500	-150.0	-152.5	0.5500	-205.5	-202.7	0.9000	-78.1	-77.4
0.3000	-168.4	-170.4	0.6000	-200.9	-197.4	0.9500	-41.7	-41.3
0.3500	-183.6	-184.5	0.6500	-191.3	-188.1			

Ternary term for the representation of  $H_{m,1+23}^E$  by equations 4.8 and 4.9:  
 $H_{m,T}^E = [x_1 x_2 x_3 / (1 - x_1 + x_3)](-535.2 + 1125.6x_1 + 1994.6x_2 - 741.1x_1^2 - 2093.7x_1x_2 - 2157.9x_2^2)$ ;  
s/(J/mol) = 0.59.



**Figure 4.1.** Excess molar enthalpies  $H_{m,1+23}^E$  for the ternary system  $x_1$  2-MTHF +  $x_2$  EBz +  $(1 - x_1 - x_2)$  *p*-Xylene at 298.15K . Experimental results:  $\diamond$   $x_2/x_3 = 0.3334$ ;  $\Delta$ ,  $x_2/x_3 = 1.0002$ ;  $\circ$ ,  $x_2/x_3 = 3.0057$ ; Curves: ..... , calculated using the equation 4.8 and 4.9

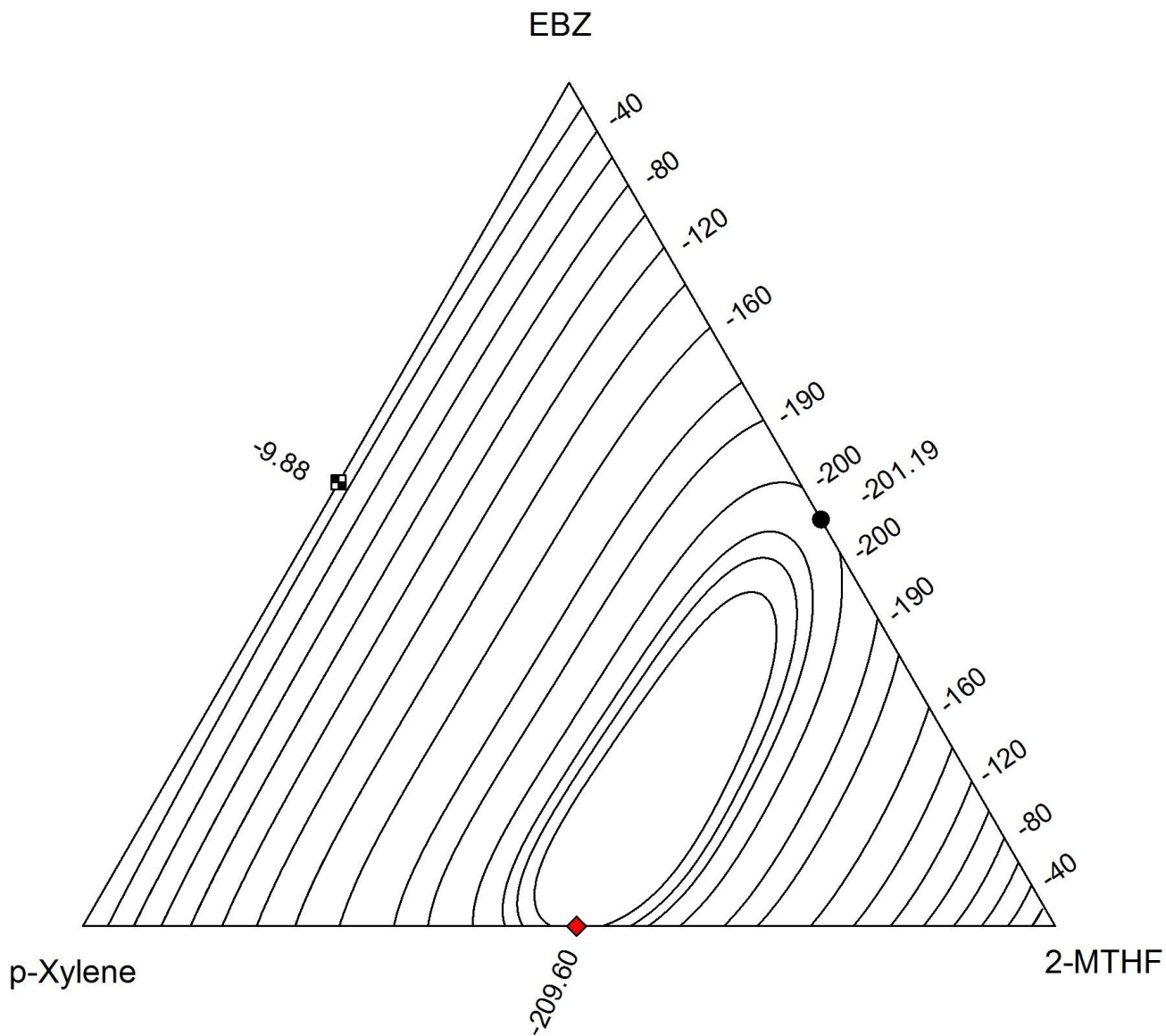


**Figure 4.2.** Constant enthalpy contours,  $H_{m,123}^E$  (J/mol) at 298.15K for the  $x_1$  2-MTHF +  $x_2$  EBz +  $(1 - x_1 - x_2)$  *p*-Xylene, calculated from the representation of the experimental results using the equation 2.3 and 2.4

**Table 4.12.** Experimental excess molar enthalpies  $H_{m,1+23}^E$  (J/mol) and the calculated values of  $H_{m,123}^E$  (J/mol) for the  $x_1$ 2-MTHF +  $x_2$  EBz +  $(1 - x_1 - x_2)$  Mesitylene ternary system at 298.15K

$x_1$	$H_{m,1+23}^E$	$H_{m,123}^E$	$x_1$	$H_{m,1+23}^E$	$H_{m,123}^E$	$x_1$	$H_{m,1+23}^E$	$H_{m,123}^E$
$x_2/x_3 = 0.3335, H_{m,23}^E = 116.93$								
0.0500	-11.8	98.7	0.4000	-57.3	13.7	0.7000	-48.8	-14.6
0.1000	-22.1	82.2	0.4500	-58.7	6.4	0.7500	-43.4	-15.6
0.1500	-31.3	67.4	0.5000	-59.0	0.2	0.8000	-37.0	-15.4
0.2000	-38.7	54.1	0.5000	-59.0	0.2	0.8500	-29.5	-13.8
0.2500	-45.5	42.1	0.5500	-58.4	-5.1	0.9000	-20.8	-10.9
0.3000	-50.5	31.5	0.6000	-56.3	-9.3	0.9500	-11.0	-6.3
0.3500	-54.6	22.0	0.6500	-53.2	-12.5			
$x_2/x_3 = 0.9921, H_{m,23}^E = 159.27$								
0.0500	-24.9	128.2	0.4000	-119.6	-24.9	0.7000	-108.2	-60.3
0.1000	-44.7	99.4	0.4500	-124.9	-37.1	0.7500	-97.2	-57.2
0.1500	-62.8	72.7	0.5000	-126.4	-46.8	0.8000	-83.3	-51.4
0.2000	-79.0	48.4	0.5000	-126.1	-46.8	0.8500	-67.0	-42.8
0.2500	-92.6	26.5	0.5500	-125.6	-54.0	0.9000	-47.0	-31.5
0.3000	-104.3	6.9	0.6000	-122.5	-58.7	0.9500	-25.6	-17.2
0.3500	-113.1	-10.2	0.6500	-116.6	-60.8			
$x_2/x_3 = 3.0005, H_{m,23}^E = 122.06$								
0.0500	-32.1	85.4	0.4000	-165.6	-93.3	0.7000	-151.3	-113.6
0.1000	-60.1	51.1	0.4500	-172.3	-105.7	0.7500	-136.1	-104.1
0.1500	-85.2	19.4	0.5000	-175.5	-114.6	0.8000	-117.0	-90.8
0.2000	-107.4	-9.5	0.5000	-174.9	-114.6	0.8500	-94.1	-73.8
0.2500	-126.9	-35.3	0.5500	-174.5	-119.8	0.9000	-67.3	-53.0
0.3000	-142.9	-58.0	0.6000	-170.4	-121.4	0.9500	-36.2	-28.4
0.3500	-156.0	-77.3	0.6500	-162.8	-119.4			

Ternary term for the representation of  $H_{m,1+23}^E$  by equation 4.8 and 4.9:  $H_{m,T}^E = [x_1 x_2 x_3 / (1 - x_1 + x_3)](-748.1 + 1506.8x_1 - 251.6x_2 - 1830.3x_1^2 - 3220.1x_1x_2)$ ; s/(J/mol) = 0.95

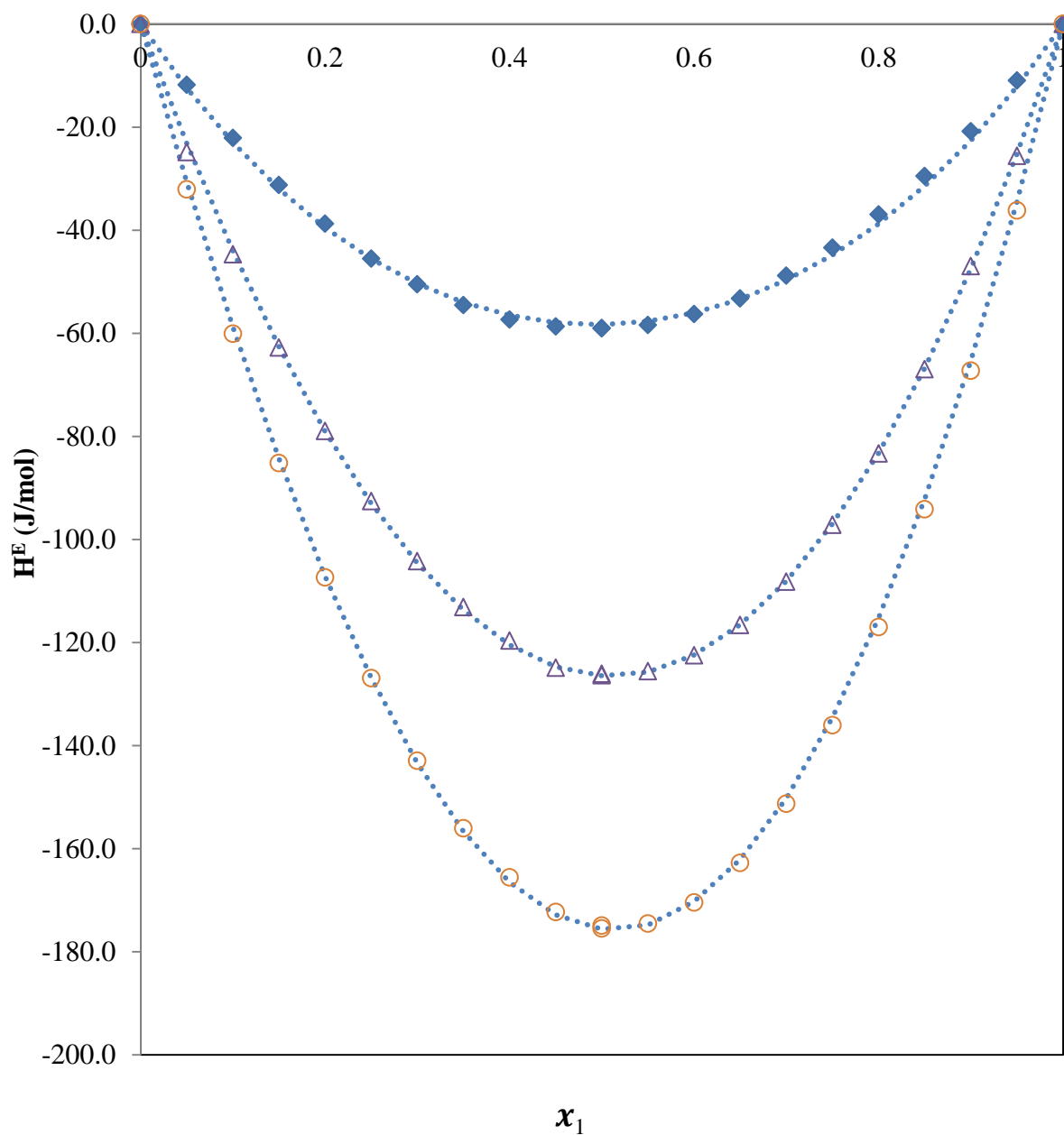


**Figure 4.3.** Excess molar enthalpies  $H_{m,1+23}^E$  for the ternary system  $x_1$  2-MTHF +  $x_2$  EBz +  $(1 - x_1 - x_2)$  Mesitylene at 298.15K . Experimental results:  $\blacklozenge$   $x_2/x_3 = 0.3335$ ;  $\blacktriangle$ ,  $x_2/x_3 = 0.9921$ ;  $\circ$ ,  $x_2/x_3 = 3.0005$ ; Curves: ..... , calculated using the equation 4.8 and 4.9

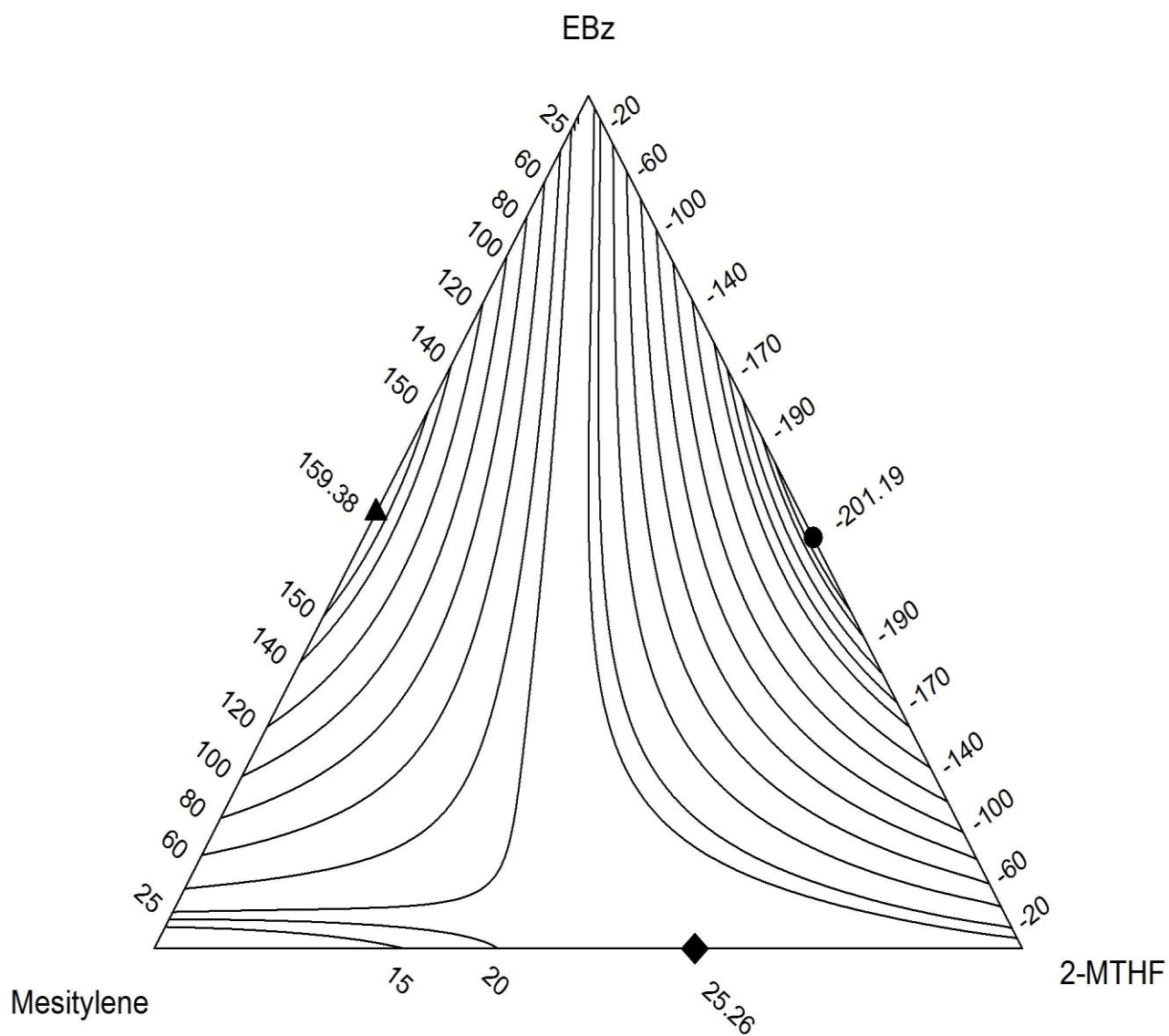


**Figure 4.4.** Constant enthalpy contours,  $H_{m,123}^E$  (J/mol) at 298.15K for the  $x_1$  2-MTHF +  $x_2$  EBz +  $(1 - x_1 - x_2)$  Mesitylene, calculated from the representation of the experimental results using the equation 2.3 and 2.4

**Table 4.13.** Experimental excess molar enthalpies  $H_{m,1+23}^E$  (J/mol) and the calculated values of  $H_{m,123}^E$  (J/mol) for the  $x_1$  2-ME +  $x_2$  EBz +  $(1 - x_1 - x_2)$ Mesitylene ternary system at 298.15K

$x_1$	$H_{m,1+23}^E$	$H_{m,123}^E$	$x_1$	$H_{m,1+23}^E$	$H_{m,123}^E$	$x_1$	$H_{m,1+23}^E$	$H_{m,123}^E$
$x_2/x_3 = 0.3335, H_{m,23}^E = 116.93$								
0.0500	417.2	536.4	0.4000	908.2	976.3	0.7000	668.9	701.6
0.1000	631.8	731.1	0.4500	893.6	957.7	0.7500	592.7	620.2
0.1500	747.7	844.2	0.5000	867.4	928.7	0.8000	503.9	526.5
0.2000	822.4	916.9	0.5000	868.3	928.7	0.8500	399.8	417.7
0.2500	869.6	960.6	0.5500	832.4	888.1	0.9000	284.3	293.7
0.3000	899.7	981.1	0.6000	789.1	835.9	0.9500	150.8	157.5
0.3500	910.7	984.7	0.6500	734.1	773.4			
$x_2/x_3 = 0.9921, H_{m,23}^E = 159.27$								
0.0500	402.2	562.2	0.4000	850.9	943.8	0.7000	607.5	654.3
0.1000	602.2	745.6	0.4500	832.2	920.3	0.7500	533.7	574.2
0.1500	714.6	847.6	0.5000	806.7	887.0	0.8000	449.8	483.7
0.2000	784.2	910.3	0.5000	806.4	887.0	0.8500	353.8	380.6
0.2500	823.0	945.7	0.5500	770.5	843.2	0.9000	249.1	265.4
0.3000	849.2	959.6	0.6000	725.3	789.1	0.9500	131.2	141.0
0.3500	856.2	957.6	0.6500	671.2	725.9			
$x_2/x_3 = 3.0005, H_{m,23}^E = 122.06$								
0.0500	404.4	515.2	0.4000	801.7	873.9	0.7000	553.3	588.8
0.1000	583.1	693.5	0.4500	781.4	848.9	0.7500	483.1	513.3
0.1500	687.5	790.2	0.5000	752.8	814.6	0.8000	404.8	429.2
0.2000	751.6	848.5	0.5000	751.4	814.6	0.8500	316.8	335.1
0.2500	786.7	880.7	0.5500	715.1	770.9	0.9000	221.7	231.8
0.3000	806.1	892.7	0.6000	670.5	718.0	0.9500	114.0	122.0
0.3500	810.5	889.2	0.6500	616.2	657.0			

Ternary term for the representation of  $H_{m,1+23}^E$  by equation 4.8 and 4.9:  $H_{m,T}^E = [x_1x_2x_3/(1 - x_1 + x_3)](1517.1 - 4987.5x_1 - 5060.5x_2 + 5638.8x_1^2 + 4677.0x_1x_2 + 5677.9x_2^2 - 2772.2x_1^3)$ ; s/(J/mol) = 2.59

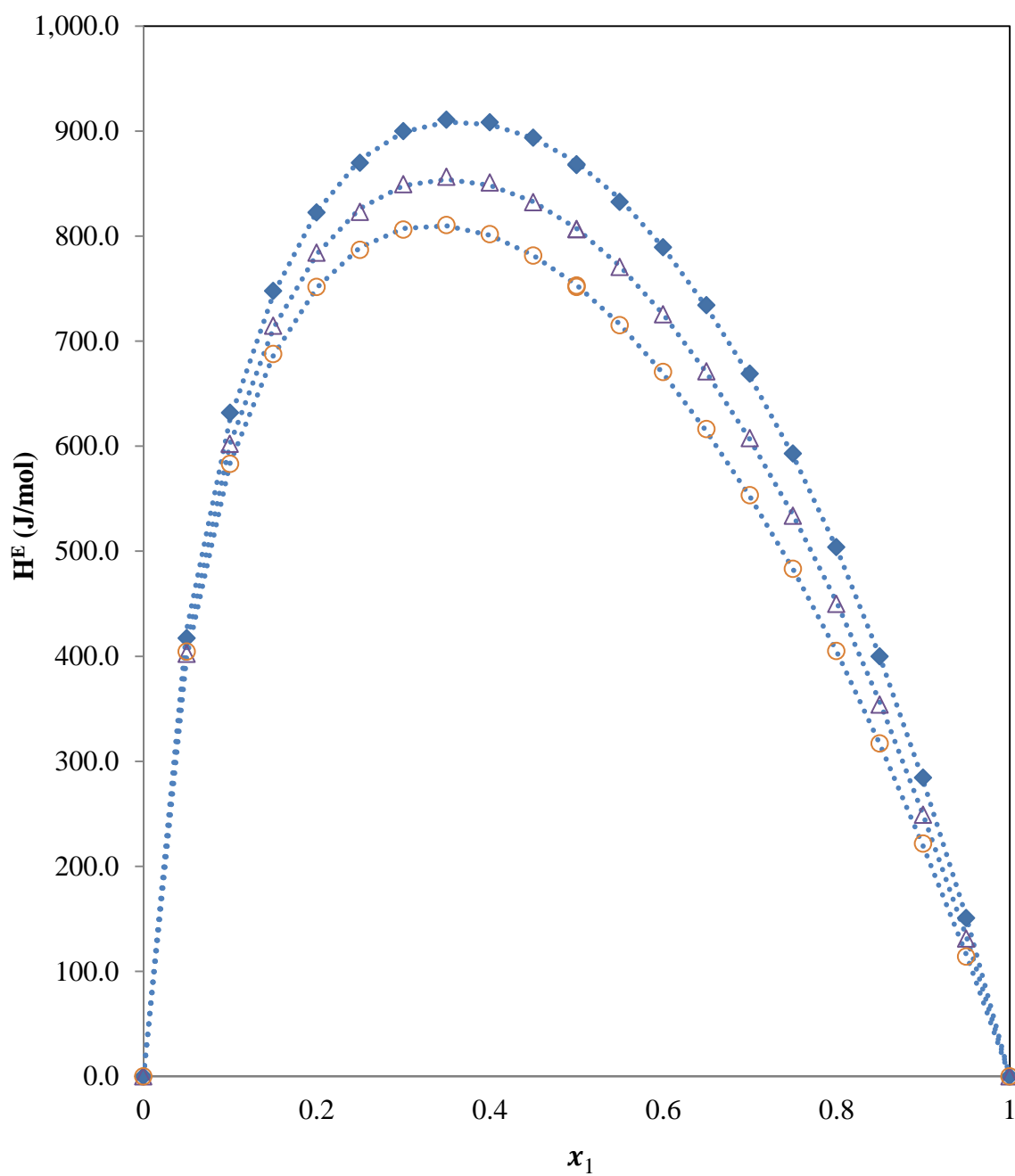


**Figure 4.5.** Excess molar enthalpies  $H_{m,1+23}^E$  for the ternary system  $x_1$  2-ME +  $x_2$  EBz +  $(1 - x_1 - x_2)$  Mesitylene at 298.15K. Experimental results:  $\blacklozenge$   $x_2/x_3 = 0.3335$ ;  $\triangle$ ,  $x_2/x_3 = 0.9921$ ;  $\circ$ ,  $x_2/x_3 = 3.0057$ ; Curves: ..... , calculated using the equation 4.8 and 4.9

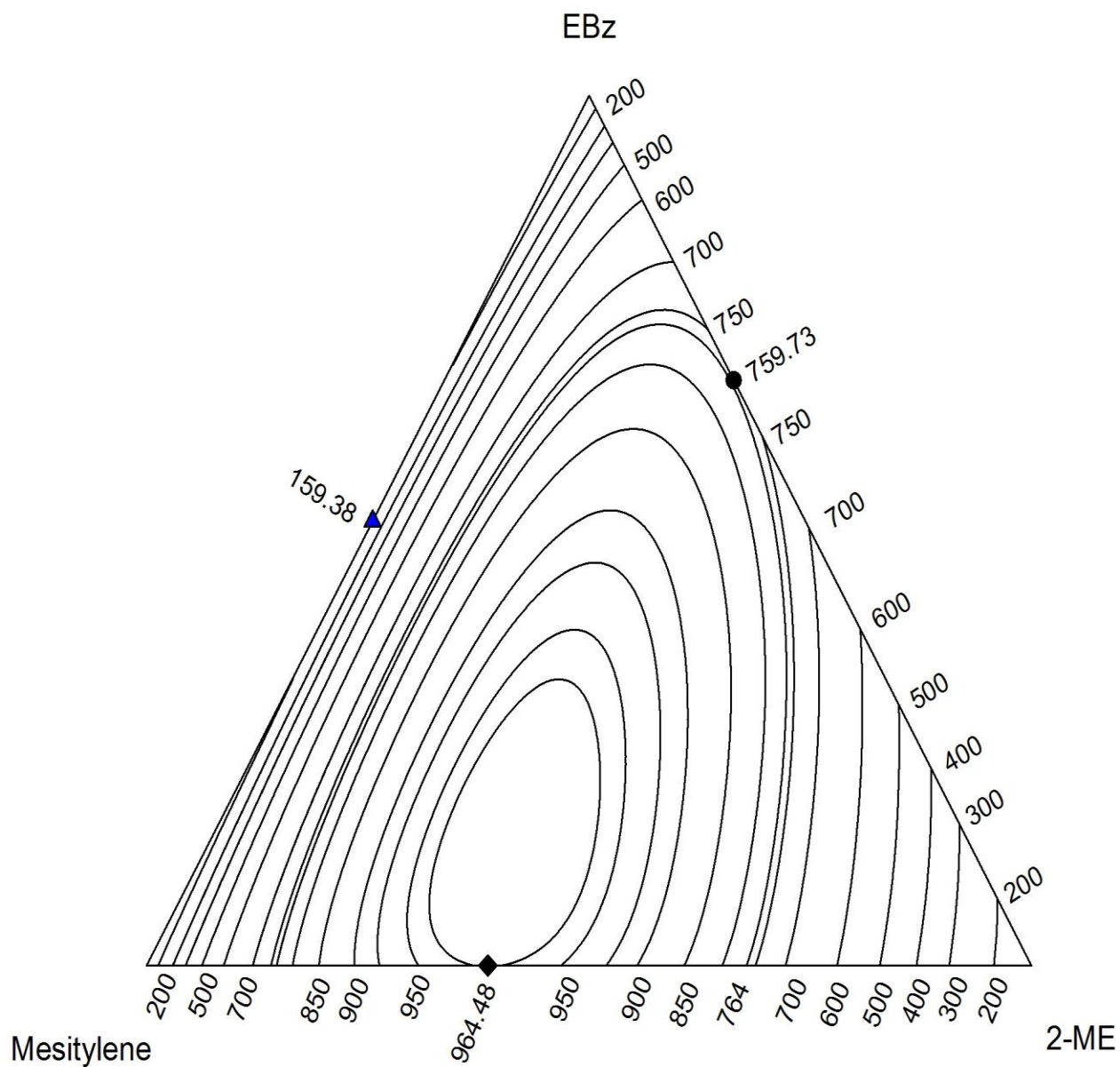


**Figure 4.6.** Constant enthalpy contours,  $H_{m,123}^E$  (J/mol) at 298.15K for the  $x_1$ 2-ME +  $x_2$  EBz +  $(1 - x_1 - x_2)$  Mesitylene, calculated from the representation of the experimental results using the equation 2.3 and 2.4

**Table 4.14.** Experimental excess molar enthalpies  $H_{m,1+23}^E$  (J/mol) and the calculated values of  $H_{m,123}^E$  (J/mol) for the  $x_1$  2-ME +  $x_2$  2-MTHF +  $(1 - x_1 - x_2)$  *p*-Xylene ternary system at 298.15K

$x_1$	$H_{m,1+23}^E$	$H_{m,123}^E$	$x_1$	$H_{m,1+23}^E$	$H_{m,123}^E$	$x_1$	$H_{m,1+23}^E$	$H_{m,123}^E$
$x_2/x_3 = 0.3334, H_{m,23}^E = -154.31$								
0.0500	251.9	130.4	0.4000	673.7	583.2	0.7000	484.9	436.5
0.1000	407.4	275.3	0.4500	665.0	582.1	0.7500	422.4	384.4
0.1500	511.3	372.3	0.5000	645.7	570.7	0.8000	355.4	325.8
0.2000	582.2	447.9	0.5000	644.5	570.7	0.8500	279.6	260.0
0.2500	626.4	506.5	0.5500	618.1	549.8	0.9000	196.3	185.4
0.3000	656.5	547.7	0.6000	582.1	520.0	0.9500	100.3	100.1
0.3500	671.3	572.5	0.6500	538.2	481.9			
$x_2/x_3 = 0.9992, H_{m,23}^E = -209.54$								
0.0500	186.4	7.4	0.4000	598.9	477.2	0.7000	451.5	382.2
0.1000	316.9	134.0	0.4500	597.2	485.3	0.7500	394.6	339.2
0.1500	413.8	229.0	0.5000	585.5	482.6	0.8000	335.5	290.0
0.2000	483.7	308.3	0.5000	584.4	482.6	0.8500	265.0	233.6
0.2500	535.9	373.1	0.5500	564.3	470.1	0.9000	185.2	168.5
0.3000	570.0	422.6	0.6000	534.6	448.5	0.9500	97.9	92.1
0.3500	590.3	456.8	0.6500	496.7	418.9			
$x_2/x_3 = 2.9963, H_{m,23}^E = -159.40$								
0.0500	146.0	3.4	0.4000	525.9	431.8	0.7000	405.3	353.3
0.1000	257.8	113.8	0.4500	526.6	441.1	0.7500	359.1	313.7
0.1500	343.9	201.2	0.5000	516.2	440.4	0.8000	302.7	267.5
0.2000	402.7	274.1	0.5000	517.7	440.4	0.8500	239.6	214.4
0.2500	457.8	333.4	0.5500	498.0	430.6	0.9000	168.7	153.2
0.3000	490.1	379.1	0.6000	472.8	412.3	0.9500	86.6	82.6
0.3500	514.3	411.5	0.6500	443.8	386.4			
Ternary term for the representation of $H_{m,1+23}^E$ by equation 4.8 and 4.9: $H_{m,T}^E = [x_1x_2x_3/(1 - x_1 + x_3)](-9249.5 + 41141.4x_1 + 4668.3x_2 - 64253.1x_1^2 - 3700.4x_1x_2 - 3881.4x_2^2 + 34960.9x_1^3)$ ; s(J/mol) = 6.2								

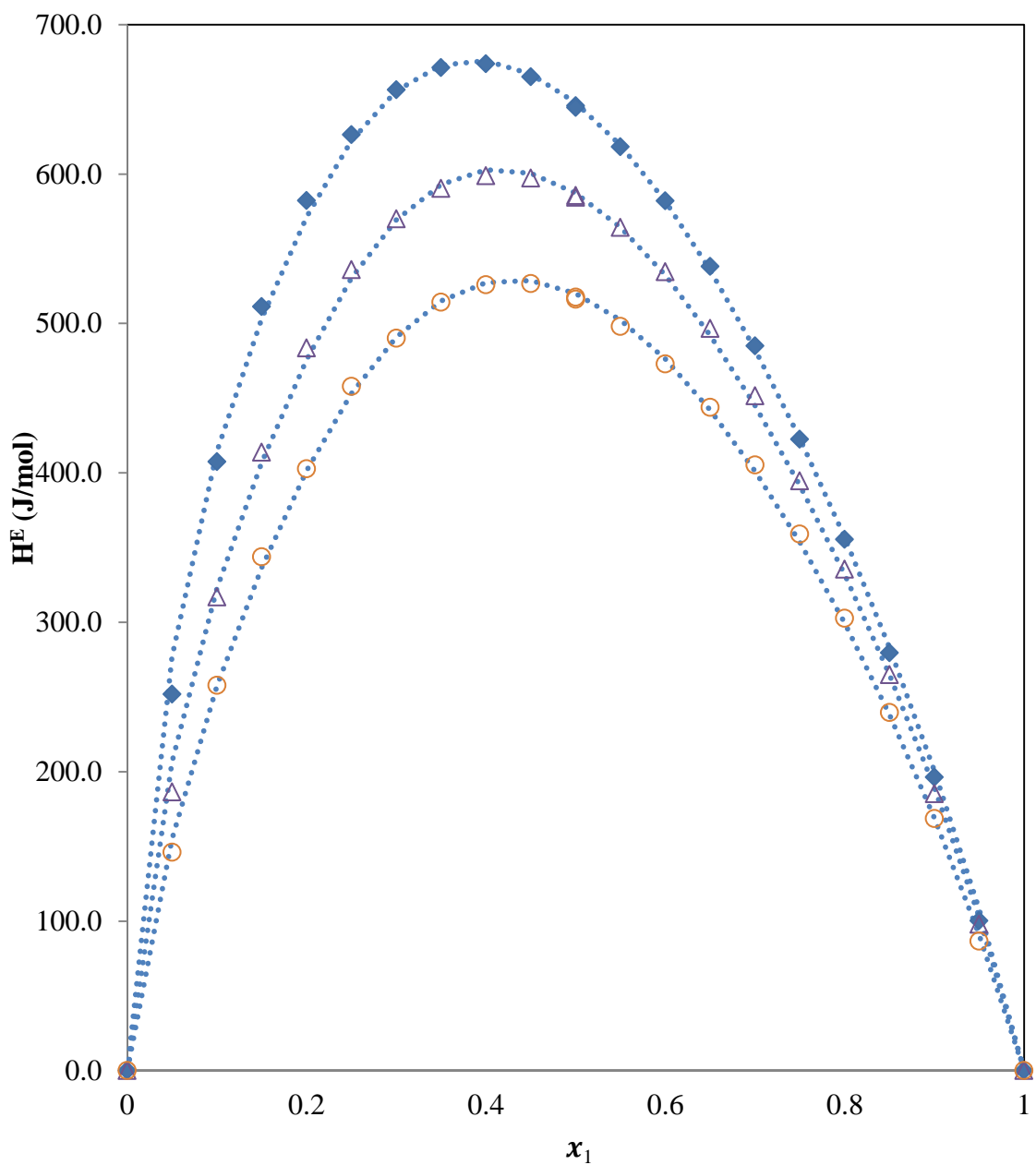


**Figure 4.7.** Excess molar enthalpies  $H_{m,1+23}^E$  for the ternary system  $x_1$  2-ME +  $x_2$  2-MTHF +  $(1 - x_1 - x_2)$  *p*-Xylene at 298.15K. Experimental results: ♦  $x_2/x_3 = 0.3334$ ; Δ,  $x_2/x_3 = 0.9992$ ; ○,  $x_2/x_3 = 2.9963$ ; Curves: ..... , calculated using the equation 4.8 and 4.9

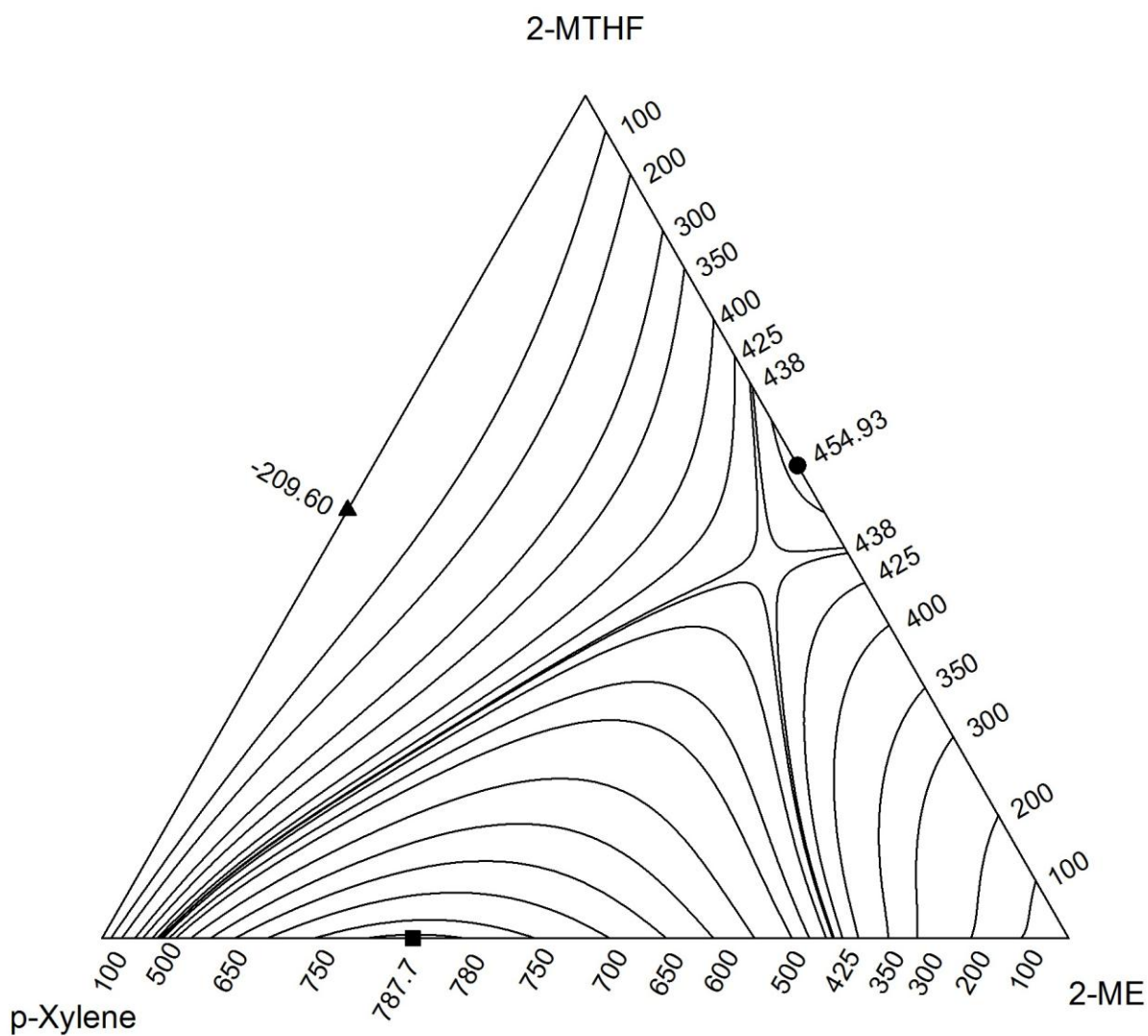


**Figure 4.8.** Constant enthalpy contours,  $H_{m,123}^E$  (J/mol) at 298.15K for the  $x_1$  2-ME +  $x_2$  2-MTHF +  $(1 - x_1 - x_2)$  *p*-Xylene, calculated from the representation of the experimental results using the equation 2.3 and 2.4.

**Table 4.15.** Experimental excess molar enthalpies  $H_{m,1+23}^E$  (J/mol) and the calculated values of  $H_{m,123}^E$  (J/mol) for the  $x_1$  1-Butanol +  $x_2$  Mesitylene +  $(1 - x_1 - x_2)$  *p*-Xylene ternary system at 298.15K

$x_1$	$H_{m,1+23}^E$	$H_{m,123}^E$	$x_1$	$H_{m,1+23}^E$	$H_{m,123}^E$	$x_1$	$H_{m,1+23}^E$	$H_{m,123}^E$
$x_2/x_3 = 0.3336, H_{m,23}^E = 5.05$								
0.0500	538.3	537.5	0.4000	1014.4	1001.5	0.7000	637.5	652.2
0.1000	751.9	768.2	0.4500	984.6	979.6	0.7500	540.7	540.9
0.1500	872.4	890.7	0.5000	938.6	944.9	0.8000	435.9	420.8
0.2000	947.2	960.6	0.5000	934.5	944.9	0.8500	328.3	299.8
0.2500	997.3	997.4	0.5500	878.1	895.7	0.9000	201.7	184.6
0.3000	1023.6	1012.0	0.6000	809.4	830.8	0.9500	79.2	78.9
0.3500	1027.7	1012.3	0.6500	728.0	749.6			
$x_2/x_3 = 0.9997, H_{m,23}^E = 6.68$								
0.0500	540.3	514.9	0.4000	1031.3	1020.1	0.7000	661.5	667.3
0.1000	756.5	768.6	0.4500	1002.9	996.5	0.7500	561.3	555.9
0.1500	884.1	909.7	0.5000	958.2	960.9	0.8000	456.4	436.8
0.2000	962.9	987.0	0.5000	961.4	960.9	0.8500	347.0	320.8
0.2500	1009.2	1023.9	0.5500	902.6	911.1	0.9000	220.9	217.4
0.3000	1038.3	1036.0	0.6000	832.4	846.1	0.9500	87.4	122.4
0.3500	1045.0	1033.2	0.6500	751.6	764.8			
$x_2/x_3 = 3.0005, H_{m,23}^E = 4.62$								
0.0500	537.3	465.9	0.4000	1049.7	1048.3	0.7000	686.2	684.1
0.1000	763.6	738.8	0.4500	1022.6	1021.5	0.7500	583.6	578.6
0.1500	890.4	904.2	0.5000	980.8	981.5	0.8000	478.0	468.6
0.2000	972.6	998.8	0.5000	978.4	981.5	0.8500	364.7	365.5
0.2500	1023.9	1046.0	0.5500	923.4	927.8	0.9000	231.3	277.9
0.3000	1050.0	1063.6	0.6000	857.4	860.2	0.9500	93.9	188.2
0.3500	1062.2	1062.6	0.6500	776.2	778.8			

Ternary term for the representation of  $H_{m,1+23}^E$  by equation 4.8 and 4.9:  $H_{m,T}^E = [x_1 x_2 x_3 / (1 - x_1 + x_3)](6005.2 - 52041.5 x_1 + 3938.6 x_2 + 125006.7 x_1^2 - 12352.1 x_1 x_2 + 2681.7 x_2^2 - 87882.3 x_1^3)$ ; s/(J/mol) = 23.0.

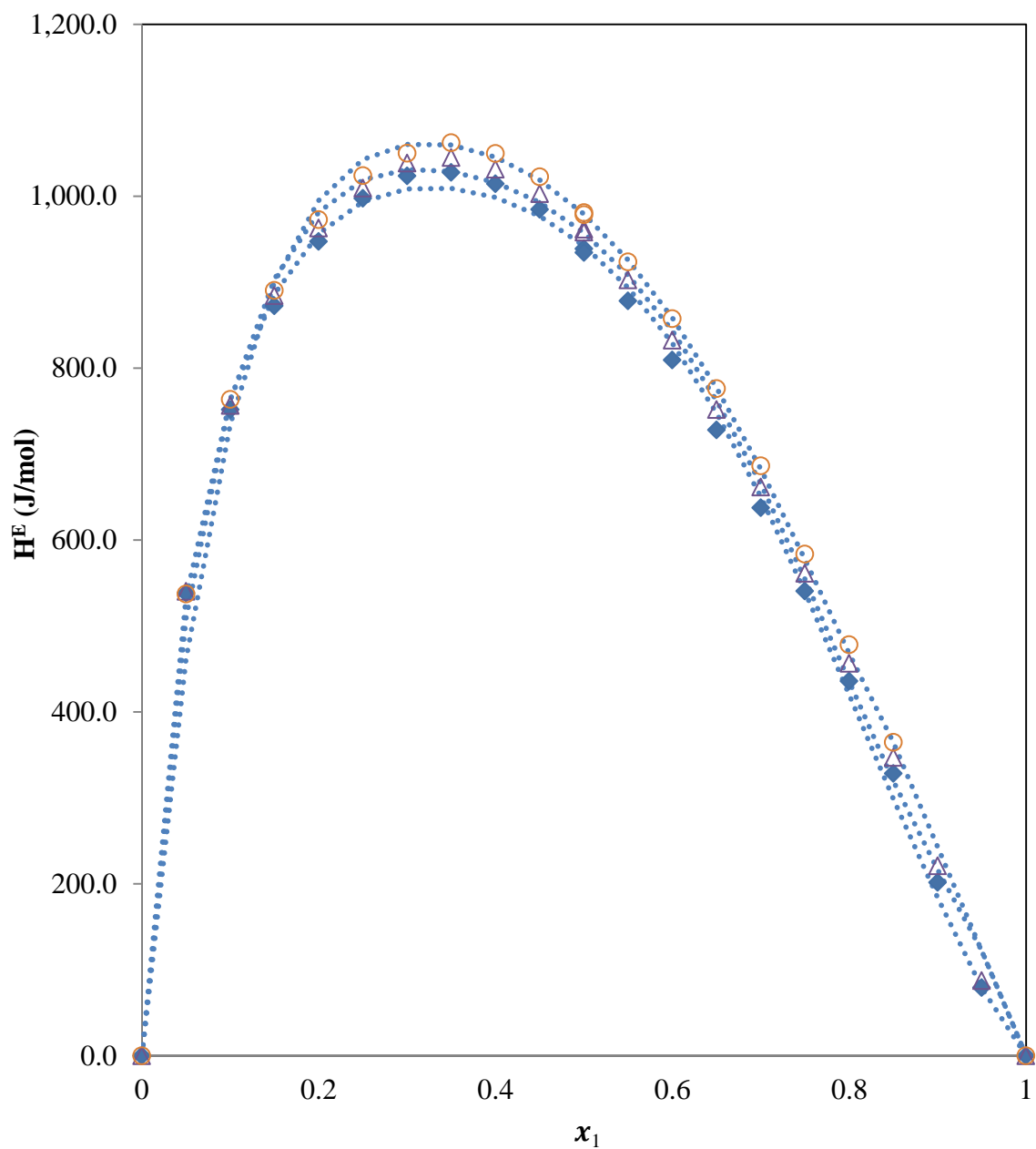


**Figure 4.9.** Excess molar enthalpies  $H_{m,1+23}^E$  for the ternary system  $x_1$  1-Butanol +  $x_2$  Mesitylene +  $(1 - x_1 - x_2)$  *p*-Xylene at 298.15K. Experimental results:  $\blacklozenge$   $x_2/x_3 = 0.3336$ ;  $\triangle$ ,  $x_2/x_3 = 0.9997$ ;  $\circ$ ,  $x_2/x_3 = 3.0005$ ; Curves: ..... , calculated using the equation 4.8 and 4.9

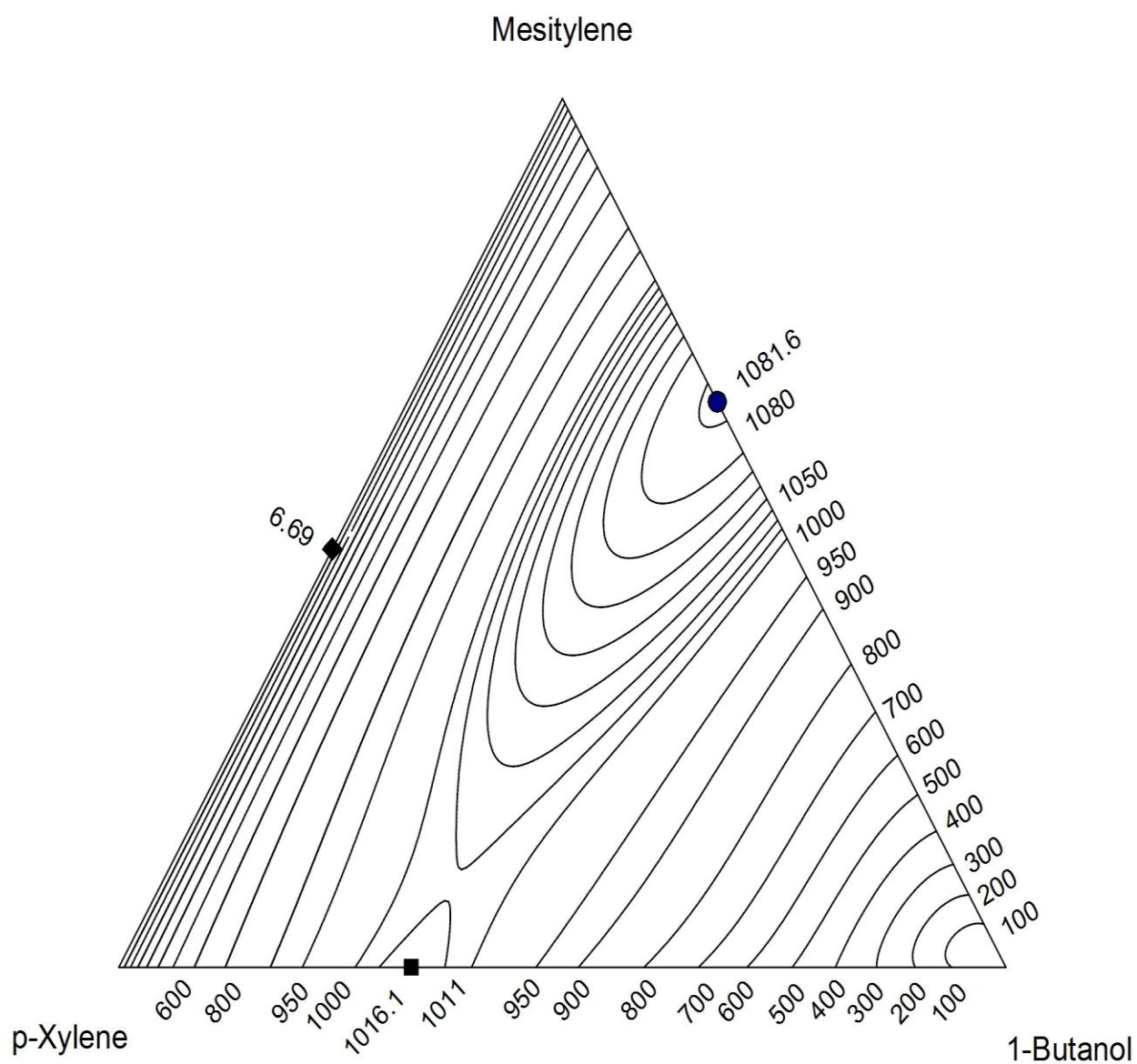


**Figure 4.10.** Constant enthalpy contours,  $H_{m,123}^E$  (J/mol) at 298.15K for the  $x_1$  1-Butanol +  $x_2$  Mesitylene +  $(1 - x_1 - x_2)$  *p*-Xylene, calculated from the representation of the experimental results using the equation 2.3 and 2.4

**Table 4.16.** Experimental excess molar enthalpies  $H_{m,1+23}^E$  (J/mol) and the calculated values of  $H_{m,123}^E$  (J/mol) for the  $x_1$  1-Butanol +  $x_2$  DNBE +  $(1 - x_1 - x_2)$  Mesitylene ternary system at 298.15K

$x_1$	$H_{m,1+23}^E$	$H_{m,123}^E$	$x_1$	$H_{m,1+23}^E$	$H_{m,123}^E$	$x_1$	$H_{m,1+23}^E$	$H_{m,123}^E$
$x_2/x_3 = 0.3334, H_{m,23}^E = 22.29$								
0.0500	453.7	503.5	0.4000	978.9	985.9	0.7000	662.1	696.2
0.1000	668.8	704.8	0.4500	957.5	977.7	0.7500	572.6	589.9
0.1500	804.8	815.9	0.5000	926.2	954.9	0.8000	473.2	470.4
0.2000	886.1	888.2	0.5000	922.7	954.9	0.8500	364.5	340.9
0.2500	944.3	935.8	0.5500	874.3	916.0	0.9000	249.4	204.6
0.3000	974.4	965.4	0.6000	815.0	860.0	0.9500	123.3	72.5
0.3500	985.0	981.5	0.6500	743.3	786.6			
$x_2/x_3 = 1.0003, H_{m,23}^E = 35.74$								
0.0500	381.1	446.4	0.4000	935.7	957.8	0.7000	638.0	608.9
0.1000	610.9	654.3	0.4500	917.8	929.9	0.7500	550.4	522.5
0.1500	746.5	785.8	0.5000	884.4	887.0	0.8000	455.8	431.3
0.2000	837.6	875.0	0.5000	884.0	887.0	0.8500	352.6	334.1
0.2500	889.1	931.7	0.5500	839.4	831.3	0.9000	240.1	227.0
0.3000	924.2	961.5	0.6000	784.1	764.8	0.9500	121.5	107.8
0.3500	940.2	969.0	0.6500	715.9	690.1			
$x_2/x_3 = 2.9944, H_{m,23}^E = 30.45$								
0.0500	350.4	354.2	0.4000	919.3	954.4	0.7000	629.7	653.0
0.1000	576.3	560.6	0.4500	902.6	928.7	0.7500	544.1	589.3
0.1500	714.1	711.4	0.5000	868.7	887.6	0.8000	448.2	521.4
0.2000	810.4	822.5	0.5000	871.0	887.6	0.8500	346.0	442.1
0.2500	865.2	898.7	0.5500	829.5	835.6	0.9000	236.2	338.8
0.3000	904.9	943.4	0.6000	774.6	777.1	0.9500	119.4	194.8
0.3500	919.0	960.7	0.6500	706.8	715.5			

Ternary term for the representation of  $H_{m,1+23}^E$  by equation 4.8 and 4.9:  $H_{m,T}^E = [x_1x_2x_3/(1 - x_1 + x_3)](9687.3 - 82469.3x_1 - 19171.7x_2 + 208054.0x_1^2 + 108548.6x_1x_2 + 45747.3x_2^2 - 151146.2x_1^3 - 236717.8x_1^2x_2)$ ; s/(J/mol) = 33.72.

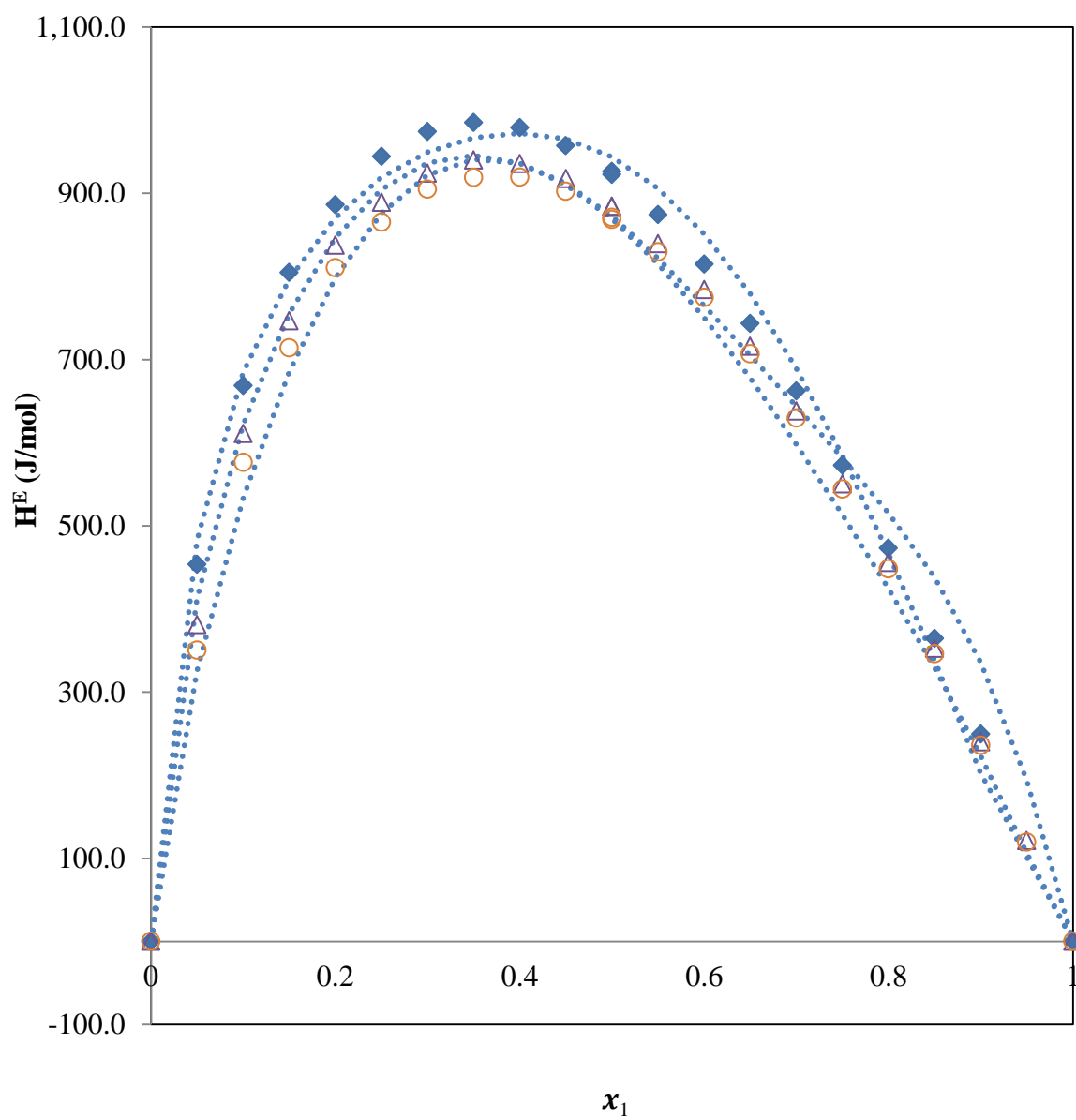


**Figure 4.11.** Excess molar enthalpies  $H_{m,1+23}^E$  for the ternary system  $x_1$  1-Butanol +  $x_2$  DNBE +  $(1 - x_1 - x_2)$  Mesitylene at 298.15K. Experimental results:  $\blacklozenge$   $x_2/x_3 = 0.3336$ ;  $\triangle$ ,  $x_2/x_3 = 0.9997$ ;  $\circ$ ,  $x_2/x_3 = 3.0005$ ; Curves: ..... , calculated using the equation 4.8 and 4.9

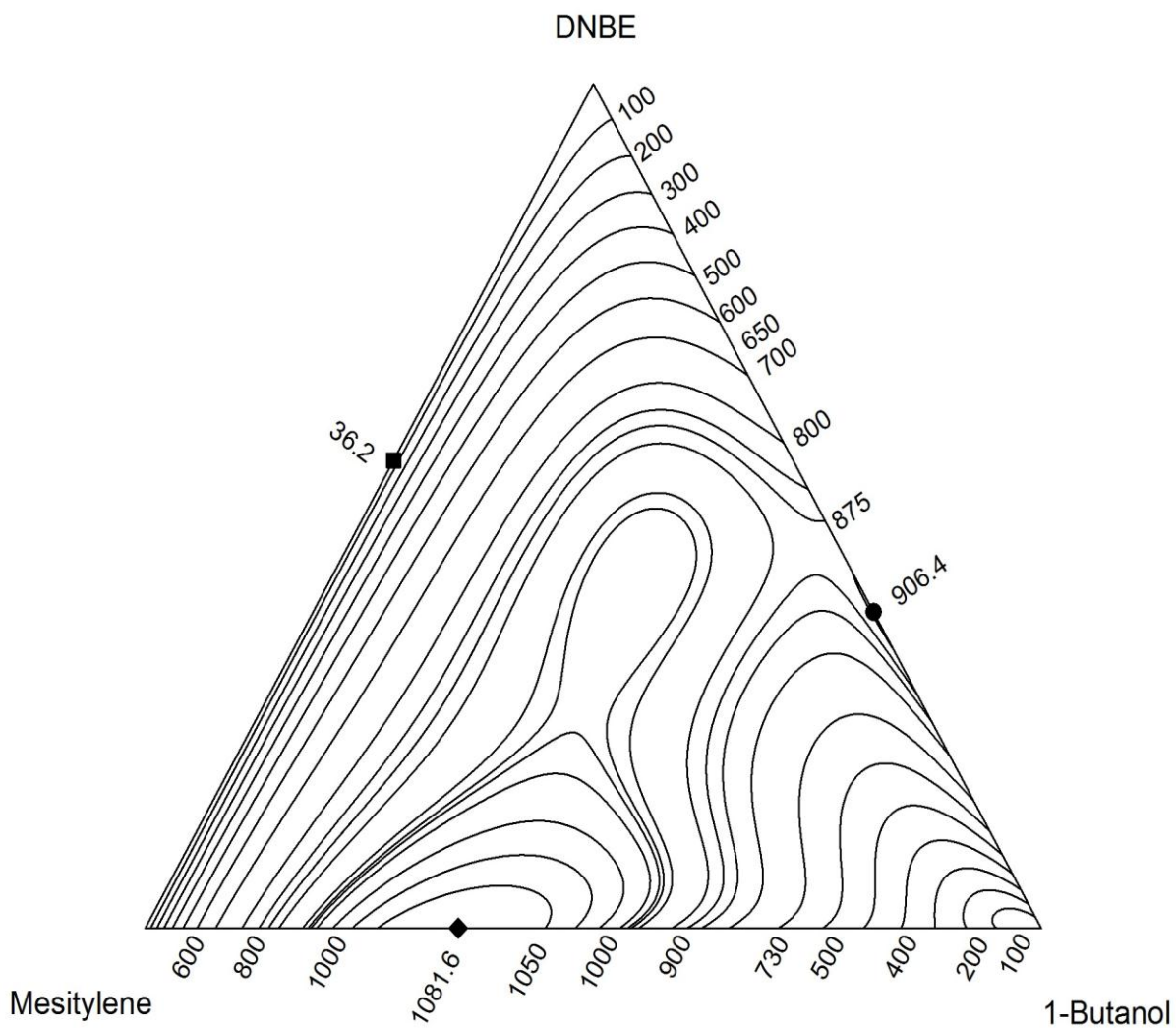


**Figure 4.12.** Constant enthalpy contours,  $H_{m,123}^E$  (J/mol) at 298.15K for the  $x_1$  1-Butanol +  $x_2$  DNBE +  $(1 - x_1 - x_2)$  Mesitylene, calculated from the representation of the experimental results using the equation 2.3 and 2.4

**Table 4.17.** Experimental excess molar enthalpies  $H_{m,1+23}^E$  (J/mol) and the calculated values of  $H_{m,123}^E$  (J/mol) for the  $x_1$  1-Butanol +  $x_2$  2-MTHF +  $(1 - x_1 - x_2)$  EBz ternary system at 298.15K

$x_1$	$H_{m,1+23}^E$	$H_{m,123}^E$	$x_1$	$H_{m,1+23}^E$	$H_{m,123}^E$	$x_1$	$H_{m,1+23}^E$	$H_{m,123}^E$
$x_2/x_3 = 0.3338, H_{m,23}^E = -144.68$								
0.0500	317.8	236.6	0.4000	875.8	796.9	0.7000	605.0	554.3
0.1000	525.8	403.9	0.4500	861.2	794.0	0.7500	523.1	478.6
0.1500	659.8	516.5	0.5000	834.0	774.0	0.8000	431.7	395.5
0.2000	754.3	611.9	0.5000	835.9	774.0	0.8500	332.2	301.1
0.2500	815.9	690.1	0.5500	792.3	737.4	0.9000	212.1	194.7
0.3000	852.0	746.8	0.6000	740.2	686.3	0.9500	92.1	86.0
0.3500	870.8	781.7	0.6500	677.9	624.1			
$x_2/x_3 = 1.0001, H_{m,23}^E = -200.91$								
0.0500	241.1	99.1	0.4000	822.6	707.1	0.7000	597.8	521.8
0.1000	428.0	258.4	0.4500	817.3	712.4	0.7500	519.4	457.3
0.1500	561.9	379.6	0.5000	798.2	700.4	0.8000	430.6	385.4
0.2000	660.1	485.0	0.5000	796.5	700.4	0.8500	335.1	302.8
0.2500	732.8	572.6	0.5500	766.0	672.8	0.9000	219.4	206.9
0.3000	780.1	638.9	0.6000	720.0	631.8	0.9500	103.9	101.7
0.3500	806.1	683.2	0.6500	665.0	580.4			
$x_2/x_3 = 2.9989, H_{m,23}^E = -156.36$								
0.0500	209.5	78.8	0.4000	791.5	701.7	0.7000	599.3	552.1
0.1000	374.1	234.7	0.4500	794.4	711.5	0.7500	522.9	490.5
0.1500	503.5	361.7	0.5000	781.2	705.0	0.8000	435.1	419.4
0.2000	604.6	470.3	0.5000	779.3	705.0	0.8500	338.2	336.2
0.2500	681.0	559.4	0.5500	753.1	683.9	0.9000	231.7	238.1
0.3000	737.3	627.3	0.6000	716.5	650.0	0.9500	105.7	124.9
0.3500	772.1	674.3	0.6500	662.8	605.5			

Ternary term for the representation of  $H_{m,1+23}^E$  by equation 4.8 and 4.9:  
 $H_{m,T}^E = [x_1x_2x_3/(1 - x_1 + x_2)](-11493.1 + 50869.6x_1 - 2819.4x_2 - 81612.9x_1^2 - 4996.3x_1x_2 + 31313.9x_2^2 + 42415.3x_1^3)$ : s(J/mol) = 15.06

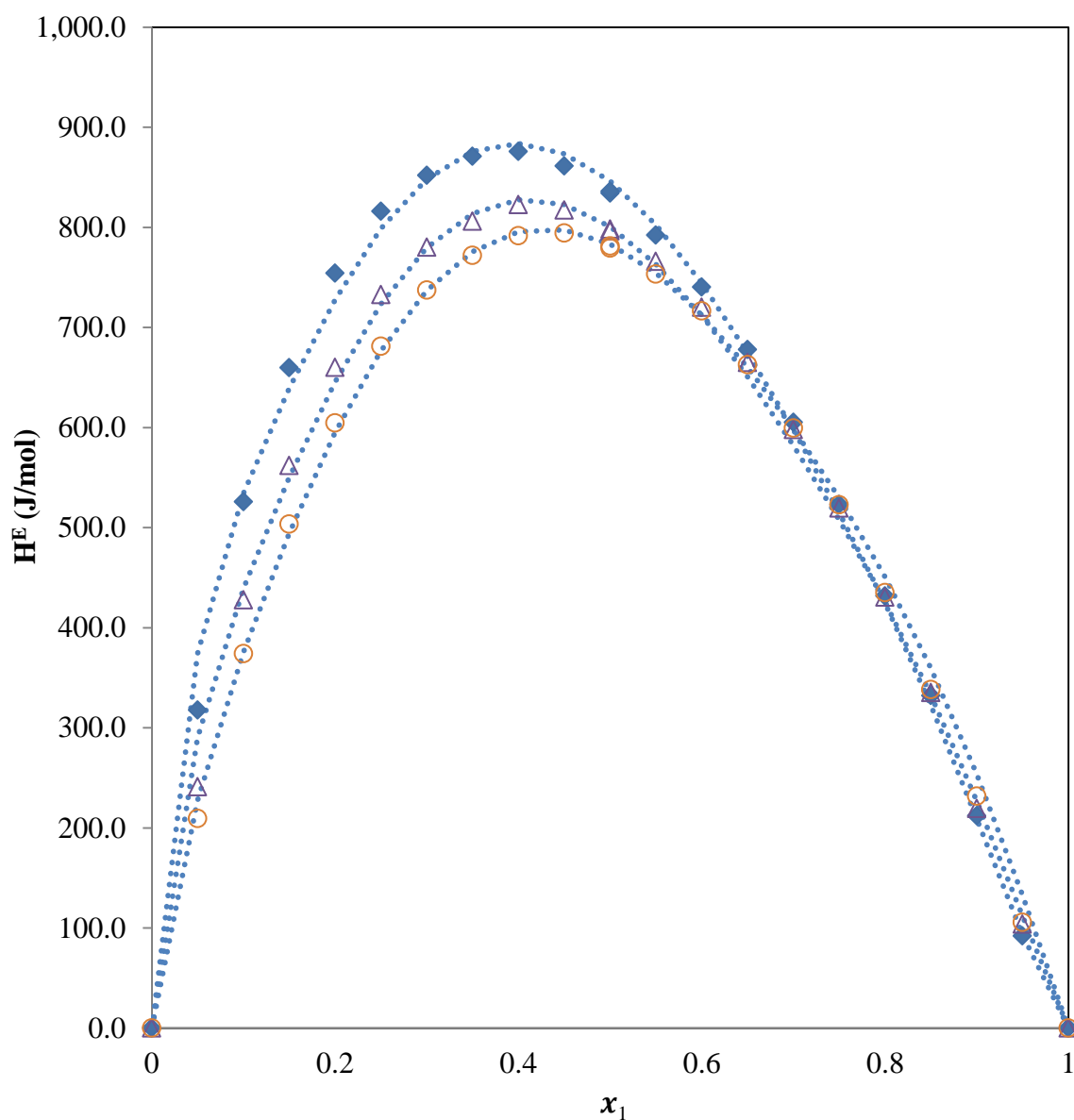


**Figure 4.13.** Excess molar enthalpies  $H_{m,1+23}^E$  for the ternary system  $x_1$  1-Butanol +  $x_2$  2-MTHF +  $(1 - x_1 - x_2)$  EBz at 298.15K. Experimental results: ♦  $x_2/x_3 = 0.3338$ ; Δ,  $x_2/x_3 = 1.0001$ ; ○,  $x_2/x_3 = 2.9989$ ; Curves: ..... , calculated using the equation 4.8 and 4.9

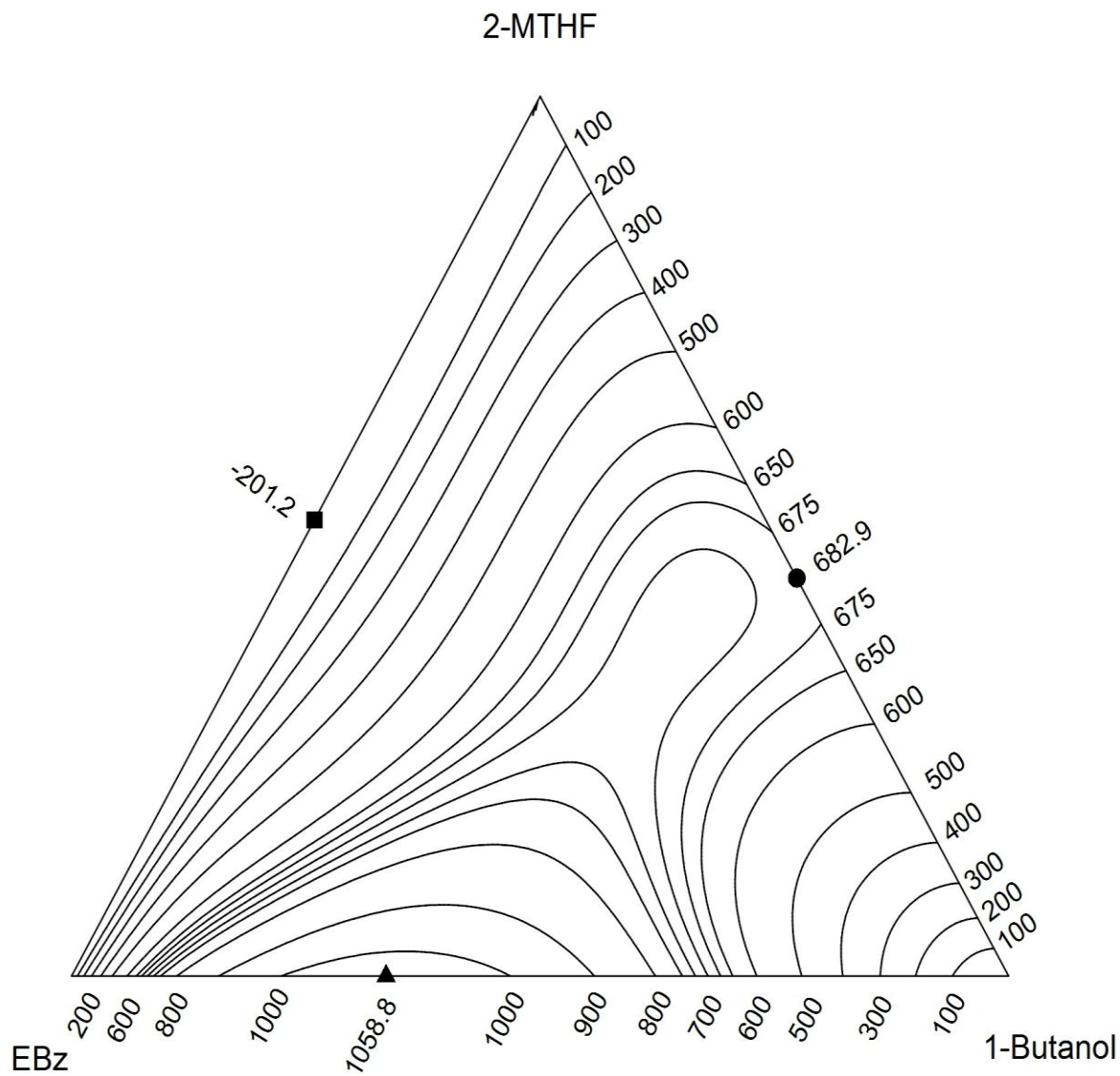


**Figure 4.14.** Constant enthalpy contours,  $H_{m,123}^E$  (J/mol) at 298.15K for the  $x_1$  1-Butanol +  $x_2$  2-MTHF +  $(1 - x_1 - x_2)$  EBz, calculated from the representation of the experimental results using the equation 2.3 and 2.4

**Table 4.18.** Experimental excess molar enthalpies  $H_{m,1+23}^E$  (J/mol) and the calculated values of  $H_{m,123}^E$  (J/mol) for the  $x_1$  DNBE +  $x_2$  2-MTHF +  $(1 - x_1 - x_2)$  EBz ternary system at 298.15K

$x_1$	$H_{m,1+23}^E$	$H_{m,123}^E$	$x_1$	$H_{m,1+23}^E$	$H_{m,123}^E$	$x_1$	$H_{m,1+23}^E$	$H_{m,123}^E$
$x_2/x_3 = 0.3338, H_{m,23}^E = -144.68$								
0.0500	35.4	-102.9	0.4000	153.3	67.2	0.7000	120.0	76.2
0.1000	65.2	-65.6	0.4500	155.1	75.8	0.7500	104.2	68.8
0.1500	90.8	-32.8	0.5000	153.6	81.1	0.8000	86.2	58.7
0.2000	111.4	-4.5	0.5000	153.6	81.1	0.8500	64.8	45.6
0.2500	127.5	19.5	0.5500	149.9	83.6	0.9000	42.2	30.0
0.3000	139.9	39.3	0.6000	142.3	83.5	0.9500	19.1	13.5
0.3500	148.5	55.2	0.6500	132.1	81.0			
$x_2/x_3 = 1.0001, H_{m,23}^E = -200.91$								
0.0500	43.1	-147.8	0.4000	189.8	69.1	0.7000	148.8	89.2
0.1000	80.1	-100.9	0.4500	191.8	81.3	0.7500	132.3	80.7
0.1500	111.0	-59.9	0.5000	190.8	89.7	0.8000	109.4	68.6
0.2000	136.2	-24.3	0.5000	190.6	89.7	0.8500	83.0	53.0
0.2500	156.2	6.1	0.5500	185.3	94.5	0.9000	52.9	34.6
0.3000	172.1	31.7	0.6000	176.7	96.0	0.9500	23.9	15.5
0.3500	183.0	52.6	0.6500	164.9	94.2			
$x_2/x_3 = 2.9989, H_{m,23}^E = -156.36$								
0.0500	44.7	-103.4	0.4000	197.6	102.8	0.7000	154.1	109.3
0.1000	83.2	-57.6	0.4500	200.2	113.3	0.7500	137.1	97.3
0.1500	115.0	-18.0	0.5000	199.2	119.8	0.8000	110.9	81.5
0.2000	140.1	16.1	0.5000	198.6	119.8	0.8500	90.1	62.0
0.2500	162.1	45.0	0.5500	191.6	122.6	0.9000	63.0	39.9
0.3000	179.9	68.9	0.6000	180.3	121.8	0.9500	31.5	17.7
0.3500	189.6	88.1	0.6500	171.4	117.3			

Ternary term for the representation of  $H_{m,1+23}^E$  by equation 4.8 and 4.9:  $H_{m,T}^E = [x_1 x_2 x_3 / (1 - x_1 + x_3)](493.7 + 2711.7x_1 + 2077.4x_2 - 6607.0x_1^2 - 3805.6x_1x_2 + 186.1x_2^2 + 4717.0x_1^3 + 8340.8x_1^2x_2)$ ; s/(J/mol) = 1.86

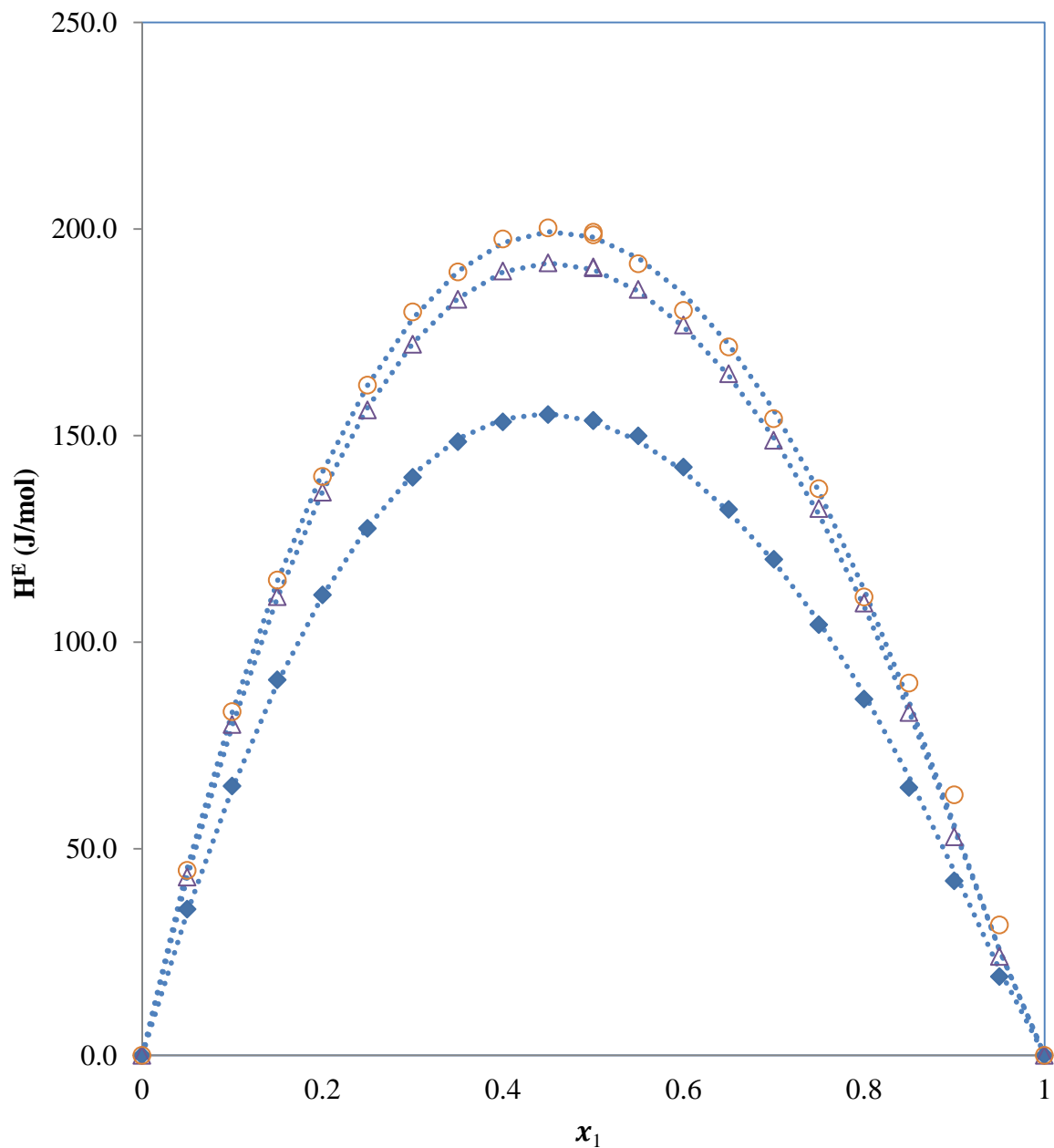


**Figure 4.15.** Excess molar enthalpies  $H_{m,1+23}^E$  for the ternary system  $x_1$  DNBE +  $x_2$  2-MTHF +  $(1 - x_1 - x_2)$  EBz at 298.15K. Experimental results:  $\blacklozenge$   $x_2/x_3 = 0.3338$ ;  $\triangle$ ,  $x_2/x_3 = 1.0001$ ;  $\circ$ ,  $x_2/x_3 = 2.9989$ ; Curves: ..... , calculated using the equation 4.5 and 4.6

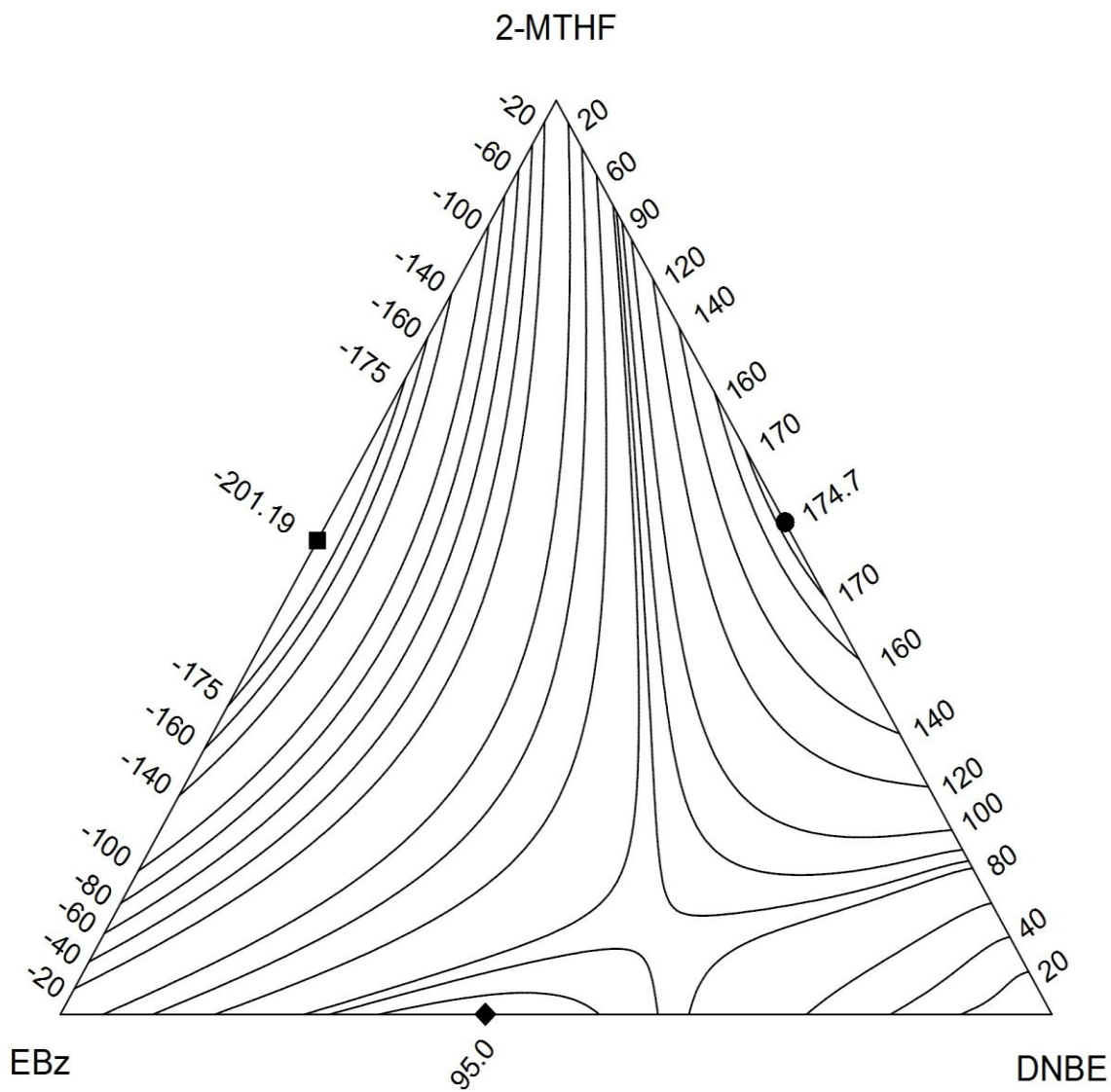


**Figure 4.16.** Constant enthalpy contours,  $H_{m,123}^E$  (J/mol) at 298.15K for the  $x_1$  DNBE +  $x_2$  2-MTHF +  $(1 - x_1 - x_2)$  EBz, calculated from the representation of the experimental results using the equation 2.3 and 2.4

**Table 4.19.** Experimental excess molar enthalpies  $H_{m,1+23}^E$  (J/mol) and the calculated values of  $H_{m,123}^E$  (J/mol) for the  $x_1$  DNBE +  $x_2$  2-MTHF +  $(1 - x_1 - x_2)$  EBz ternary system at 298.15K

$x_1$	$H_{m,1+23}^E$	$H_{m,123}^E$	$x_1$	$H_{m,1+23}^E$	$H_{m,123}^E$	$x_1$	$H_{m,1+23}^E$	$H_{m,123}^E$
$x_2/x_3 = 0.3336, H_{m,23}^E = 5.05$								
0.0500	-8.0	-2.5	0.4000	-26.3	-23.5	0.7000	-18.2	-16.5
0.1000	-13.8	-8.7	0.4500	-26.2	-23.2	0.7500	-15.8	-14.1
0.1500	-18.0	-13.6	0.5000	-25.1	-22.6	0.8000	-12.7	-11.5
0.2000	-21.3	-17.4	0.5000	-25.0	-22.6	0.8500	-9.5	-8.5
0.2500	-23.5	-20.1	0.5500	-23.9	-21.6	0.9000	-6.1	-5.2
0.3000	-25.3	-22.0	0.6000	-22.4	-20.2	0.9500	-3.3	-1.8
0.3500	-26.3	-23.1	0.6500	-20.6	-18.5			
$x_2/x_3 = 0.9997, H_{m,23}^E = 6.68$								
0.0500	-4.3	2.5	0.4000	-10.0	-5.9	0.7000	-3.4	-1.8
0.1000	-6.9	-0.9	0.4500	-9.1	-5.3	0.7500	-2.3	-1.0
0.1500	-8.9	-3.3	0.5000	-7.9	-4.6	0.8000	-1.3	-0.5
0.2000	-10.3	-4.8	0.5000	-7.8	-4.6	0.8500	-0.3	0.0
0.2500	-10.6	-5.8	0.5500	-7.0	-3.9	0.9000	0.5	0.7
0.3000	-11.0	-6.3	0.6000	-5.8	-3.3	0.9500	0.6	1.5
0.3500	-10.7	-6.3	0.6500	-4.6	-2.5			
$x_2/x_3 = 3.0005, H_{m,23}^E = 4.62$								
0.0500	-0.2	4.5	0.4000	9.4	12.2	0.7000	13.4	14.9
0.1000	0.3	4.4	0.4500	10.7	13.6	0.7500	12.7	14.0
0.1500	1.4	5.2	0.5000	12.3	14.6	0.8000	11.6	12.3
0.2000	2.9	6.4	0.5000	12.1	14.6	0.8500	10.1	10.1
0.2500	4.5	7.7	0.5500	12.7	15.2	0.9000	7.4	7.8
0.3000	6.0	9.1	0.6000	13.4	15.4	0.9500	3.5	5.5
0.3500	7.7	10.7	0.6500	13.5	15.3			

Ternary term for the representation of  $H_{m,1+23}^E$  by equation 4.8 and 4.9:  $H_{m,T}^E = [x_1x_2x_3/(1 - x_1 + x_3)](-584.0 + 934.7x_1 + 980.4x_2 - 593.9x_1^2 - 1063.0x_1x_2 - 885.3x_2^2)$ ; s/(J/mol) = 0.35

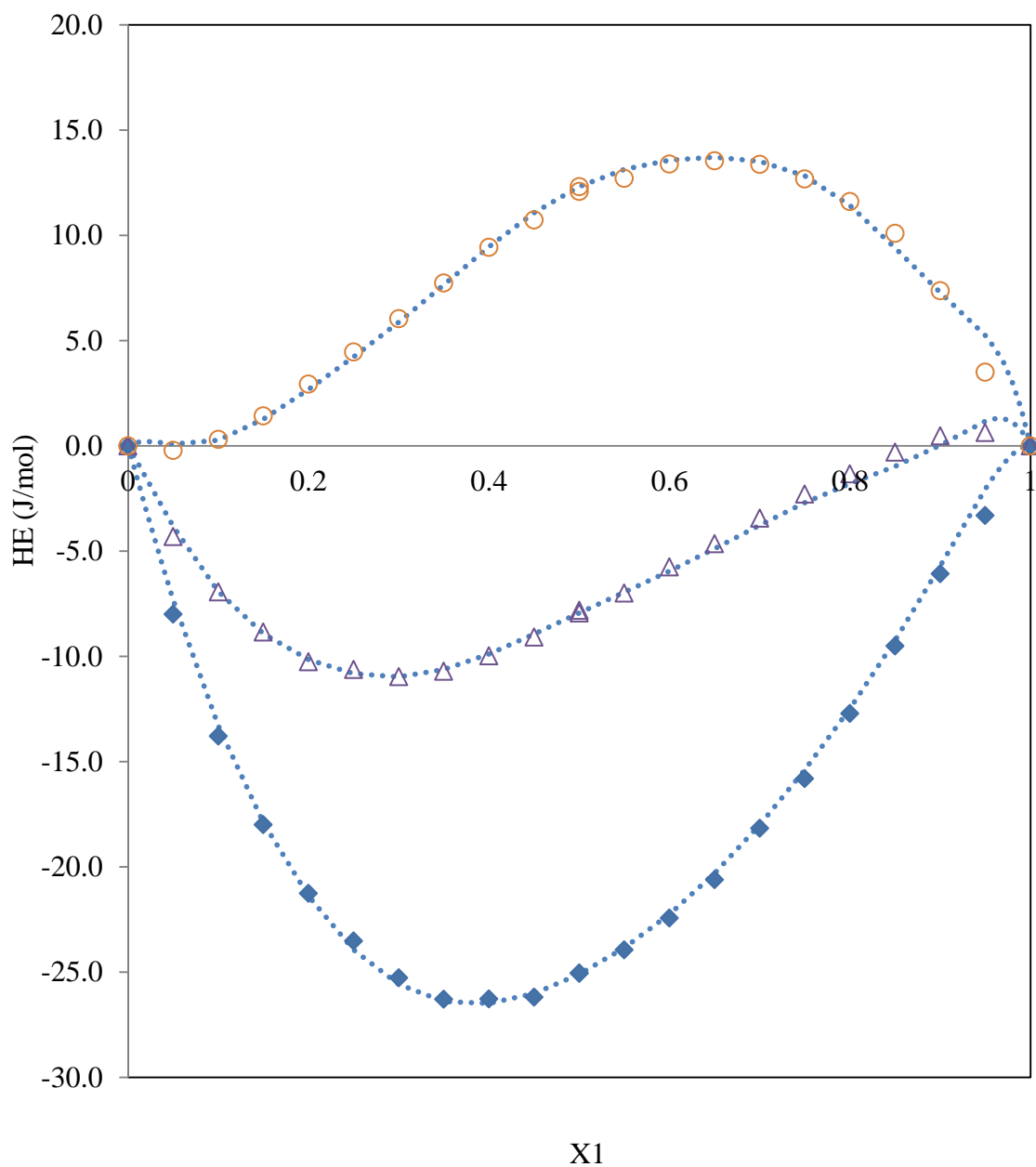


**Figure 4.17.** Excess molar enthalpies  $H_{m,1+23}^E$  for the ternary system  $x_1$  DNBE +  $x_2$  Mesitylene +  $(1 - x_1 - x_2)$  *p*-Xylene at 298.15K. Experimental results:  $\blacklozenge$   $x_2/x_3 = 0.3338$ ;  $\triangle$ ,  $x_2/x_3 = 1.0001$ ;  $\circ$ ,  $x_2/x_3 = 2.9989$ ; Curves: ..... , calculated using the equation 4.8 and 4.9

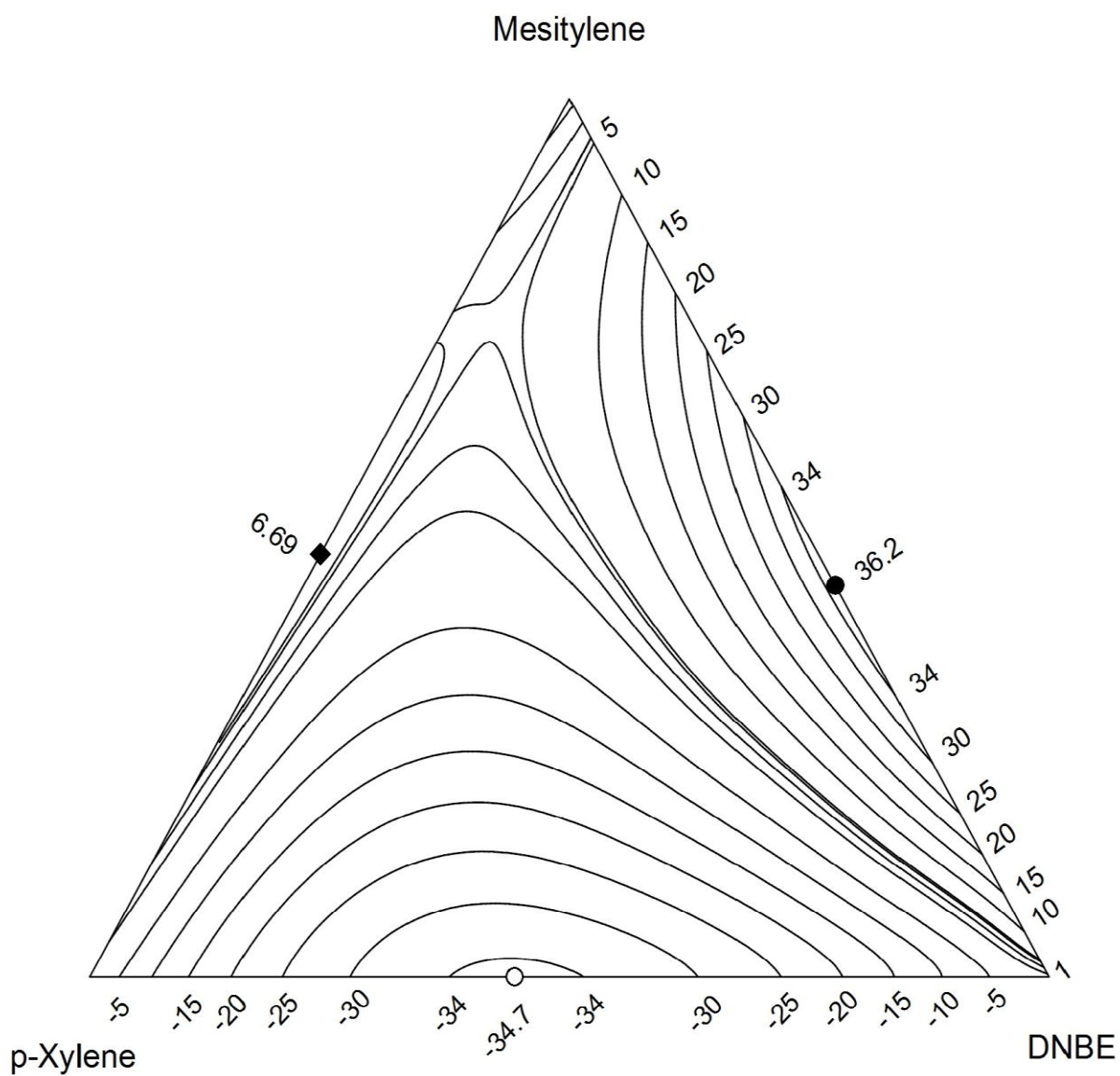


**Figure 4.18.** Constant enthalpy contours,  $H_{m,123}^E$  (J/mol) at 298.15K for the  $x_1$  DNBE +  $x_2$  Mesitylene +  $(1 - x_1 - x_2)$  *p*-Xylene, calculated from the representation of the experimental results using the equation 2.3 and 2.4

#### 4.3.2 Prediction of experimental data by Liebermann - Fried solution theory model

The ternary excess molar enthalpy values were also predicted by means of the Liebermann-Fried model. Only the pure component properties and the interaction parameters were required for the constituent binaries. Table 4.20 shows the standard deviation 's' of the excess molar enthalpy values predicted by the Liebermann-Fried model for the ternary system. The table serves to indicate that the Liebermann-Fried model was fairly able to predict the ternary excess molar enthalpy values of few systems.

**Table 4.20.** Standard deviation 's' for the ternary enthalpy values predicted by the Liebermann-Fried model for the ternary systems.

Ternary	Component			Std. deviation 's' J/mol
	1	2	3	
1	2-MTHF	EBz	<i>p</i> -Xylene	8.1
2	2-MTHF	EBz	Mesitylene	3.6
3	2-ME	EBz	Mesitylene	47.6
4	2-ME	2-MTHF	<i>p</i> -Xylene	20.0
5	1-Butanol	Mesitylene	<i>p</i> -Xylene	41.8
6	1-Butanol	DNBE	Mesitylene	43.9
7	1-Butanol	2-MTHF	EBz	33.0
8	DNBE	2-MTHF	EBz	7.2
9	DNBE	Mesitylene	<i>p</i> -Xylene	9.1

For the 2-MTHF (1) + EBz (2) + Mesitylene (3) ternary system the Liebermann-Fried model was able to predict the ternary contours more accurately than the Tsao-Smith model. But in general

the Liebermann-fried model was not that successful in predicting the ternary contours. No internal maximum exists for all the nine ternary systems. An internal saddle points exists for the 2-ME (1) + 2-MTHF (2) + *p*-Xylene (3), (1-Butanol or DNBE) (1) + 2-MTHF (2) + EBz (3) ternary systems. The standard deviation is relatively higher for the ternary systems involving 1-Butanol and 2-ME as the component 1.

## 5.0 CONCLUSIONS AND RECOMMENDATIONS

### 5.1 Conclusions

The experimental excess molar enthalpy values for 15 binaries and nine ternary systems at 298.15K have been satisfactorily carried out using an LKB (10700-1) flow microcalorimeter. The following conclusions can be drawn based on the results obtained in this study.

- The binary mixtures studied shows, systems exhibiting positive and negative excess molar enthalpy values. The reason for exothermic and endothermic mixing behavior of specific mixtures was analyzed in this study.
- The Liebermann-Fried model was able to represent the experimental excess molar enthalpy of some binary and ternary systems with reasonable accuracy with a standard deviation ranging from 0.3 - 59.5 J/mol for the binary systems and 3.6 - 47.6 J/mol for the ternary systems.
- The Tsao-Smith model was closely able to represent the excess molar enthalpy of all ternary systems except the 1-Butanol ternary system.
- The Liebermann-fried model was able to predict the ternary excess molar enthalpies of (2-MTHF + hydrocarbons) and (DNBE + 2-MTHF + EBz) ternary systems, for the other seven ternary systems the model predicts the enthalpy values with high standard deviation.

## 5.2 Recommendations

Following recommendations are suggested for future studies.

- Vapor liquid equilibrium (VLE) values for the binary systems studied in this research work can be experimentally measured. The measured values can be compared with the values calculated using the Liebermann-Fried model binary interaction parameters, determined in this study.
- Out of the possible 35 ternary systems involving the chosen seven chemicals, nine ternary systems have been studied in this research work. It would be interesting to study the excess molar enthalpy of the other 26 ternary systems.
- For further studies it is desirable to apply other thermodynamic models to predict the binary and ternary excess molar enthalpies values measured in this research work and can be compared with the models used in this study.

## 6.0 REFERENCES

- Abe, A., Flory, P. (1965). The thermodynamic properties of mixtures of small, nonpolar molecules. *Journal of the American Chemical Society*, 87(9), 1838-1846.
- Abrams, D. S., Prausnitz, J. M. (1975). Statistical thermodynamics of liquid mixtures: a new expression for the excess Gibbs energy of partly or completely miscible systems. *AIChE Journal*, 21(1), 116-128.
- Aicart, E., Junquera, E., Letcher, T. M. (1995). Isobaric thermal expansivity and isothermal compressibility of several nonsaturated hydrocarbons at 298.15 K. *Journal of Chemical and Engineering Data*, 40(6), 1225-1227.
- Ancillotti, F., Fattore, V. (1998). Oxygenate fuels: Market expansion and catalytic aspect of synthesis. *Fuel Processing Technology*, 57(3), 163-194.
- Baud, M. (1915). Thermal analysis of binary mixtures. *Bull. Soc. Chim. Fr*, 17, 329-345.
- Bauer, N. (1959). Determination of Density. *Physical Methods of Organic Chemistry, Part I*; Arnold Weissberger. editor, Interscience: New York, 1959, chapter IV.
- Bevington, P. R., Robinson, D. K. (2003). Data reduction and error analysis for the physical sciences. *Data reduction and error analysis for the physical sciences*; McGraw-Hill, New York, 2003.
- Bose, E. (1907). Calorimetric studies. *Z. Phys. Chem*, 58, 585-624.
- Brandreth, D. A., O'Neill, S. P., Missen, R. W. (1966). Thermodynamic excess functions of binary solutions involving a fluoroalcohol. *Transactions of the Faraday Society*, 62(0), 2355-2366.

- CEPA. (1990). Ministry of Justice Retrieved from <http://laws-lois.justice.gc.ca/PDF/SOR-90-247.pdf>.
- Cerdeiriña, C. A., Tovar, C. A., González, D., Carballo, E., Romaní, L. (2001). Thermodynamics of the nitromethane + 1-butanol system near the upper critical point. *Fluid Phase Equilibria*, 179(1–2), 101-115.
- Christensen, J., Hansen, L., Eatough, D., Izatt, R., Hart, R. (1976). Isothermal high pressure flow calorimeter. *Review of Scientific Instruments*, 47(6), 730-734.
- Christensen, J. J., Johnston, H. D., Izatt, R. M. (1968). An Isothermal Titration Calorimeter. *Review of Scientific Instruments*, 39(9), 1356-1359.
- Clarke, B. (1905). Determination of Several Heats of Mixing. *Phys. Z*, 5, 154-159.
- Cobos, J. C., Garcia, I., Gonzalez, J. A., Casanova, C. (1988). Excess enthalpy. 2-Methoxyethanol - 1-butanol system. *International DATA Series, Selected Data on Mixtures, Series A: Thermodynamic Properties of Non-Reacting Binary Systems of Organic Substances*(2), 85.
- Davis, J. M., Farland, W. H. (2001). The paradoxes of MTBE. *Toxicological Sciences*, 61(2), 211-217.
- Elliott, K., Wormald, C. J. (1976). A precision differential flow calorimeter the excess enthalpy of benzene + cyclohexane between 280.15 K and 393.15 K. *The Journal of Chemical Thermodynamics*, 8(9), 881-893.
- Flory, P. (1965). Statistical thermodynamics of liquid mixtures. *Journal of the American Chemical Society*, 87(9), 1833-1838.

- Francesconi, R., Comelli, F. (1997). Excess Molar Enthalpies, Densities, and Excess Molar Volumes of Diethyl Carbonate in Binary Mixtures with Seven n-Alkanols at 298.15 K. *Journal of Chemical and Engineering Data*, 42(1), 45-48.
- George, J., Sastry, N. V. (2003). Densities, excess molar volumes, viscosities, speeds of sound, excess isentropic compressibilities, and relative permittivities for  $C_mH_{2m+1}(OCH_2CH_2)_nOH$  ( $m=1$  or  $2$  or  $4$  and  $n=1$ ) + benzene, + toluene, + (o-, m-, and p-) xylenes, + ethylbenzene, and + cyclohexane. *Journal of Chemical and Engineering Data*, 48(4), 977-989.
- Gill, P., Moghadam, T. T., Ranjbar, B. (2010). Differential scanning calorimetry techniques: applications in biology and nanoscience. *Journal of biomolecular techniques: JBT*, 21(4), 167.
- Giner, B., Artigas, H., Carrion, A., Lafuente, C., Royo, F. (2003). Excess thermodynamic properties of isomeric butanols with 2-methyl-tetrahydrofuran. *Journal of molecular liquids*, 108(1-3), 303-311.
- Harsted, B. S., Thomsen, E. S. (1974). Excess enthalpies from flow microcalorimetry 1. Experimental method and excess enthalpies for carbon tetrachloride + cyclohexane, +benzene, and +octamethylcyclotetrasiloxane, and of n-hexane + cyclohexane. *The Journal of Chemical Thermodynamics*, 6(6), 549-555.
- Hassan, S. M. N. (2010). *Excess molar enthalpies of binary and ternary systems involving hydrocarbons and ethers*. (Master of Science), University of Saskatchewan, Saskatoon.

- Hirobe, H. I. (1925). Thermochemical studies II. The thermochemistry of concentrated solution. *The Journal of the College of Science, Imperial University of Tokyo*, 1, 155-222.
- Höhne, G., Hemminger, W., Flammersheim, H.-J. (2003). *Differential scanning calorimetry*: Springer
- Holt, D. L., Smith, B. D. (1974). Measurement of excess enthalpies with Tronac titration calorimeter. Data for some C<sub>8</sub> aromatic binaries. *Journal of Chemical and Engineering Data*, 19(2), 129-133.
- Hsu, K.-Y., Lawrence Clever, H. (1975). The excess enthalpies of the 15 binary mixtures formed from cyclohexane, benzene, toluene, 1, 4-dimethylbenzene, 1, 2, 4-trimethylbenzene, and 1, 3, 5-trimethylbenzene at 298.15 K. *The Journal of Chemical Thermodynamics*, 7(5), 435-442.
- Jablonski, P., Müller-Blecking, A., Borchard, W. (2003). A method to determine mixing enthalpies by DSC. *Journal of Thermal Analysis and Calorimetry*, 74(3), 779-787.
- Kammerer, K., Lichtenthaler, R. (1998). Excess properties of binary alkanol–ether mixtures and the application of the ERAS model. *Thermochimica Acta*, 310(1), 61-67.
- Kimura, F., Benson, G. C., Halpin, C. J. (1983). Excess enthalpies of binary mixtures of n-heptane with hexane isomers. *Fluid Phase Equilibria*, 11(3), 245-250.
- Kinart, C., Kinart, W., Ćwiklińska, A. (2002). 2-Methoxyethanol–Tetrahydrofuran–Binary Liquid System. Viscosities, densities, excess molar volumes and excess Gibbs activation energies of viscous flow at various temperatures. *Journal of Thermal Analysis and Calorimetry*, 68(1), 307-317.

- Lasdon, L. S., Waren, A. D., Jain, A., Ratner, M. (1978). Design and testing of a generalized reduced gradient code for nonlinear programming. *ACM Transactions on Mathematical Software (TOMS)*, 4(1), 34-50.
- Liao, W.-C., Lin, H.-M., Lee, M.-J. (2009a). Excess Molar Enthalpies of Binary Systems of 2-Octanone or 3-Octanone with Dodecane, Tetradecane, or Hexadecane at 298.15 K. *Journal of Chemical and Engineering Data*, 55(1), 217-222.
- Liao, W.-C., Lin, H.-M., Lee, M.-J. (2009b). Excess Molar Enthalpies of Binary Systems of n-Valeric Anhydride or n-Hexanoic Anhydride with n-Dodecane, n-Tetradecane, or n-Hexadecane at 298.15 K. *Journal of Chemical and Engineering Data*, 56(4), 757-762.
- Liao, W.-C., Lin, H.-m., Lee, M.-J. (2012). Excess molar enthalpies of binary systems containing 2-octanone, hexanoic acid, or octanoic acid at 298.15 K. *The Journal of Chemical Thermodynamics*, 44(1), 51-56.
- Liebermann, E., Fried, V. (1972a). Estimation of the Excess Gibbs Free Energy and Enthalpy of Mixing of Binary Nonassociated Mixtures. *Industrial and Engineering Chemistry Fundamentals*, 11(3), 350-354.
- Liebermann, E., Fried, V. (1972b). The temperature dependence of the excess Gibbs free energy of binary nonassociated mixtures. *Industrial and Engineering Chemistry Fundamentals*, 11(3), 354-355.
- Marquardt, D. W. (1963). An algorithm for least-squares estimation of nonlinear parameters. *Journal of the Society for Industrial and Applied Mathematics*, 11(2), 431-441.

- Marsh, K. N., Niamskul, P., Gmehling, J., Bölts, R. (1999). Review of thermophysical property measurements on mixtures containing MTBE, TAME, and other ethers with non-polar solvents. *Fluid Phase Equilibria*, 156(1), 207-227.
- Mato, M., Illobre, M., Verdes, P., Paz Andrade, M. (2006). Excess molar enthalpies of the ternary system mtbe+ ethanol+ hexane. *Journal of Thermal Analysis and Calorimetry*, 84(1), 291-295.
- Monk, P., Wadsö, I. (1968). A flow micro reaction calorimeter. *Acta chem. scand*, 22(6), 1842-1852.
- Morris, J. W., Mulvey, P. J., Abbott, M. M., Van Ness, H. C. (1975). Excess thermodynamic functions for ternary systems. I. Acetone-chloroform-methanol at 50. deg. *Journal of Chemical and Engineering Data*, 20(4), 403-405.
- Mrazek, R. V., Van Ness, H. C. (1961). Heats of mixing: Alcohol- aromatic binary systems at 25°, 35°, and 45°C. *AIChE Journal*, 7(2), 190-195.
- Navidi, W. C. (2008). *Statistics for engineers and scientists*: McGraw-Hill Higher Education.
- Nayak, J. N., Aralaguppi, M. I., Aminabhavi, T. M. (2002). Density, viscosity, refractive index, and speed of sound in the binary mixtures of ethyl chloroacetate with aromatic liquids at 298.15, 303.15, and 308.15 K. *Journal of Chemical and Engineering Data*, 47(4), 964-969.
- Nishimoto, M., Tabata, S., Tamura, K., Murakami, S. (1997). Thermodynamic properties of the mixture of methoxyethanol and cyclohexane: Measurements at the temperatures 293.15, 298.15 and 303.15 K above and below UCST. *Fluid Phase Equilibria*, 136(1), 235-247.

- O'Shea, S. J., Stokes, R. H. (1986). Activity coefficients and excess partial molar enthalpies for (ethanol + hexane) from 283 to 318 K. *The Journal of Chemical Thermodynamics*, 18(7), 691-696.
- Ott, J. B., Sipowska, J. T. (1996). Applications of calorimetry to nonelectrolyte solutions. *Journal of Chemical and Engineering Data*, 41(5), 987-1004.
- Peng, D.-Y., Benson, G. C., Lu, B. C.-Y. (1998). Excess enthalpies of {2-methoxyethanol+methyl 1, 1-dimethylethyl ether, or n-heptane} at the temperature 298.15 K. *The Journal of Chemical Thermodynamics*, 30(9), 1141-1146.
- Peng, D.-Y., Benson, G. C., Lu, B. C.-Y. (2002). Excess enthalpies of (di- n-butyl ether + 2, 2, 4-trimethylpentane + heptane, or octane) at the temperature 298.15 K. *The Journal of Chemical Thermodynamics*, 34(4), 413-422.
- Peng, D.-Y., Wang, Z., Benson, G. C., Lu, B. C. Y. (2001). Predicting the excess enthalpies and vapor–liquid equilibria of multicomponent systems containing ether and hydrocarbons. *Fluid Phase Equilibria*, 182(1–2), 217-227.
- Picker, P. (1974). New concepts in design and applications of flow microcalorimetry *Can Res. Dev*, Jan - Feb, 11-16.
- Polák, J., Murakami, S., Lam, V., Pflug, H., Benson, G. (1970). Molar excess enthalpies, volumes, and Gibbs free energies of methanol-isomeric butanol systems at 25 C. *Canadian Journal of Chemistry*, 48(16), 2457-2465.
- Prchal, M., Dohnal, V., Veselý, F. (1982). Representation of binary excess enthalpy data. *Collection of Czechoslovak Chemical Communications*, 47(12), 3171-3176.

- Renon, H., Prausnitz, J. M. (1968). Local compositions in thermodynamic excess functions for liquid mixtures. *AIChE Journal*, 14(1), 135-144.
- Riddick, J. A., Bunger, W. B., Sakano, T. K. (1986). Organic solvents: physical properties and methods of purification; Wiley: New York.
- Rodríguez de Rivera, M., Socorro, F., Matos, J. S. (2009). Heats of mixing using an isothermal titration calorimeter: associated thermal effects. *International journal of molecular sciences*, 10(7), 2911-2920.
- Rodríguez de Rivera, M., & Socorro, F. (2007). Flow microcalorimetry and thermokinetics of liquid mixtures. *Journal of Thermal Analysis and Calorimetry*, 87(2), 591-594.
- Rogalski, M., Malanowski, S. (1977). A new equation for correlation of vapour-liquid equilibrium data of strongly non-ideal mixtures. *Fluid Phase Equilibria*, 1(2), 137-152.
- Smith, J. M., Van Ness, H. C., Abbott, M. M. (2005). *Introduction to chemical engineering thermodynamics* (7th ed.). Boston: McGraw-Hill.
- Tanaka, R., Benson, G. C. (1976). Excess enthalpies of some ethylbenzene + aromatic hydrocarbon mixtures at 298.15 K. *The Journal of Chemical Thermodynamics*, 8(3), 259-268.
- Tanaka, R., D'Arcy, P. J., Benson, G. C. (1975). Application of a flow microcalorimeter to determine the excess enthalpies of binary mixtures of non-electrolytes. *Thermochimica Acta*, 11(2), 163-175.
- Tsao, C., Smith, J. (1953). *Heats of mixing of liquids*. Paper presented at the Chem. Eng. Prog. Symp. Ser.

- Wadso, I. (1968). Design and testing of a micro reaction calorimeter. *Acta Chemica Scandinavica*, 22.
- Wang, L., Benson, G. C., Lu, B. C. Y. (1992). Excess enthalpies of (ethanol + hexane + decane or dodecane) at the temperature 298.15 K. *The Journal of Chemical Thermodynamics*, 24(11), 1135-1143.
- Wang, Z., Benson, G. C., Lu, B. C. Y. (2001). Excess Enthalpies of 2-Methyltetrahydrofuran + n-Alkane Binary Mixtures at 298.15 K. *Journal of Chemical and Engineering Data*, 46(5), 1188-1189.
- Wang, Z., Lan, C. Q., Lu, B. C.-Y. (2006). Excess molar enthalpies of the ternary mixtures:(tetrahydrofuran or 2-methyltetrahydrofuran+ methyl tert-butyl ether+< i> n-octane) at the temperature 298.15 K. *The Journal of Chemical Thermodynamics*, 38(5), 572-577.
- Wang, Z., Lu, B. C. Y. (2000). Prediction of isobaric vapour–liquid equilibrium from excess enthalpies for (methyl tert -butyl ether , alkane(s)) mixtures. *The Journal of Chemical Thermodynamics*, 32(2), 175-186.
- Wang, Z., Lu, B. C. Y., Peng, D. Y., Lan, C. Q. (2005). Liebermann-fried model parameters for calculating vapour-liquid equilibria of oxygenate and hydrocarbon mixtures. *Journal of the Chinese Institute of Engineers*, 28(7), 1089-1105.
- Wilson, G. M. (1964). Vapor-liquid equilibrium. XI. A new expression for the excess free energy of mixing. *Journal of the American Chemical Society*, 86(2), 127-130.
- Wormald, C. J., Lewis, K. L., Mosedale, S. (1977). The excess enthalpies of hydrogen + methane, hydrogen + nitrogen, methane + nitrogen, methane + argon, and nitrogen +

argon at 298 and 201 K at pressures up to 10.2 MPa. *The Journal of Chemical Thermodynamics*, 9(1), 27-42.

Zudkevitch, D. (1978). Impact of thermodynamic and fluid properties on design and economics of separation processes. In J. McKetta (Ed.), *Encyclopedia of chemical processing and design*.

## **Appendix A**

### **A1 Pump Constant Calculation**

## A1 Pump constant calculation

The volumetric flow rate of the individual pumps are calculated using the expression

$$Q = K_p GR$$

where  $Q$  is the flow rate in cc/s,  $G$  is the gear ratio (0.01 the default gear ratio for both the motors),  $R$  is the motor speed in counts/sec and  $K_p$  is the pump constant which is determined experimentally and is explained as follows

The pump constant  $K_p$  is determined for both pump A and pump B respectively at 298.15K. The syringe A and syringe B was filled with reverse osmosis water and water is pumped through one syringe at a time at specified motor speed and time interval. The water coming out of the calorimeter exit was collected in a plastic bottle. The plastic bottle was weighed before and after the collection of water, the difference in the weight of the plastic bottle gives the amount of water collected for the fixed amount of time and specified motor speed.

The volumetric flow rate of the pump is calculated using the formula

$$\text{Volumetric flow rate } Q = \frac{m}{\rho * t}$$

where  $m$  is the weight of the water collected in grams,  $\rho$  is the density of water in g/cm<sup>3</sup> at 298.15K, and  $t$  is the time interval in seconds 's' for which the water had been collected. Table A1.1 and A1.2 summarize the results for both the pumps A and B.

**Table A1.1** Pump A calibration results

<b>Motor speed R (counts/s)</b>	<b>Time (s)</b>	<b>Mass of water (g)</b>	<b>Volumetric flow rate (Q) (cm<sup>3</sup> / s)</b>
20000.4	1800.0	9.055	0.005045
20000.4	1800.0	9.060	0.005048
18000.4	1800.0	8.143	0.004537
18000.6	1800.0	8.139	0.004535
13000.1	2500.0	8.164	0.003275
13000.1	2500.0	8.176	0.003280
8000.3	4050.0	8.149	0.002018
8000.4	4050.0	8.147	0.002018
3000.6	10800.0	8.156	0.000757
3000.8	10800.0	8.144	0.000756

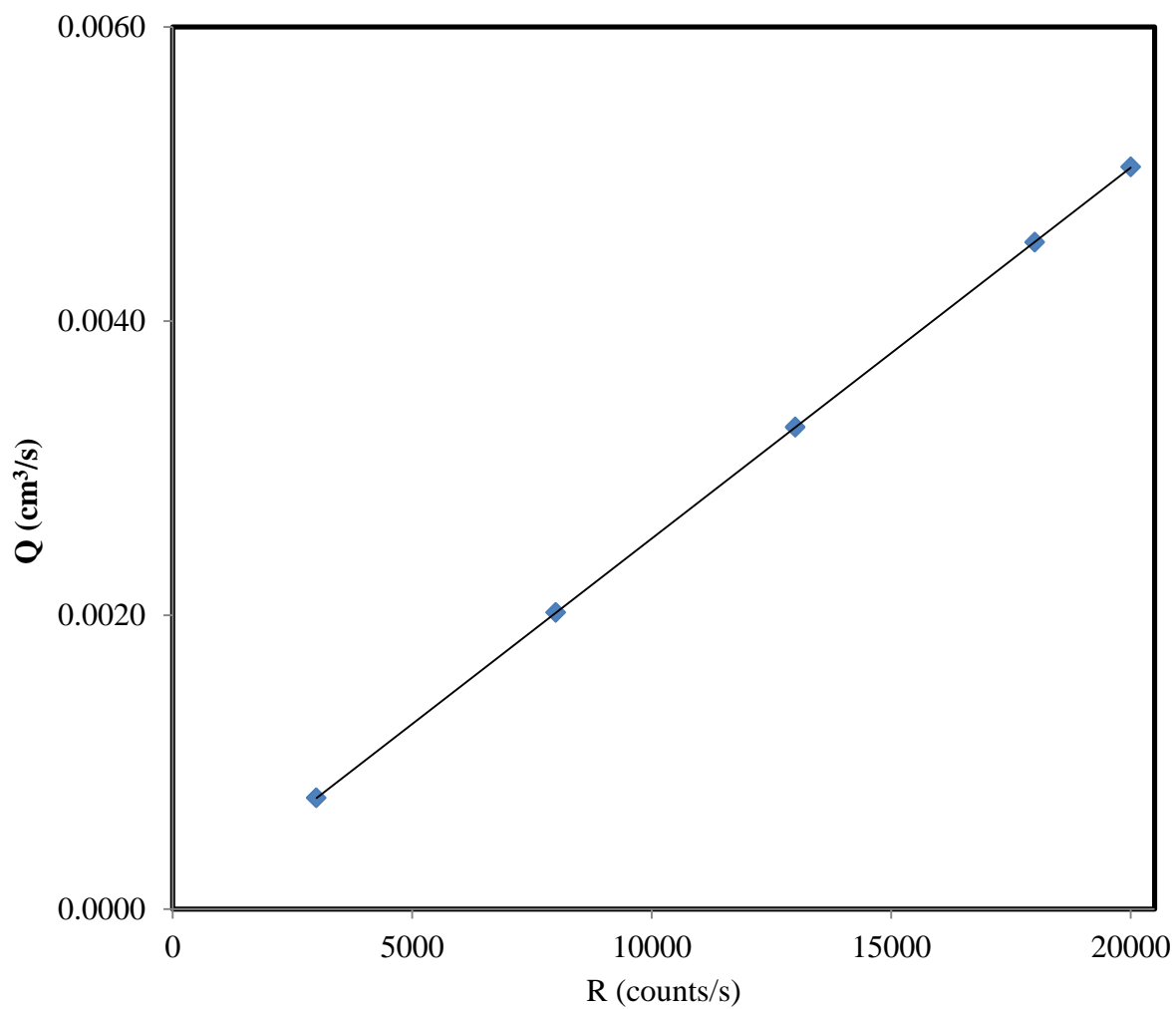


**Figure A1.1.** Pump A calibration plot. Volumetric flow rate  $Q$  against motor speed  $R$ . Experimental results; ♦, Experimental data; Curves : —, calculated from equation A1.1

**Table A1.2.** Pump B calibration results

<b>Motor speed R (count/s)</b>	<b>Time (s)</b>	<b>Mass of water (g)</b>	<b>Volumetric flow rate (Q) (cm<sup>3</sup> / s)</b>
20000.4	1800.0	9.053	0.005044
20000.4	1800.0	9.079	0.005059
20000.4	1800.0	9.087	0.005063
18000.5	1800.0	8.171	0.004553
18000.6	1800.0	8.201	0.004570
13000.0	2500.0	8.201	0.003290
13000.0	2500.0	8.201	0.003290
8000.4	4050.0	8.162	0.002021
8000.4	4050.0	8.173	0.002024
3000	10800.0	8.135	0.000755
3000	10800	8.14	0.000756

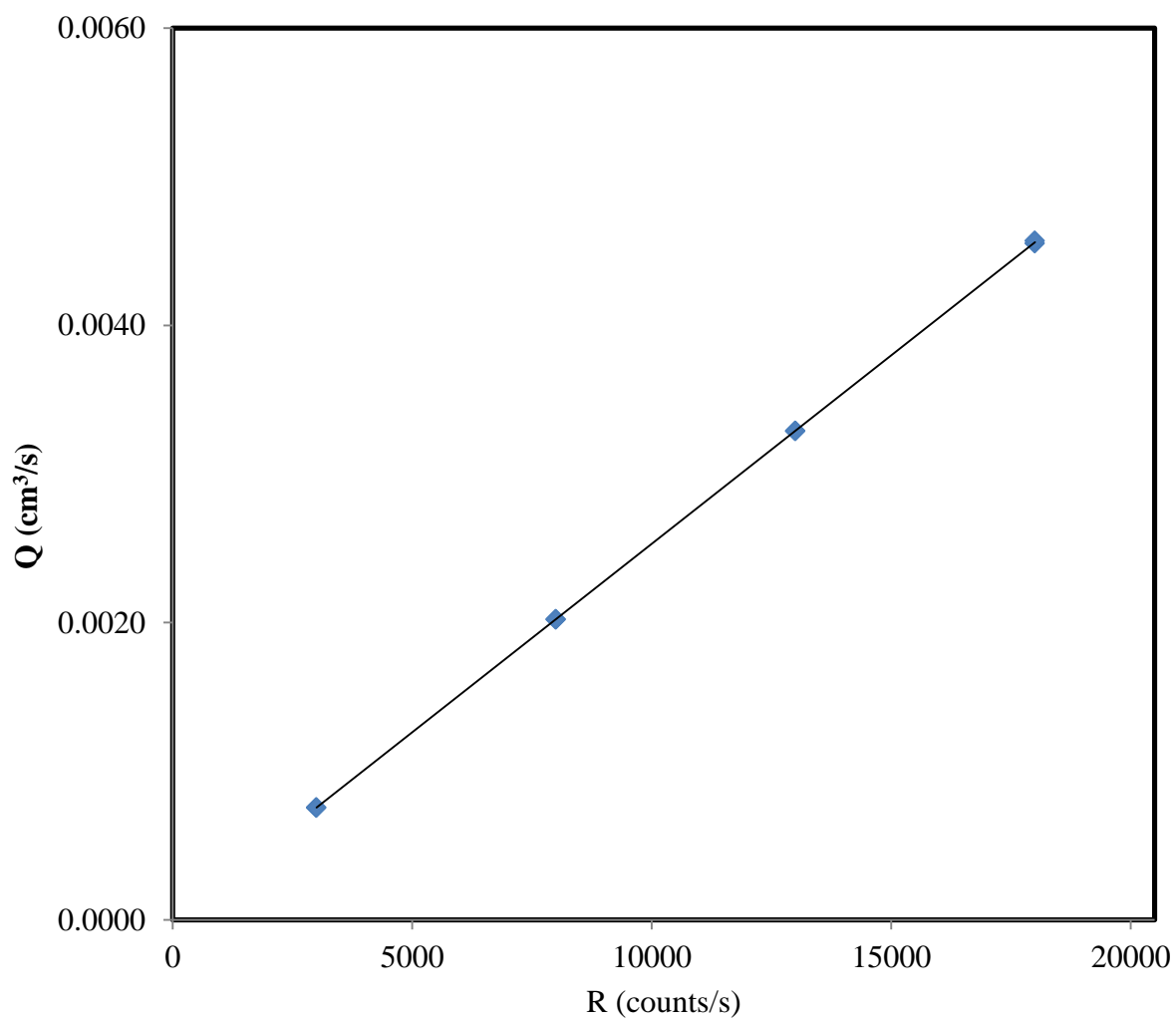


**Figure A1.2.** Pump B calibration plot. Volumetric flow rate  $Q$  against motor speed  $R$ . Experimental results;  $\blacklozenge$ , Experimental data; Curves: —, calculated from equation A1.1

A plot between volumetric flow rate 'Q' against the motor speed 'R' was plotted for both pump A and pump B. The calibration results for both pumps were correlated with equation A1.1 using the least squares method. The pump constants obtained from this analysis are given by the equations  $Q = 2.5220 \times 10^{-7}R - 2.4841 \times 10^{-7}$  for pump A and  $Q = 2.5312 \times 10^{-7}R - 2.2488 \times 10^{-7}$  for pump B respectively.

The pump constants  $K_p$  of this study is also compared with results of Hassan (2010) and Tanaka *et al.* (1975) and summarized in table A1.3

**Table A1.3.** Pump Constant  $K_p$  comparison

Author	$K_p$	
	Pump A	Pump B
Tanaka <i>et al.</i> (1975)	$4.1882 \times 10^{-6}$	$4.1889 \times 10^{-6}$
Hassan (2010)	$2.7847 \times 10^{-6}$	$2.7867 \times 10^{-6}$

## **Appendix B**

B1. Heats of mixing calculations for binary mixtures

B2. Weight corrections for buoyancy effect of air

## B1 Heats of mixing calculations

The basic parameters required for calculating the heats of mixing values are molecular weight of the components, density of the components at 298.15K and calibration results of the pure components

For sample calculations the DNBE (1) + 2-MTHF (2) system is taken as a basis

**Table B1.1.** Pure component properties

Component	Molecular weight (g/mol)	Density (g/cm <sup>3</sup> )
DNBE	130.22792	0.763705
2-MTHF	86.1323	0.847973

**Table B1.2.** Calibration results of DNBE in pump A

Motor Speed R (counts/s)	Baseline Voltage $E_Q^0$ (mV)	Observed Voltage $E_Q$ (mV)	$\Delta E$ (mV)	I (amp)	Calibration constant $\varepsilon = I^2 \Omega / \Delta V$ (J/s/V)
3999.9	-0.001204	-0.352843	0.351639	0.010559	15.700464
7000.7	-0.001328	-0.352504	0.351176	0.010557	15.716718
10000.2	-0.001023	-0.351599	0.350576	0.010560	15.751952
13000.0	-0.001291	-0.351334	0.350043	0.010559	15.772958
16000.0	-0.001016	-0.350421	0.349406	0.010558	15.799338
18999.8	-0.001159	-0.349784	0.348625	0.010560	15.838302

The calibration constant ' $\epsilon$ ' is plotted against motor speed ' $R$ ' and the experimental data was fitted to the equation 3.2 and the expression for the calibration constant has the form

$$\epsilon = 15.6584 + 0.9125 \times 10^{-5} R$$

where  $R$  is the motor speed in counts/sec.

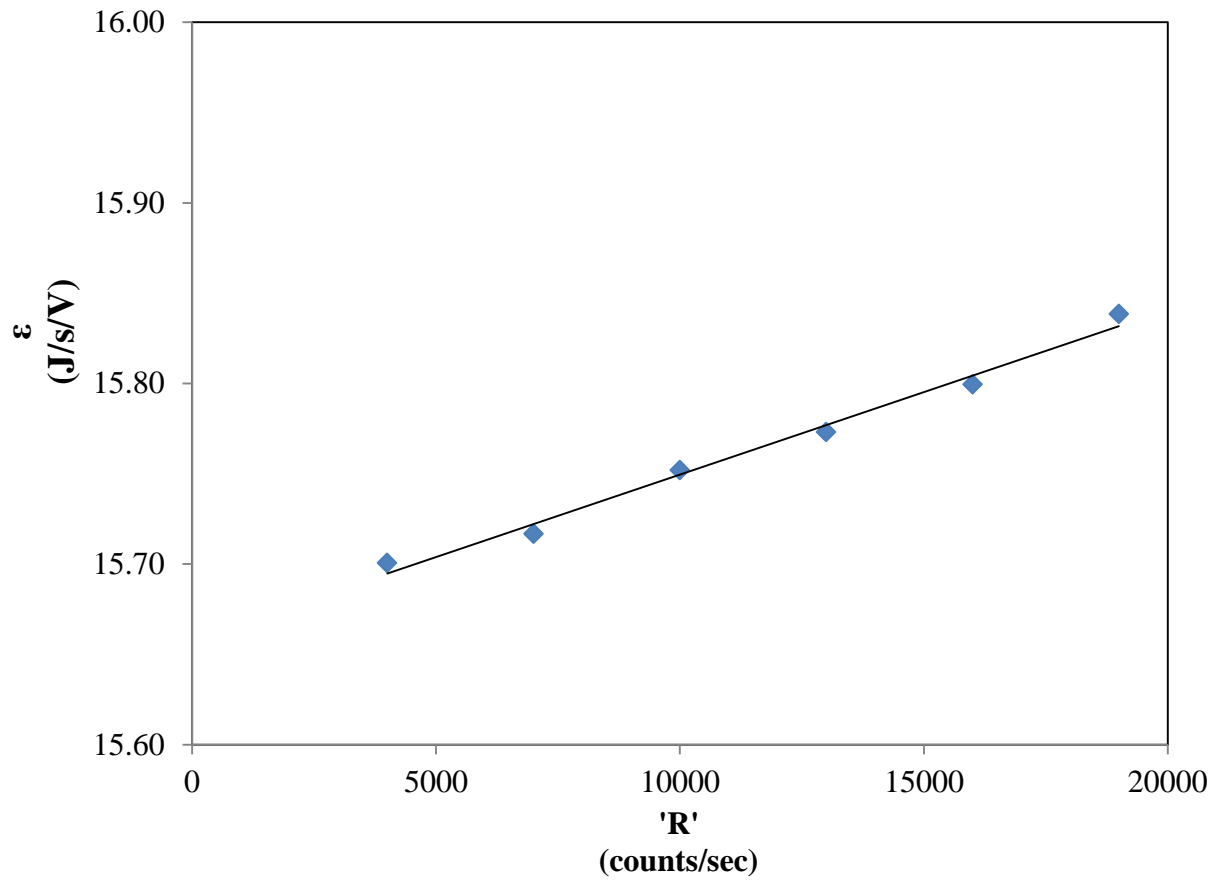


**Figure B1.1.** Calibration curve for DNBE in pump A

**Table B1.3.** Calibration results of 2-MTHF in pump B

<b>Motor Speed R (counts/s)</b>	<b>Baseline Voltage <math>E_Q^0</math> (mV)</b>	<b>Observed Voltage <math>E_Q</math> (mV)</b>	<b><math>\Delta E</math> (mV)</b>	<b>I (amp)</b>	<b>Calibration constant <math>\varepsilon = I^2\Omega/\Delta V</math> (J/s/V)</b>
3999.9	-0.002523	-0.349612	0.347089	0.010480	15.669167
7000.0	-0.002708	-0.349094	0.346386	0.010475	15.687498
10000.2	-0.002369	-0.348255	0.345886	0.010477	15.715268
13000.0	-0.002650	-0.348056	0.345406	0.010481	15.749104
16000.0	-0.002526	-0.347124	0.344598	0.010481	15.786031
19000.0	-0.002522	-0.346257	0.343735	0.010481	15.825689

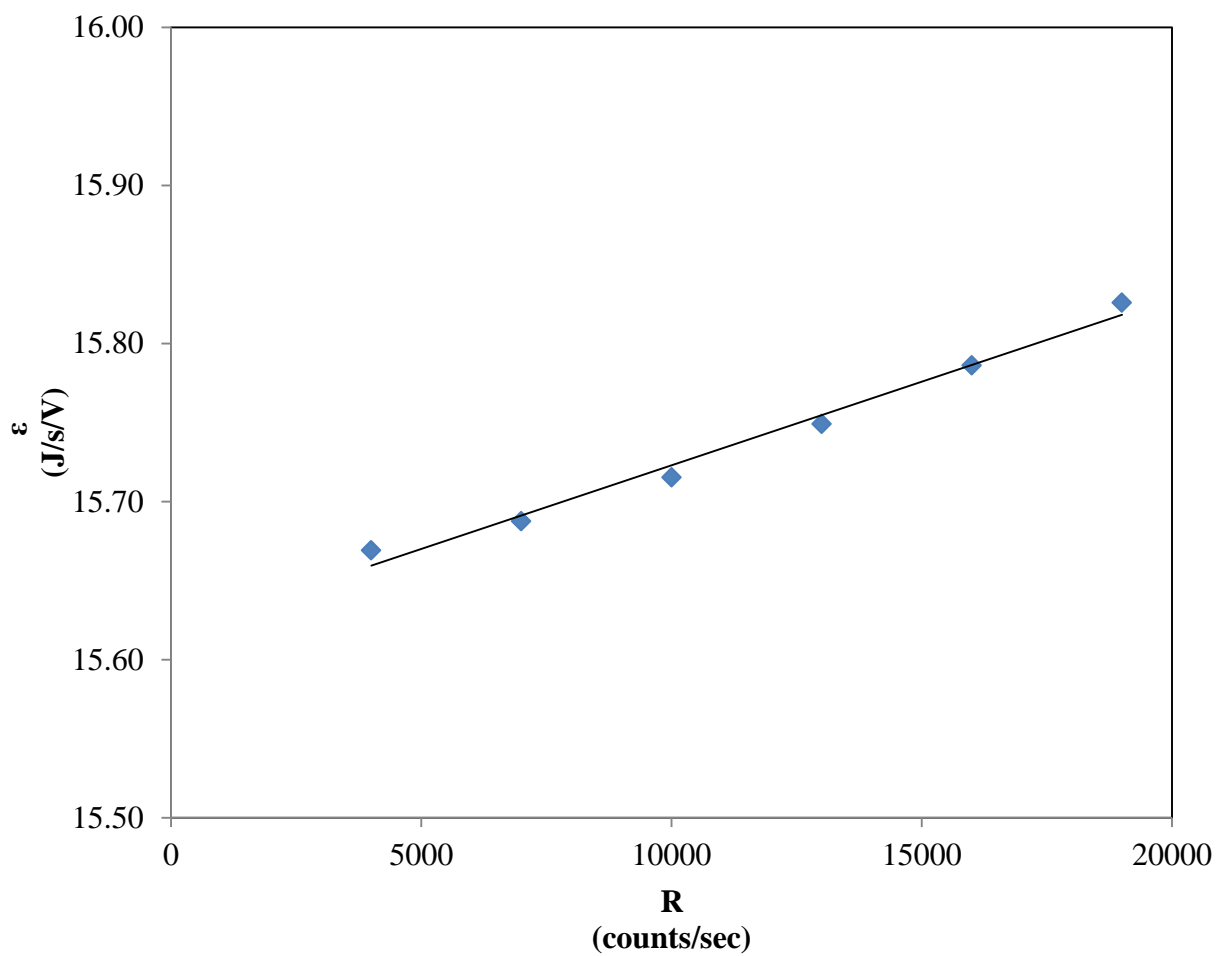


**Figure B1.2.** Calibration curve for 2-MTHF in pump B

The expression for the calibration constant for 2-MTHF in pump is of the form

$$\varepsilon = 15.6170 + 1.0591 \times 10^{-5} R$$

**Table B1.4.** Experimental data of the DNBE (1) + 2-MTHF binary system

Pump	#	Component	Molecular weight (g/mol)	Den (g/cc)	$k_0$	$k_1 \times 10^{-4}$
A	1	DNBE	130.22792	0.763705	15.65836	0.091245
B	2	2-MTHF	86.13230	0.847973	15.61700	0.105908
Point No.		$R_A$ /(Counts/sec)		$R_B$ /(Counts/sec)	$E(\mu V)$	
1		0		19762.2	-2.2751	
2		1610.9		18158.5	112.7610	
3		2225.0		17545.7	152.2340	
4		3117.9		16656.8	205.3530	
5		4531.8		15247.7	277.2710	
6		5861.7		13922.7	332.4670	
7		7114.5		12674.0	370.6030	
8		8296.7		11497.1	399.5640	
9		9413.6		10383.3	414.5500	
10		10471.5		9330.4	418.2570	
11		11474.3		8331.3	414.1300	
12		12426.2		7382.3	402.6580	
13		12426.2		7382.3	399.2660	
14		13330.2		6481.4	381.6620	
15		14192.0		5623.5	360.3250	
16		15012.2		4805.6	322.8720	
17		15795.1		4025.8	288.4310	
18		16542.1		3281.6	245.8750	
19		17257.0		2568.8	198.7600	
20		17941.0		1887.8	146.5860	
21		18595.8		1234.8	92.7543	
22		19223.8		609.9	38.0215	
23		19826.8		0	-1.5154	

### Sample calculation for calculating heats of mixing values

To explain the method for calculating the heat of mixing values from the raw experimental data, point 12 in table B1.4 is taken as basis.

#### Motor speed R

$$R_A = 12426.2 \text{ counts/sec}$$

$$R_B = 7382.3 \text{ counts/sec}$$

#### Volumetric flow rate

$$Q_1 = 2.5220 \times 10^{-7} R - 2.4841 \times 10^{-7} = 0.003134 \text{ cm}^3/\text{s}$$

$$Q_2 = 2.5312 \times 10^{-7} R - 2.2488 \times 10^{-7} = 0.001866 \text{ cm}^3/\text{s}$$

#### Overall flow rate

$$Q = Q_1 + Q_2 = 0.00500 \text{ cm}^3/\text{s}$$

$$\text{Volume fraction of fluid A } \phi_1 = \frac{Q_1}{Q} = 0.626722$$

$$\text{Volume fraction of fluid B } \phi_2 = \frac{Q_2}{Q} = 0.373278$$

$$\begin{aligned} \text{Calibration constant of the mixture } \varepsilon_M &= \left( k_{1A} + k_{0A} \frac{R}{\phi_1} \phi_1 \right) + \left( k_{1B} + k_{0B} \frac{R}{\phi_2} \phi_2 \right) \\ &= 15.4385 \text{ J/v/cm}^3 \end{aligned}$$

**Molar flow rate 'f'**

$$f_1 = \frac{Q_1}{V_{m1}} = 1.8377 \times 10^{-5}$$

$$f_2 = \frac{Q_2}{V_{m2}} = 1.8375 \times 10^{-5}$$

where  $V_m$  is the molar volume and it is calculated using the formula  $V_m = \frac{M}{\rho}$

Total molar flow rate,  $f = f_1 + f_2 = 3.6751 \times 10^{-5}$  mol/s

**Pure component baseline voltage**

$$E_1^0 = -1.51544 \mu V$$

$$E_2^0 = -2.27511 \mu V$$

**Mixture baseline voltage**

$$E_M^0 = (E_1^0 \times Q_1 + E_2^0 \times Q_2) / Q$$

$$= -1.77990 \mu V$$

**Observed Voltage**

$$E = 402.658 \mu V$$

Corrected Voltage  $E_{corr}$

$$E_{corr} = E - E_M^0$$

$$= 404.457\mu V$$

$$\text{Mole fraction } x_1 = \frac{f_1}{f}$$

$$= 0.50003$$

$$\text{Enthalpy } H_m^E = \frac{E_M^0 \times E_{corr} \times 10^{-6}}{f}$$

$$= 174.26 \text{ J/mol}$$

### Error Estimation

Calculation of error or uncertainty is an important aspect in this research work; it reflects the accuracy of the measurements and methods. In this study the uncertainty of the data is calculated using the error propagation method explained by Hassan (2010) thesis work.

The error propagation method is explained as follows

Let U be a dependent variable and it is a function of several measured variables,  $u_1, u_2$ , etc.

$$U = f(u_1, u_2, \dots) \quad (\text{B1.1})$$

The error in the variable U is given by Bevington and Robinson (2003)

$$S_U = \sqrt{\left(\frac{\partial U}{\partial u_1}\right)^2 S_{u_1}^2 + \left(\frac{\partial U}{\partial u_2}\right)^2 S_{u_2}^2 + \dots} \quad (\text{B1.2})$$

where  $S_U$  is the standard deviation of the U dependent variable,  $S_{u_1}, S_{u_2}$  are the standard deviation of the  $u_1$  and  $u_2$  variable respectively.

$\frac{\partial U}{\partial u_i}$  is the partial derivative of the variable U with respect to  $u_i$

In this study a simpler approximation of the error propagation method is used.

Consider the variables  $u_1$  and  $u_2$  have errors  $\Delta u_1$  and  $\Delta u_2$  respectively, then uncertainties  $\Delta U$  in the dependent variable will be

i) For addition and subtraction:  $U = u_1 + u_2$  or  $U = u_1 - u_2$

$$\Delta U = \sqrt{\Delta u_1^2 + \Delta u_2^2} \quad (\text{B1.3})$$

ii) For multiplication and division:  $U = u_1 \times u_2$  or  $U = u_1 / u_2$

$$\Delta U = |U| \cdot \sqrt{\left(\frac{\Delta u_1}{u_1}\right)^2 + \left(\frac{\Delta u_2}{u_2}\right)^2} \quad (\text{B1.4})$$

The uncertainties of the mole fraction and excess molar enthalpy were determined using the equations B1.3 and B1.4.

## Sample calculation

### Molefraction uncertainty calculation

Error in volumetric flow rate

$$\text{Volumetric flow rate } Q_i = \frac{m_i}{\rho_{\text{water}} \times \text{time}}$$

Error

$$\Delta Q_i = |Q_i| \sqrt{\left(\frac{\Delta m_i}{m_i}\right)^2 + \left(\frac{\Delta \rho_{\text{water}}}{\rho_{\text{water}}}\right)^2 + \left(\frac{\Delta \text{time}_i}{\text{time}_i}\right)^2}$$

where,  $m = 9.055\text{g}$ ,  $\Delta m = \pm 0.001\text{g}$ ,  $\rho_{\text{water}} = 0.99705 \text{ g/cm}^3$ ,  $\Delta \rho = \pm 0.00001 \text{ g/cm}^3$ ,  $\text{time} = 1800 \text{ s}$ ,  $\Delta \text{time} = \pm 0.1 \text{ s}$ . Then the error in the flow rate corresponding to  $Q_1 = 0.005045 \text{ cm}^3/\text{s}$  is  $\Delta Q_1 = \pm 0.0000006 \text{ cm}^3/\text{s}$ .

Error in counter reading

$$\Delta R_A = \pm 0.5 \text{ counts/s and } \Delta R_B = \pm 0.5 \text{ counts/s}$$

Error in molar volume

Molar volume

$$V_{m_i} = \frac{M_i}{\rho_i}$$

$$\Delta V_{m_i} = |V_{m_i}| \cdot \sqrt{\left(\frac{\Delta M_i}{M_i}\right)^2 + \left(\frac{\Delta \rho_i}{\rho_i}\right)^2}$$

where,  $M_1 = 170.5212 \text{ g/mol}$ ,  $\Delta M_1 = 0$ ;  $\rho_1 = 0.763705 \text{ g/cm}^3$ ,  $\Delta \rho = \pm 0.00001 \text{ g/cm}^3$ . Then the error in the molar volume corresponding to  $V_{m_1} = 170.512 \text{ g/cm}^3$  is  $\Delta V_{m_1} = \pm 0.0022 \text{ cm}^3/\text{mol}$ .

In the same way  $V_{m_2} = 101.5743 \text{ g/cm}^3$  is  $\Delta V_{m_2} = \pm 0.0012 \text{ cm}^3/\text{mol}$ .

Error in molar flow rate

$$\text{Molar flow rate } f_i = \frac{Q_i}{V_{m_i}}$$

$$\Delta f_i = |f_i| \cdot \sqrt{\left(\frac{\Delta Q_i}{Q_i}\right)^2 + \left(\frac{\Delta V_{m_i}}{V_{m_i}}\right)^2}$$

when,  $Q_1 = 0.003134 \text{ cm}^3/\text{s}$  and  $f_1 = 0.000018376 \text{ mol/s}$ , the error,

$$\Delta f_1 = \pm 3.67678 \times 10^{-9} \text{ mol/s}$$

when,  $Q_2 = 0.001866 \text{ cm}^3/\text{s}$  and  $f_1 = 0.0000183745 \text{ mol/s}$ , the error,

$$\Delta f_1 = \pm 6.16533 \times 10^{-9} \text{ mol/s}$$

Therefore the error in the total molar flow rate  $f$  is

$$\begin{aligned}\Delta f &= \sqrt{(\Delta f_1)^2 + (\Delta f_2)^2} \\ &= 7.17844 \times 10^{-9} \text{ mol/s}\end{aligned}$$

Molefraction

$$x_1 = \frac{f_1}{f}$$

Error in molefraction is calculated using the equation

$$\Delta x_1 = |x_1| \cdot \sqrt{\left(\frac{\Delta f_1}{f_1}\right)^2 + \left(\frac{\Delta f}{f}\right)^2}$$

so for  $x_1 = 0.50003$  the error in molefraction is  $\Delta x_1 = 0.0000977$

Error in excess molar enthalpy

Excess molar enthalpy is given by the formula

$$H_m^E = \frac{\varepsilon_M X E_{corr}}{f X Q}$$

where,

$\varepsilon_M = \varepsilon_1 Q_1 + \varepsilon_2 Q_2 = A + B$ , where  $A = \varepsilon_1 Q_1$  and  $B = \varepsilon_2 Q_2$  and error in A and B can be calculated using the equation

$$\Delta A = |A| \cdot \sqrt{\left(\frac{\Delta \varepsilon_1}{\varepsilon_1}\right)^2 + \left(\frac{\Delta Q_1}{Q_1}\right)^2}$$

and

$$\Delta B = |B| \cdot \sqrt{\left(\frac{\Delta \varepsilon_2}{\varepsilon_2}\right)^2 + \left(\frac{\Delta Q_2}{Q_2}\right)^2}$$

The error  $\varepsilon_M$  can be calculated by the relation

$$\varepsilon_M = \sqrt{(\Delta X)^2 + (\Delta Y)^2}$$

The uncertainty in the calibration constants of the pure components are estimated to be

$$\Delta \varepsilon_1 = 0.005033 \text{ J/s/V and } \Delta \varepsilon_2 = 0.006516 \text{ J/s/V}$$

Using the above values the error in the calibration constant for the mixture for  $\varepsilon_M$  value of 15.8345 J/v/cm<sup>3</sup>, is found to be  $\Delta \varepsilon_M = 0.00002398 \text{ J/V/cm}^3$ .

Assuming the uncertainty in the voltage measurement to be  $\Delta E_{corr} = \pm 0.01 \mu\text{V}$ , the uncertainty in the excess molar enthalpy value of  $H_m^E = 174.26 \text{ J/mol}$  is calculated using the equation

$$\Delta H_m^E = |H_m^E| \cdot \sqrt{\left(\frac{\Delta \varepsilon_M}{\varepsilon_M}\right)^2 + \left(\frac{\Delta E_{corr}}{E_{corr}}\right)^2 + \left(\frac{\Delta Q}{Q}\right)^2 + \left(\frac{\Delta f}{f}\right)^2} = \pm 0.04 \text{ J/mol}.$$

Heat of mixing calculations for pseudo-binary mixture is same as the pure binary mixture; in pseudo-binary system the component 2 is prepared from component 2 and component 3 of the respective ternary system. The molecular weight and molefraction of the prepared pseudo binary mixture is calculated after correcting the weights for buoyancy effect of air. The density of the pseudo-binary mixture at 2698.15K was measured using the densitometer.

Details for calculating the molefraction of the pseudo-binary mixture and for correcting weights to eliminate the buoyancy effect of air was explained in detail in appendix B2.

## B2 Weight corrections for buoyancy effect of air

Hassan, 2010 in his thesis explained (Bauer, 1959) method for correcting the weights to eliminate the buoyancy effect of air. The formula is of the form

$$m_c = m_0 \frac{\left(1 - \frac{\rho_a}{\rho_B}\right)}{\left(1 - \frac{\rho_a}{\rho_s}\right)} \quad (\text{B2.1})$$

where,  $m_c$  , corrected mass of the sample,  $\rho_s$  density of the weighed sample,  $m_0$  measured weight of the sample,  $\rho_a$  density of air,  $\rho_B$  density of brass (built in weights of the balance used and has a value of 8.4 g/cm<sup>3</sup>)

### Density of air $\rho_a$ calculation

In general, most weight measurements are made in an environment surrounded by air, the density of air acts as a buoyancy force on the weighed sample. The density of the air needs to be calculated to eliminate the buoyancy effect of air. Bauer, 1959 equation can be used to calculate the density of air

$$\rho_a / (\text{g/cm}^3) = \frac{0.000001701 \times (P - 0.0038 H \times P_{\text{water}}^v)}{(1 + 0.00367 \times t)} \quad (\text{B2.2})$$

where, P is the atmospheric pressure in mmHg,  $R_H$  the relative humidity of the surrounding in %, and t is the room temperature in °C, and  $P_{\text{water}}^v$  is the vapor pressure of water at room temperature and it is calculated using Antoine equation

$$\log_{10}(P_{\text{water}}^v / (\text{mmHg})) = A - \frac{B}{c + t}$$

where, A = 8.184254, B = 1791.3, C = 238.1. (Riddick *et al.*, 1986)

Sample calculations for correcting weights to buoyancy effect

**Table B2.1.** Ambient conditions and pure component properties for preparing EBz (1) + *p*-Xylene (2) mixture of molefraction  $x_1 \approx 0.2500$

Ambient conditions		
Temperature	Pressure	Relative Humidity
21.725 C	707.8 mmHg	14%
Pure component properties		
Component	Molecular weight (g/mol)	Density (g/cm <sup>3</sup> )
EBz	106.165	0.862598
<i>p</i> -Xylene	106.165	0.856574

**Table B2.2.** Summary of weighing

Component	Weight (g)
EBz	38.6193
<i>p</i> -Xylene	115.8177

Weight correction for EBz

$$P_{water}^v / (mmHg) = 10^{\left(8.184254 - \left(\frac{1791.3}{238.1 + 21.725}\right)\right)}$$

$$P_{water}^v = 19.49836 \text{ mmHg}$$

$$\rho_a = \frac{1.701 \times 10^{-6} (707.8 - (0.0038 \times 14 \times 19.4984))}{1 + 0.00367 \times 21.725}$$

$$\rho_a = 0.00120 \text{ g/cm}^3$$

$$\rho_b = 8.4 \text{ g/cm}^3$$

$$m_c = 38.6193 \left( \frac{1 - \frac{0.00120}{8.4}}{1 - \frac{0.00120}{0.862598}} \right)$$

$$m_c = 38.6677 \text{ g}$$

similarly for *p*-Xylene the corrected weight is 115.9531 g

The molefraction of the mixture is then calculated as follows

$$x_1 = \frac{\frac{m_1}{M_1}}{\frac{m_1}{M_1} + \frac{m_2}{M_2}} = \frac{\frac{38.6677}{106.165}}{\frac{38.6677}{106.165} + \frac{115.9531}{106.165}} = 0.25006$$

and the molecular weight of the mixture is calculated using the equation

$$M_{mix} = x_1 M_1 + (1 - x_1) M_2 = 106.165 \text{ g/mol}$$

## **Appendix C**

C1. Statistics of data Correlation

C2. Liebermann-Fried model representation of ternary systems

## C1 Statistics of data correlation

The experimental excess molar enthalpy data was fitted to empirical equations and solution theory model by means of unweighted least square method. This study continued the method used by (Hassan, 2010) for performing the statistical tests. The Marquardt method (Levenberg-Marquardt algorithm; (Marquardt, 1963) was used for finding the best Redlich-Kister fit parameters and Microsoft excel solver function was used to fit the Liebermann-Fried model and the Tsao and Smith equation. The solver function uses the Generalized Reduced Gradient (GRG2) Algorithm (Lasdon *et al.*, 1978) for solving nonlinear problems. The standard error was used as the objective function for both methods and it is expressed as

$$s = \sqrt{\frac{\sum_{i=1}^n (\text{Experimental values} - \text{calculated values})^2}{n - p}}$$

where, n is the number of data points, and p is the number of adjustable parameters of the model. The parameters are selected based on the minimization of the objective function. The total numbers of parameters representing the best fit of the experimental values are chosen by means of F - statistical test.

### F-statistical test

When experimental data are fitted to a model, a model with large number of parameters will have a low standard error than a model with less number of parameters. Quite often it is assumed that a model with large number of parameter provides the best fit of the experimental data, but it does not always represent the statistically better fit than a model with less number of parameters. In this case, statistical tests help to choose the model which most accurately represents the

experimental data. There are different types of statistical tests used; in our study the F-statistical test was selected.

The formula for doing the F-statistical test is as follows

$$F(v, l) = \frac{\frac{(SSE_1 - SSE_2)}{(p_2 - p_1)}}{\left(\frac{SSE_2}{(n - p_2)}\right)}$$

where,  $SSE_1$  and  $SSE_2$  are the sum of squares of the error of model #1 and model #2 respectively,  $v = n - p_1$  is the degree of freedom of model # 1 and  $l = n - p_2$  is the degree of freedom of model # 2.

The value of  $F_{(v,l)}$  will have an F distribution, with an assumption that errors because of lack of fit are normally distributed. At 5% significance level the value of the  $F_{(v,l)}$  is compared with values of  $F_{(1-q)}(v, l)$ .

If  $F_{(v,l)}$  is greater than  $F_{(1-q)}(v, l)$ , it is decided that model # 2 is a better model than model # 1 (Bevington and Robinson, 2003; Navidi, 2008)

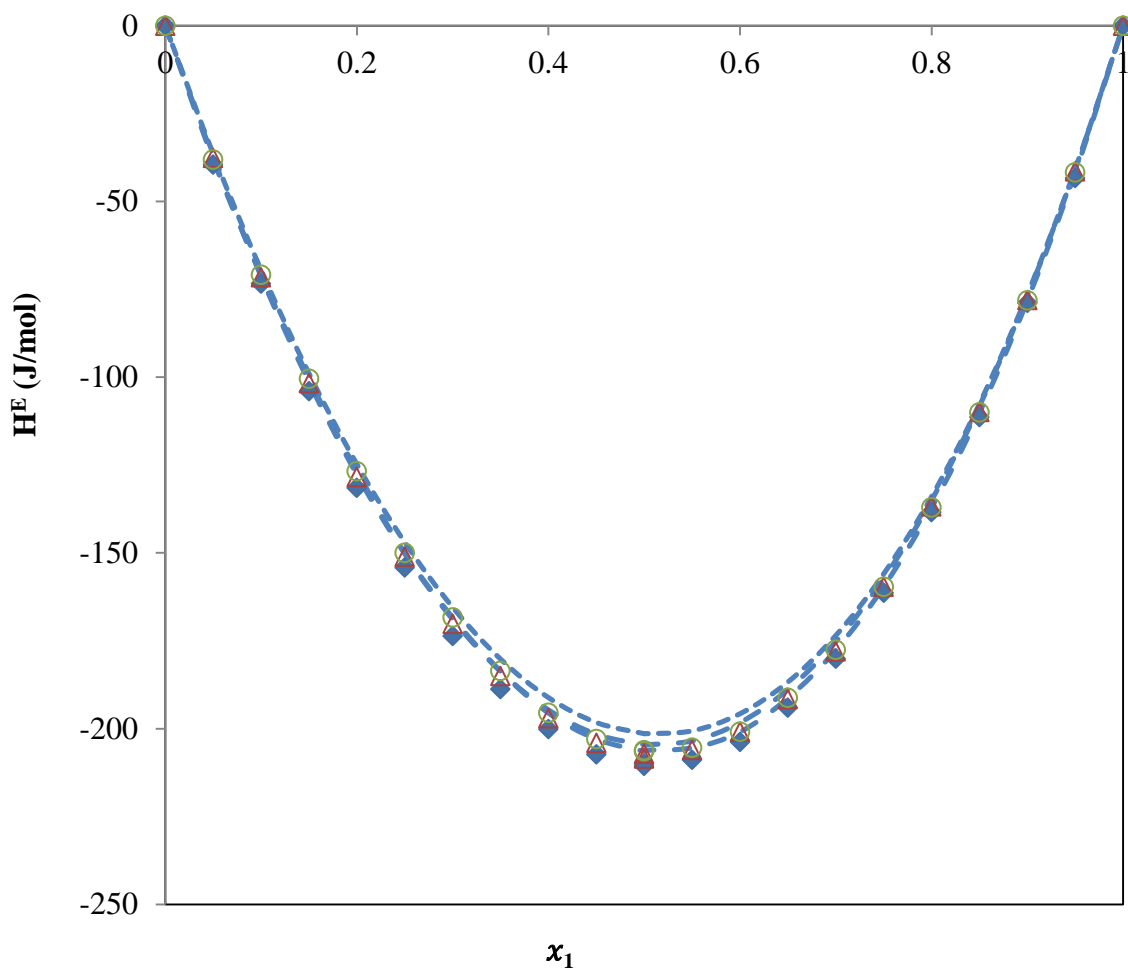
To illustrate the F-statistical test, fitting of the experimental data of DNBE (1) + 2-MTHF (2) binary system to of Redlich - Kister equation is demonstrated.

**Table C1.1.** Summary of F-statistical test ( $q=0.05$ )

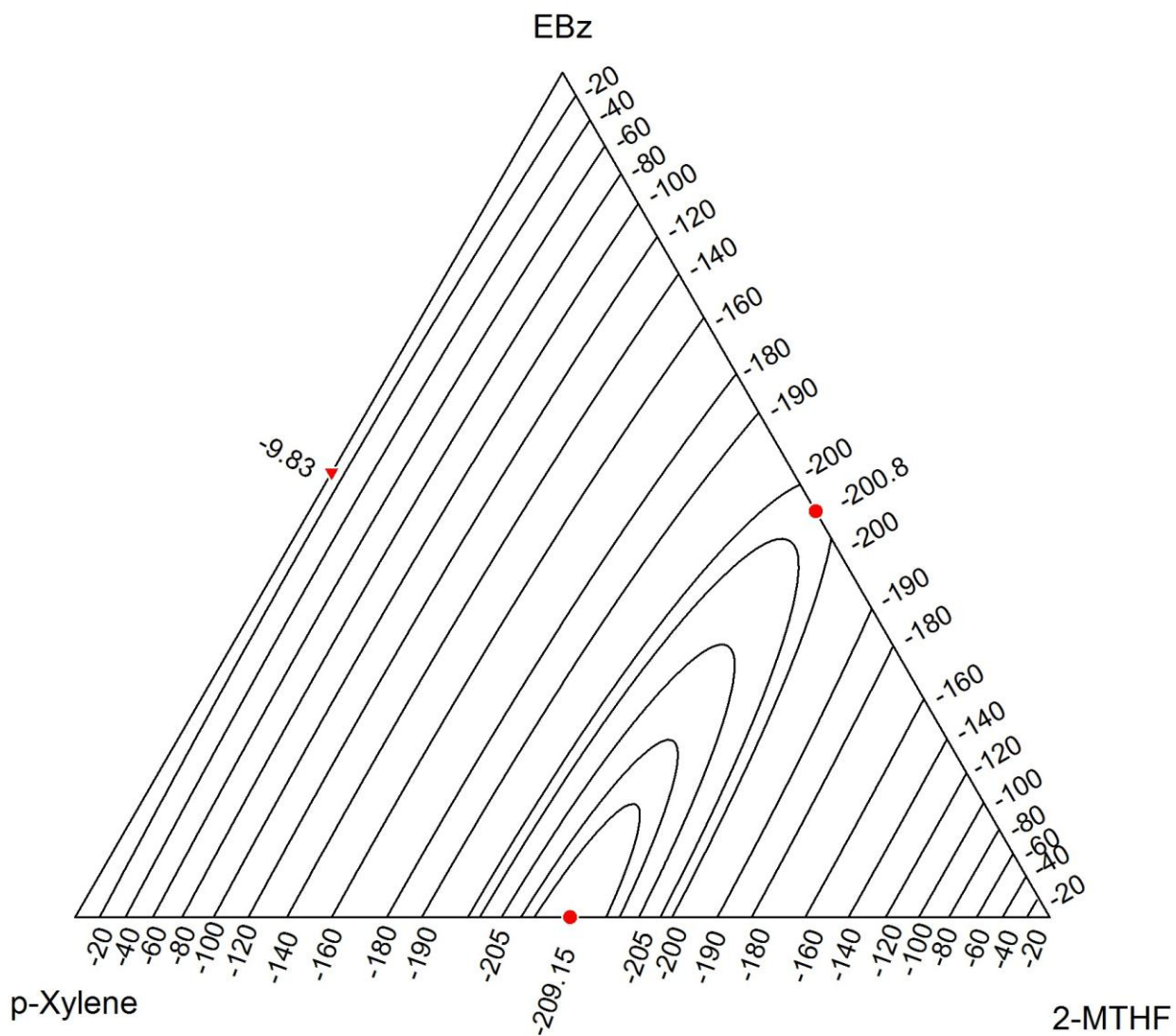
Test no	Parameters	s (J/mol)	SSE (J/mol)	DoF	$F$	$F_{(1-q)}$	Result
1	5	0.92	12.73	15	9.87	2.463	$F > F_{(1-q)}$
	6	0.73	7.45	14			
2	6	0.71	6.57	13	1.73	2.554	$F < F_{(1-q)}$
	7	0.71	6.57	13			
3	7	0.72	6.18	12	7.4	2.660	$F > F_{(1-q)}$
	8	0.72	6.18	12			

From the table, is observed that the model with six number of parameter gives a better fit than the model with seven and eight parameters and the reliability of the model is supported by the F statistical test.

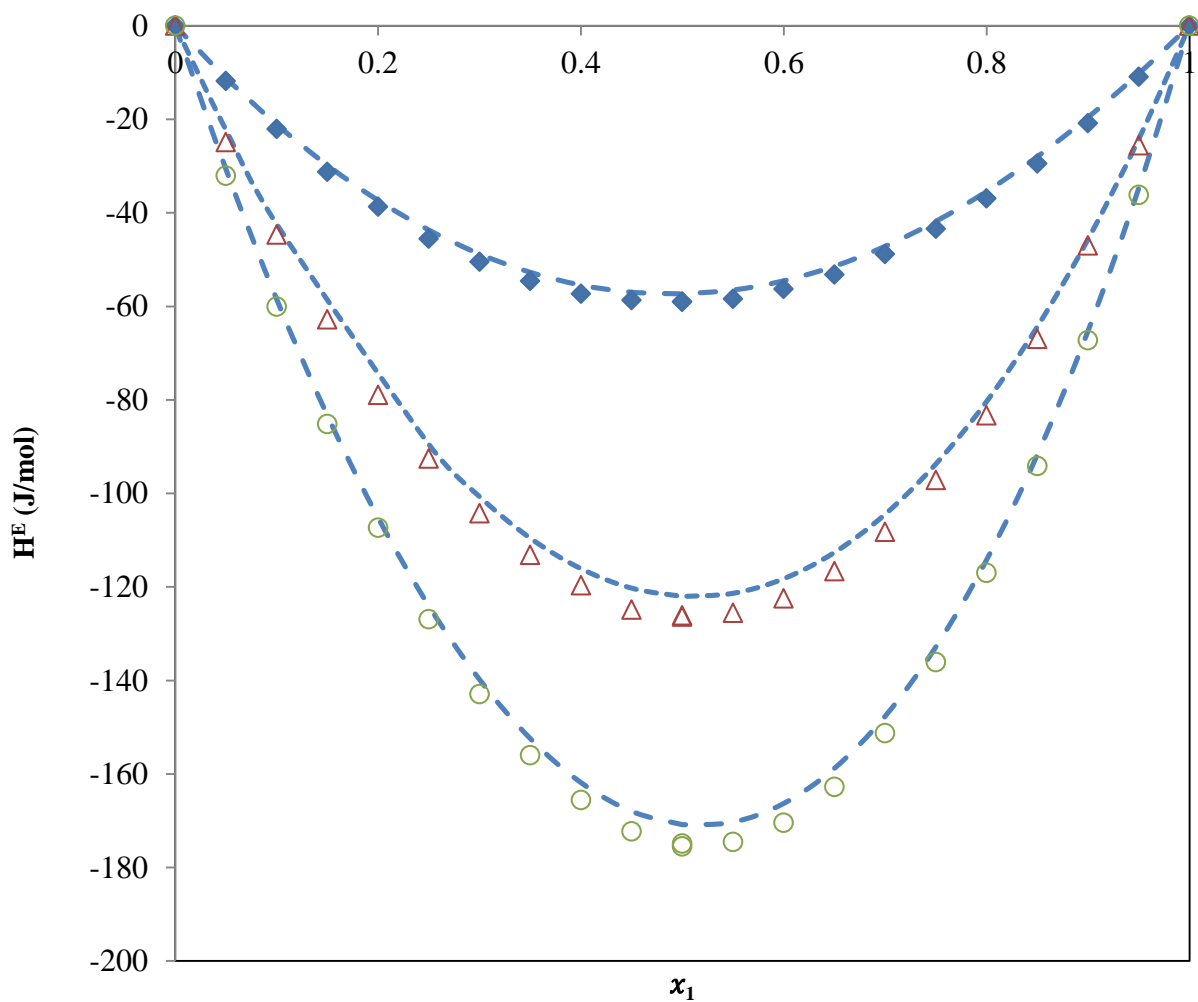
C2 Representation of ternary excess molar enthalpy using the Liebermann-Fried model.



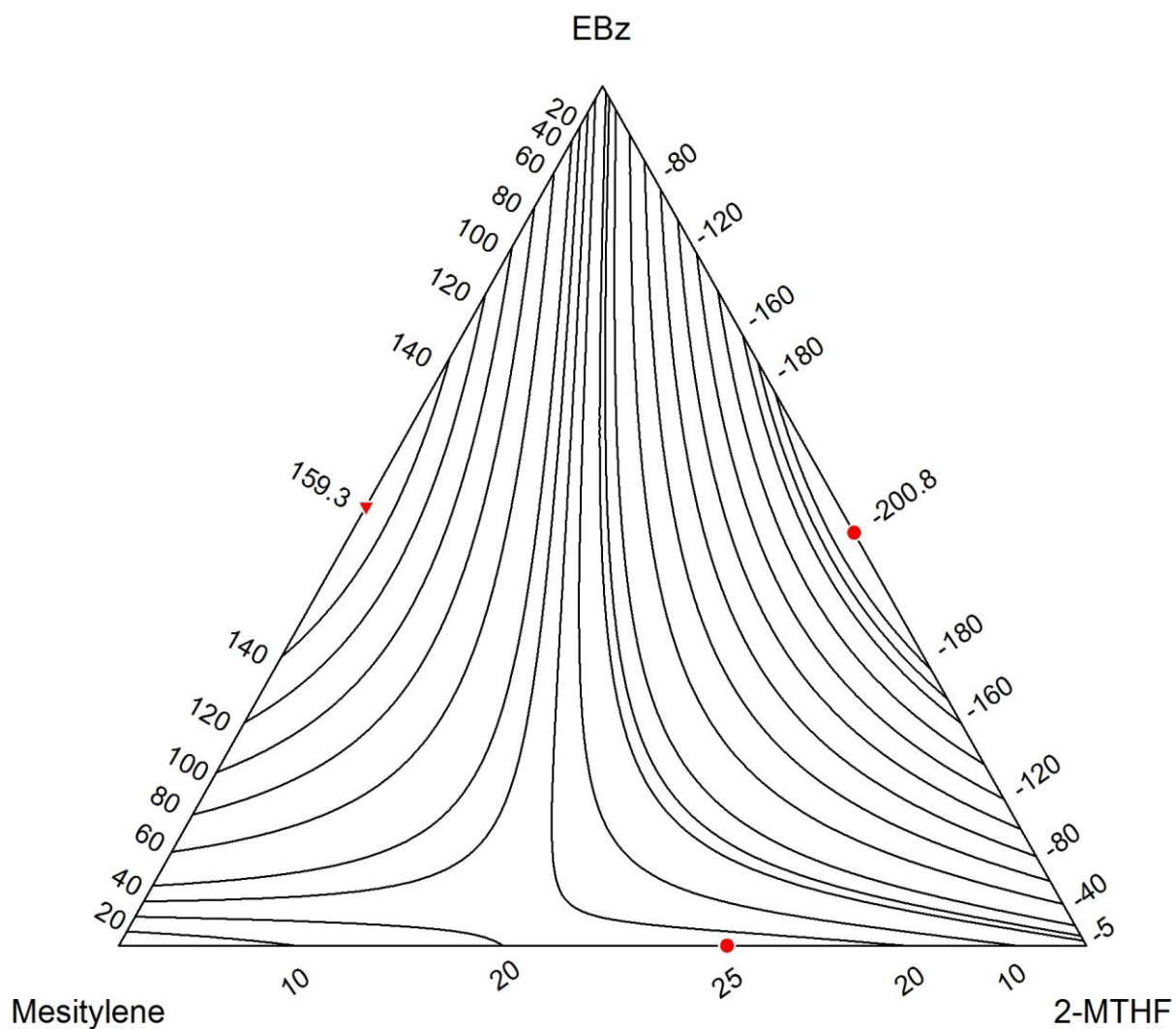
**Figure C2.1.** Excess molar enthalpies  $H_{m,1+23}^E$  for the ternary system  $x_1$  2-MTHF +  $x_2$  EBz +  $(1 - x_1 - x_2)$  *p*-Xylene at 298.15K . Experimental results:  $\diamond$   $x_2/x_3 = 0.3334$ ;  $\Delta$ ,  $x_2/x_3 = 1.0002$ ;  $\circ$ ,  $x_2/x_3 = 3.0057$ ; Curves: ..... , calculated using the Liebermann-Fried model



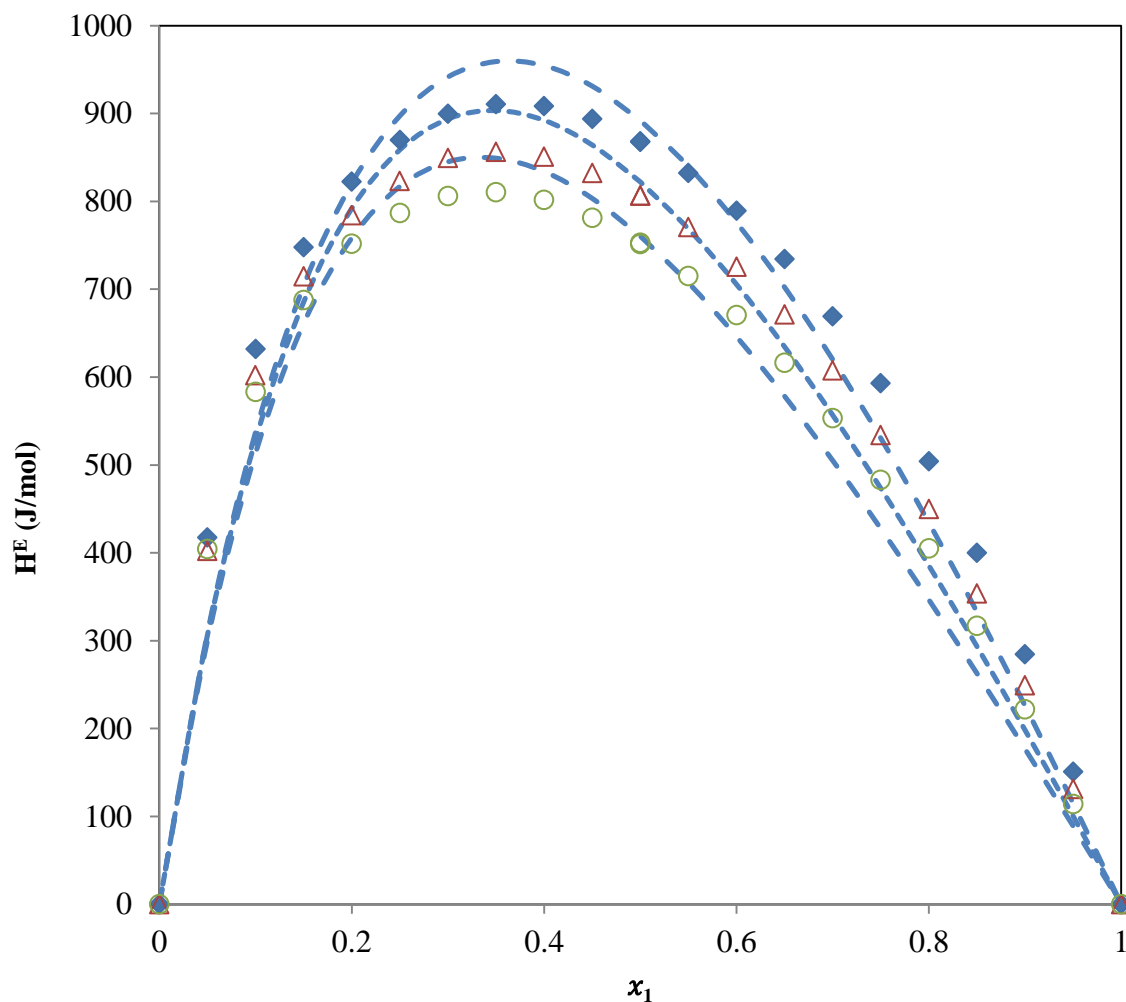
**Figure C2.2.** Constant enthalpy contours,  $H_{m,123}^E$  (J/mol) at 298.15K for the  $x_1$  2-MTHF +  $x_2$  EBz +  $(1 - x_1 - x_2)$  p-Xylene, calculated from the representation of the experimental results using the Liebermann-Fried model.



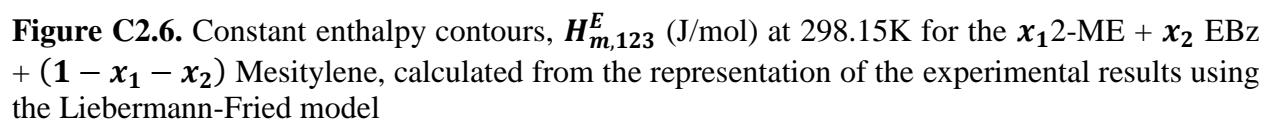
**Figure C2.3.** Excess molar enthalpies  $H_{m,1+23}^E$  for the ternary system  $x_1$  2-MTHF +  $x_2$  EBz +  $(1 - x_1 - x_2)$  Mesitylene at 298.15K . Experimental results:  $\blacklozenge$   $x_2/x_3 = 0.3335$ ;  $\triangle$ ,  $x_2/x_3 = 0.9921$ ;  $\circ$ ,  $x_2/x_3 = 3.0005$ ; Curves: ..... , calculated using the Liebermann-Fried model.



**Figure C2.4.** Constant enthalpy contours,  $H_{m,123}^E$  (J/mol) at 298.15K for the  $x_1$ 2-MTHF +  $x_2$  EBz +  $(1 - x_1 - x_2)$  Mesitylene, calculated from the representation of the experimental results using the Liebermann-Fried model.



**Figure C2.5.** Excess molar enthalpies  $H_{m,1+23}^E$  for the ternary system  $x_1$  2-ME +  $x_2$  EBz +  $(1 - x_1 - x_2)$  Mesitylene at 298.15K. Experimental results: ♦  $x_2/x_3 = 0.3335$ ; Δ,  $x_2/x_3 = 0.9921$ ; ○,  $x_2/x_3 = 3.0057$ ; Curves: ..... , calculated using the Liebermann-Fried model



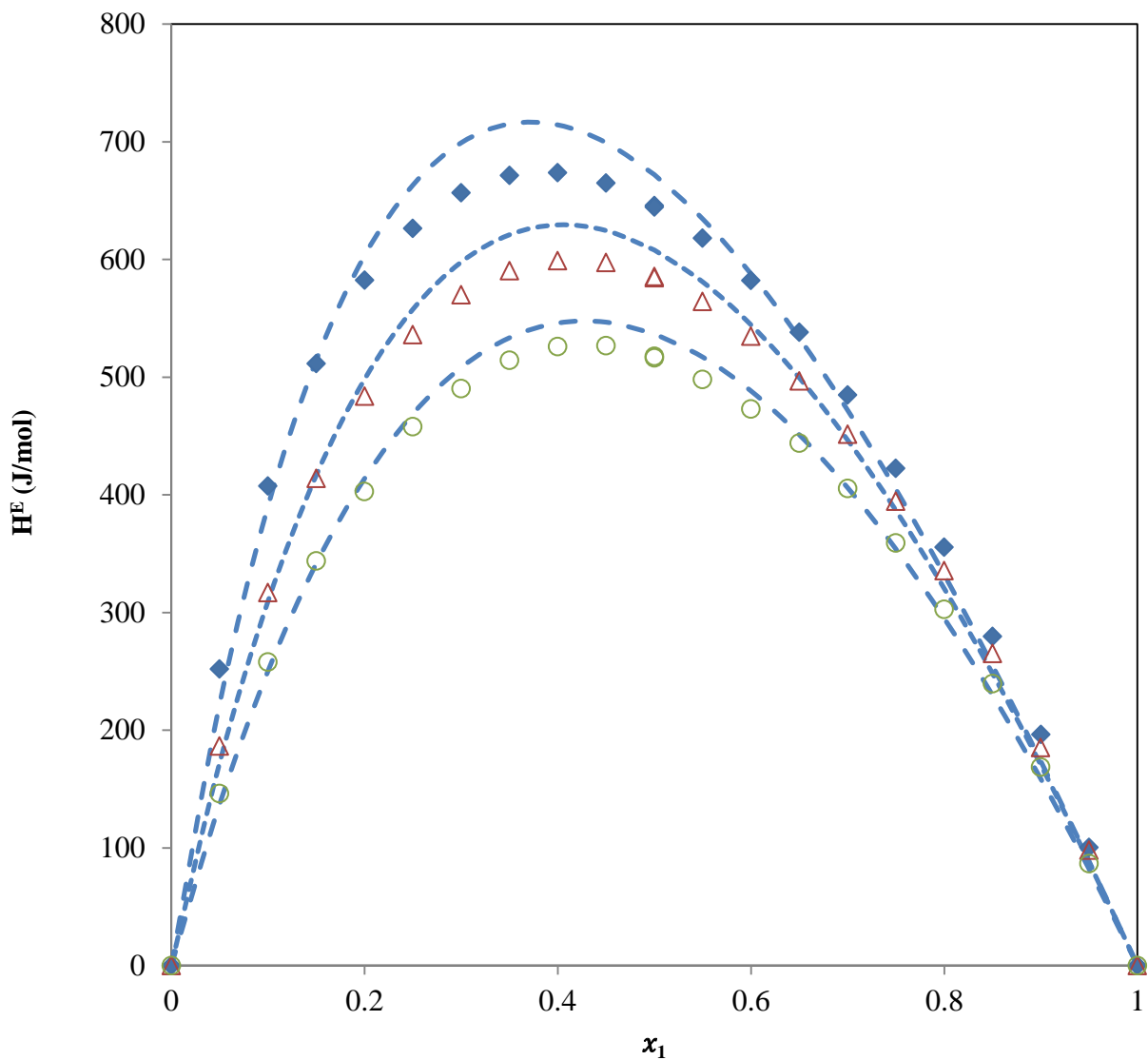


**Figure C2.7.** Excess molar enthalpies  $H_{m,1+23}^E$  for the ternary system  $x_1$  2-ME +  $x_2$  2-MTHF +  $(1 - x_1 - x_2)$  *p*-Xylene at 298.15K. Experimental results:  $\blacklozenge$   $x_2/x_3 = 0.3334$ ;  $\triangle$ ,  $x_2/x_3 = 0.9992$ ;  $\circ$ ,  $x_2/x_3 = 2.9963$ ; Curves: ..... , calculated using the Liebermann-Fried model.

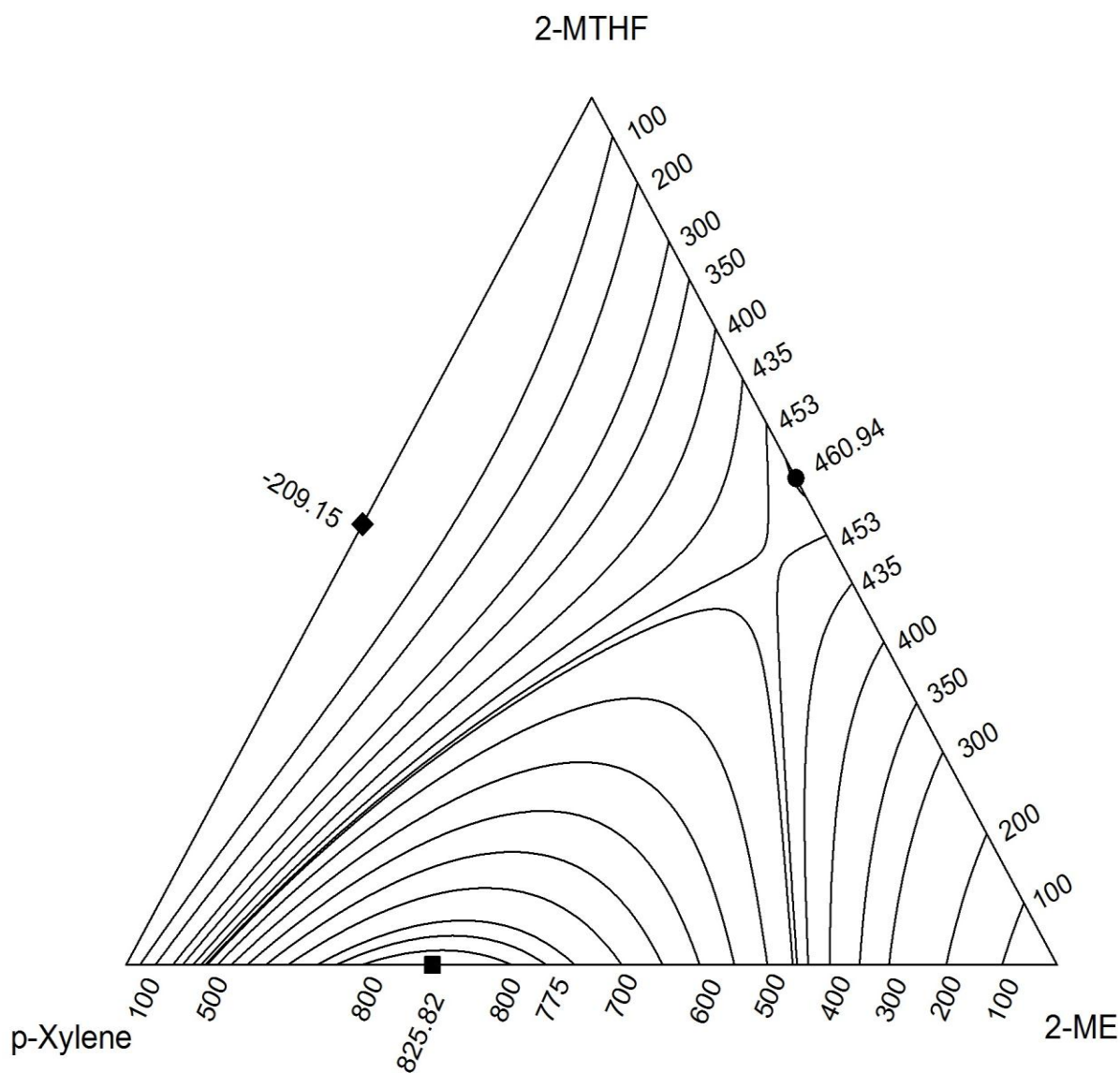


**Figure C2.8.** Constant enthalpy contours,  $H_{m,123}^E$  (J/mol) at 298.15K for the  $x_1$  2-ME +  $x_2$  2-MTHF +  $(1 - x_1 - x_2)$  *p*-Xylene, calculated from the representation of the experimental results using the Liebermann-Fried model.

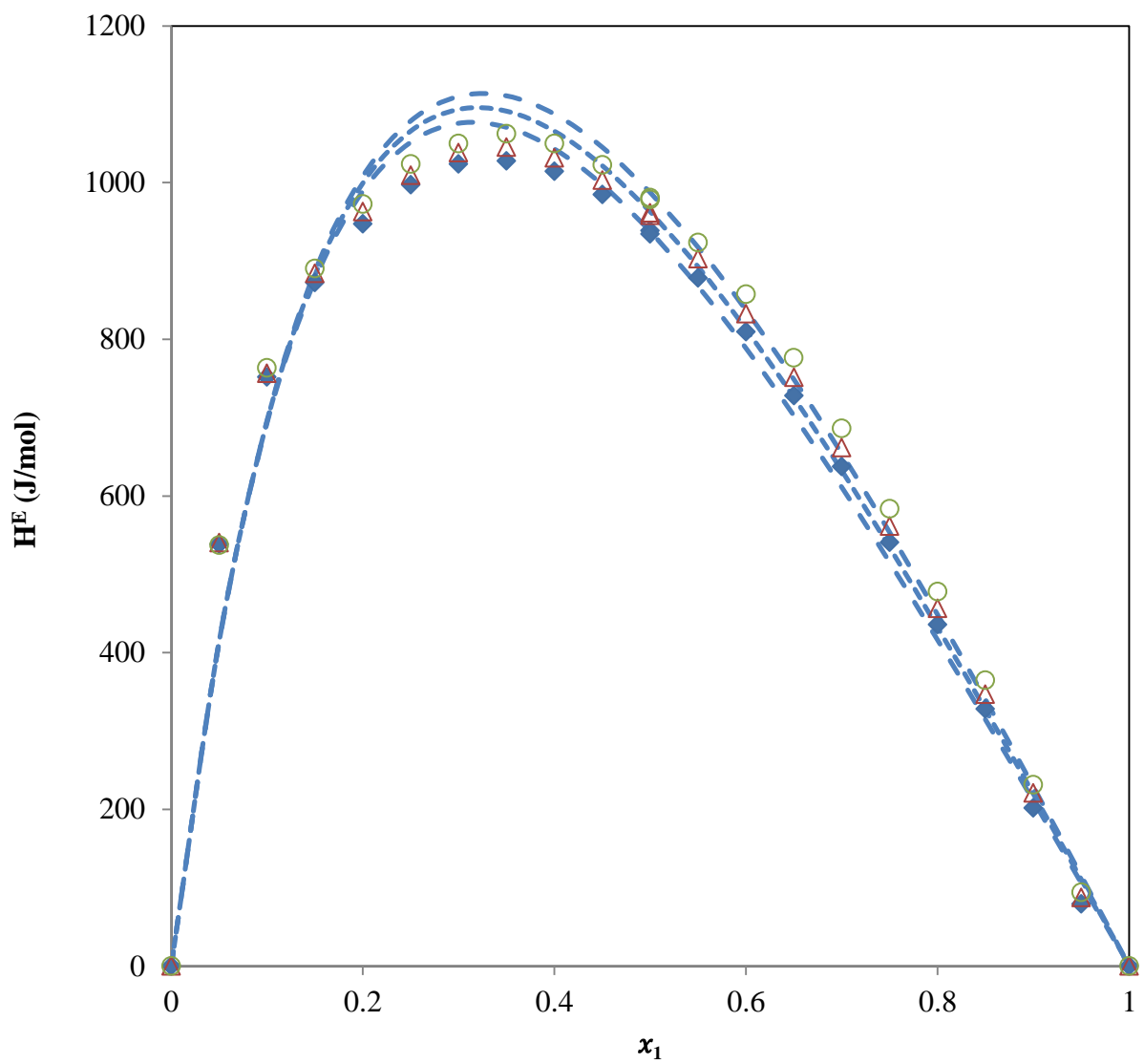


**Figure C2.9.** Excess molar enthalpies  $H_{m,1+23}^E$  for the ternary system  $x_1$  1-Butanol +  $x_2$  Mesitylene +  $(1 - x_1 - x_2)$  *p*-Xylene at 298.15K. Experimental results:  $\blacklozenge$   $x_2/x_3 = 0.3336$ ;  $\triangle$ ,  $x_2/x_3 = 0.9997$ ;  $\circ$ ,  $x_2/x_3 = 3.0005$ ; Curves: ..... , calculated using the Liebermann-Fried model.

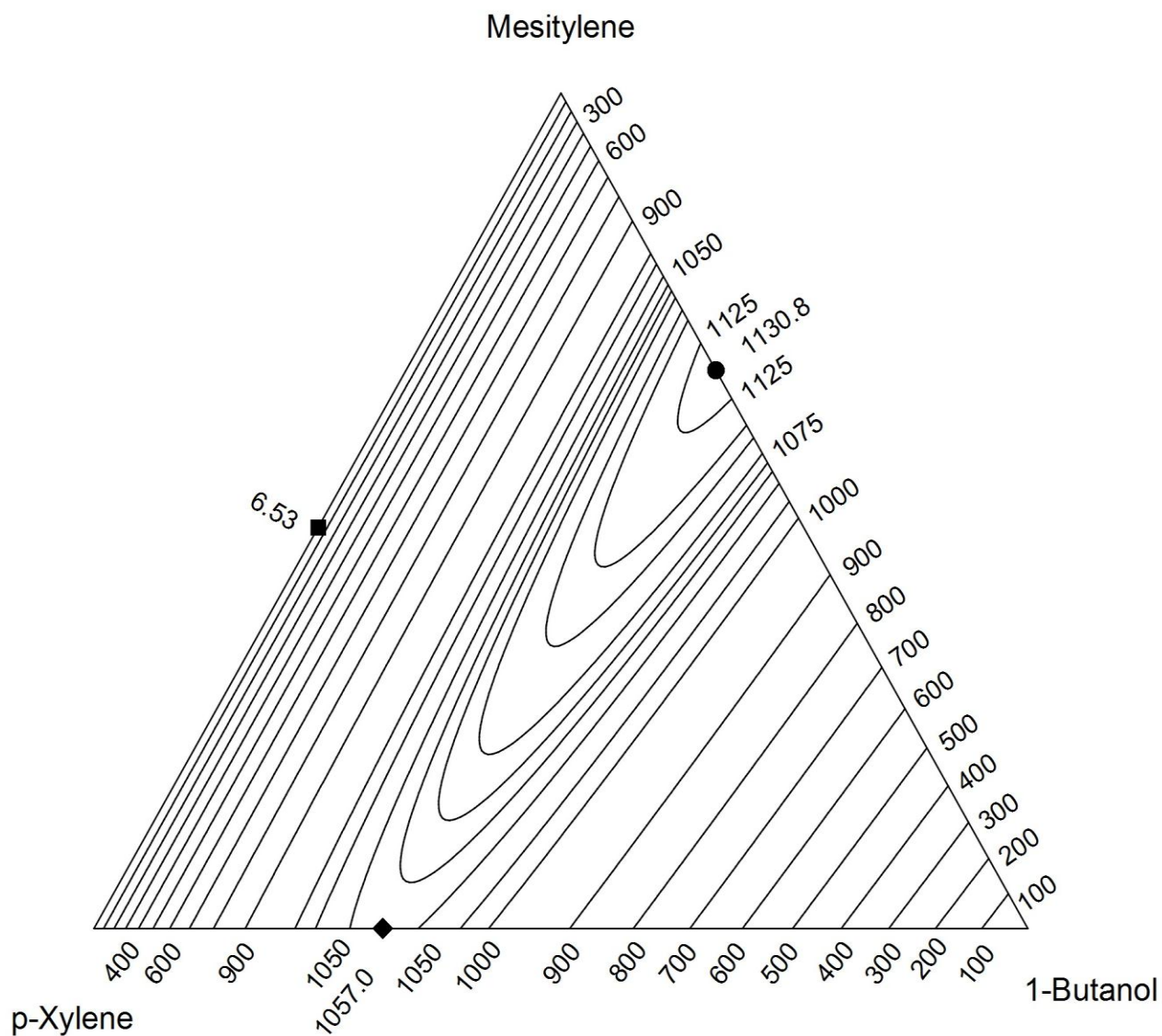


**Figure C2.10.** Constant enthalpy contours,  $H_{m,123}^E$  (J/mol) at 298.15K for the  $x_1$  1-Butanol +  $x_2$  Mesitylene +  $(1 - x_1 - x_2)$  p-Xylene, calculated from the representation of the experimental results using the Liebermann-Fried model

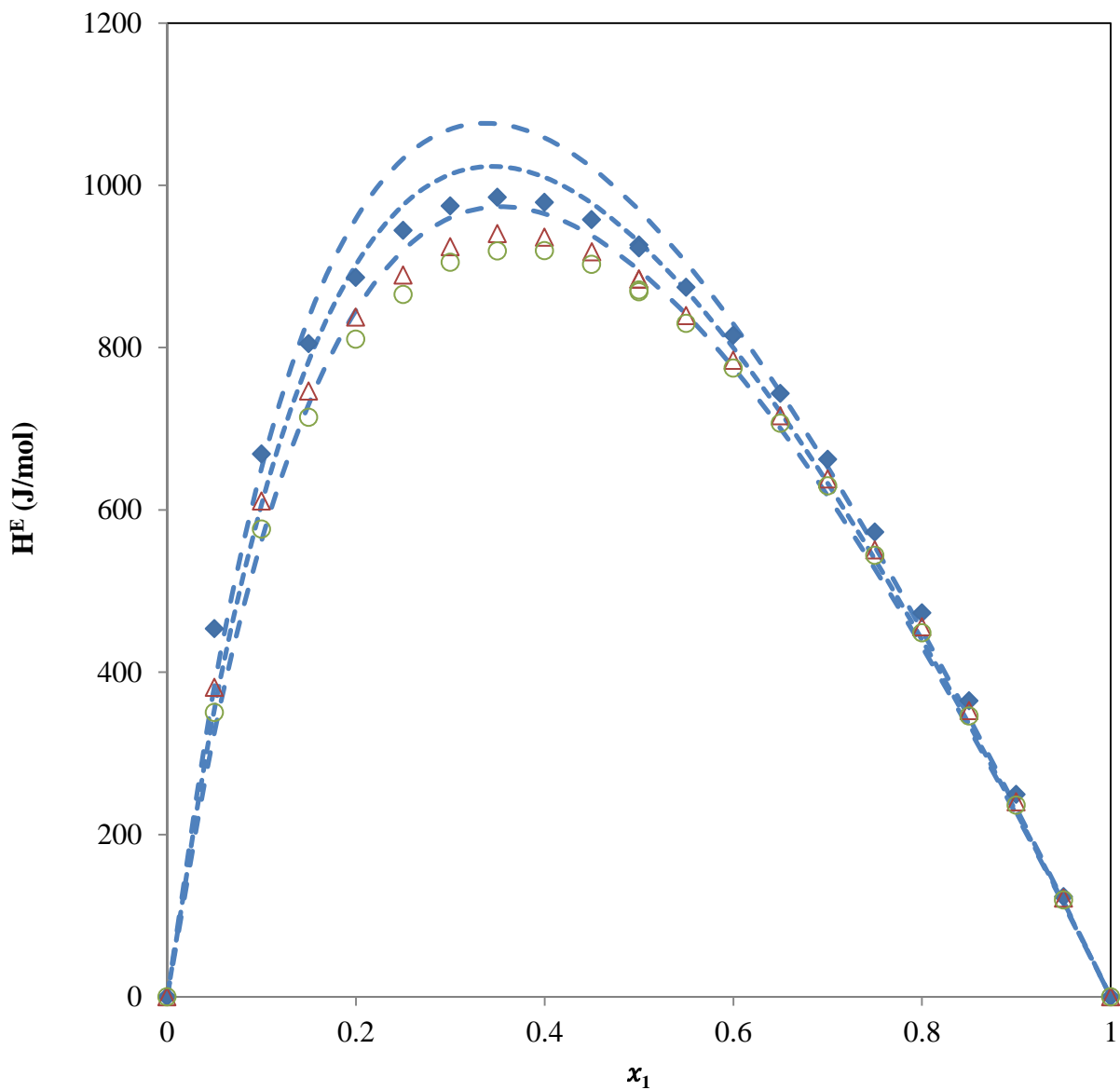


**Figure C2.11.** Excess molar enthalpies  $H_{m,1+23}^E$  for the ternary system  $x_1$  1-Butanol +  $x_2$  DNBE +  $(1 - x_1 - x_2)$  Mesitylene at 298.15K. Experimental results:  $\blacklozenge$ ,  $x_2/x_3 = 0.3336$ ;  $\triangle$ ,  $x_2/x_3 = 0.9997$ ;  $\circ$ ,  $x_2/x_3 = 3.0005$ ; Curves: ..... , calculated using the Liebermann-Fried model.

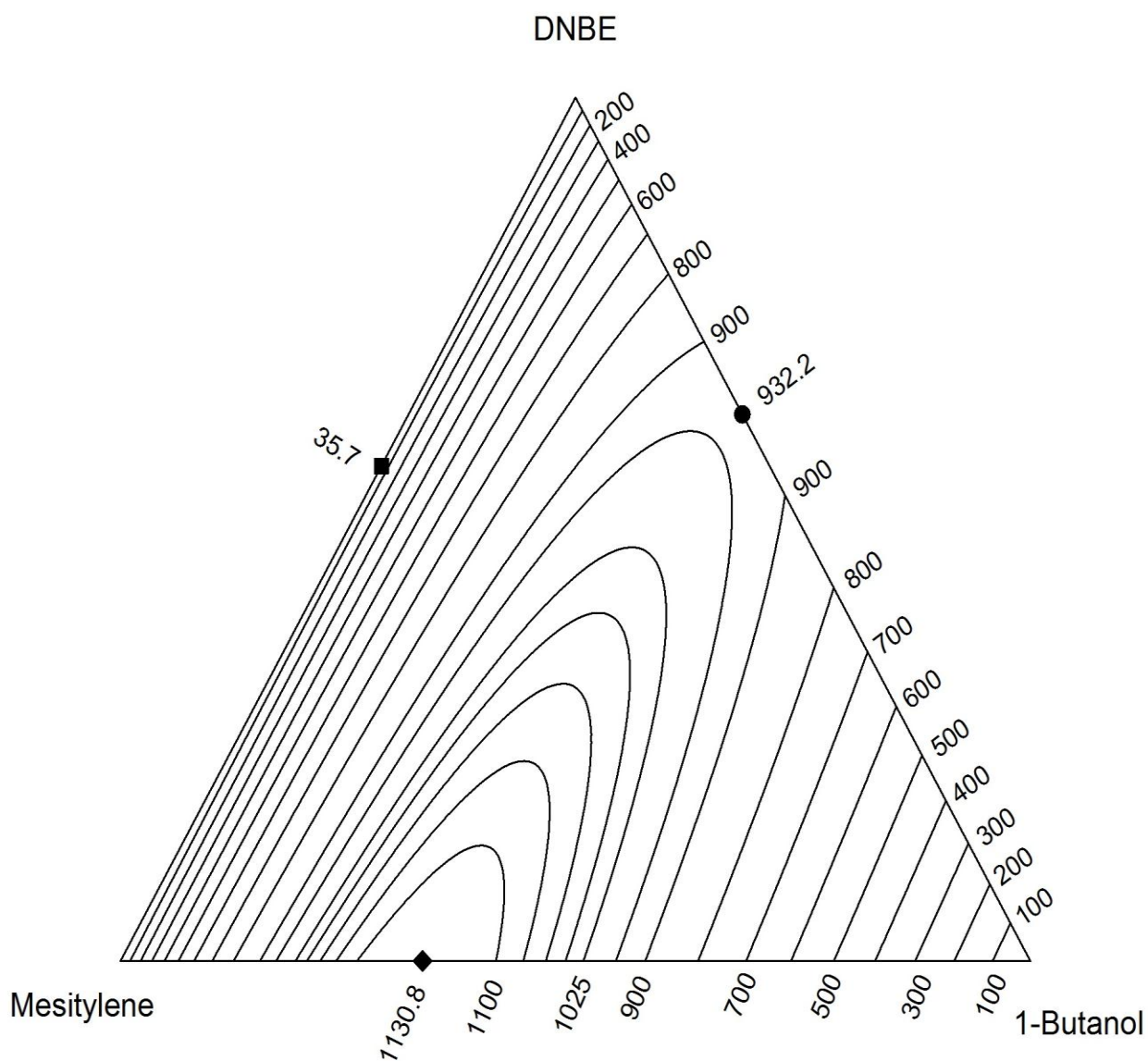


**Figure C2.12.** Constant enthalpy contours,  $H_{m,123}^E$  (J/mol) at 298.15K for the  $x_1$  1-Butanol +  $x_2$  DNBE +  $(1 - x_1 - x_2)$  Mesitylene, calculated from the representation of the experimental results using the Liebermann-Fried model.

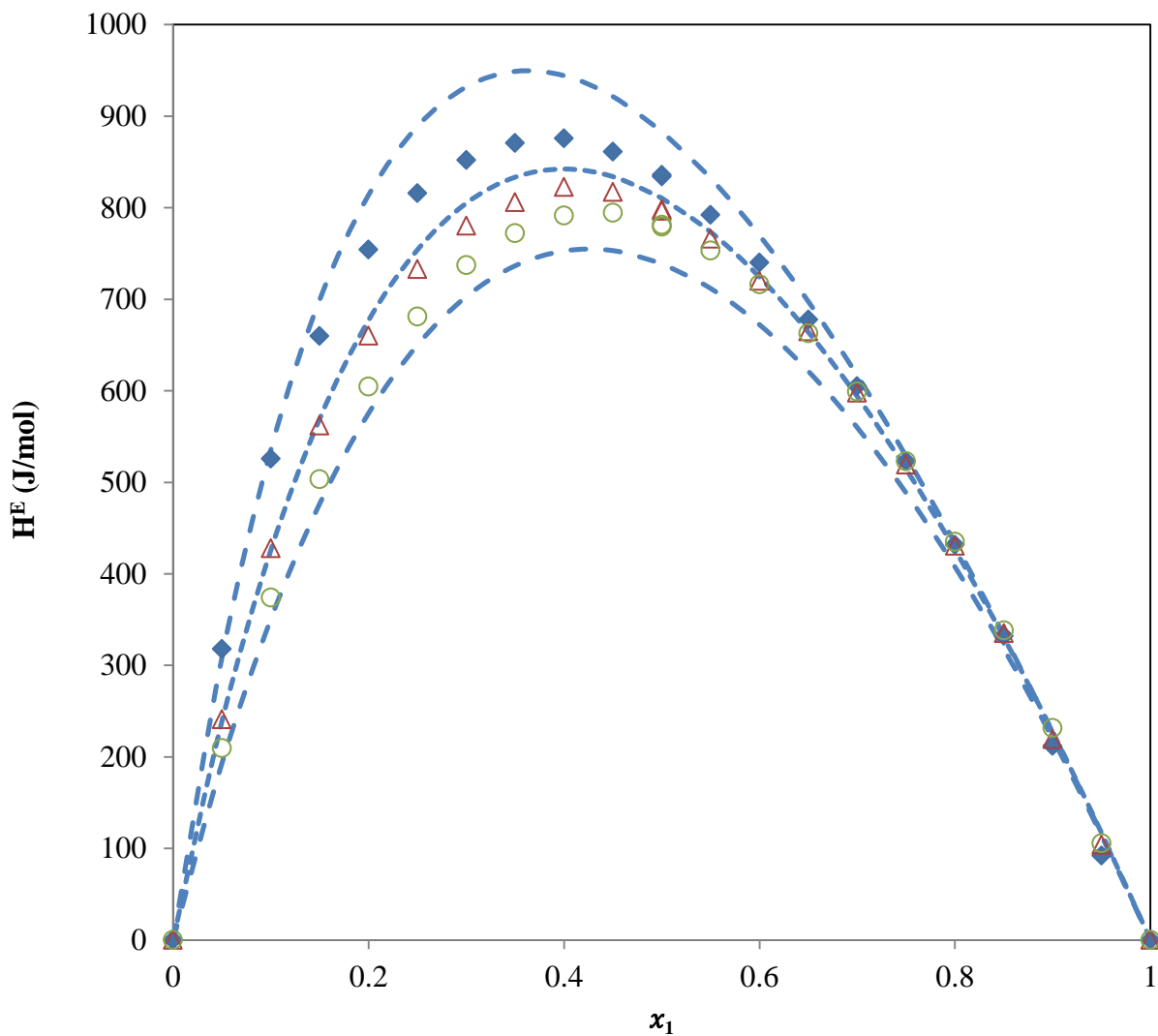


**Figure C2.13** Excess molar enthalpies  $H_{m,1+23}^E$  for the ternary system  $x_1$  1-Butanol +  $x_2$  2-MTHF +  $(1 - x_1 - x_2)$  EBz at 298.15K. Experimental results:  $\blacklozenge$   $x_2/x_3 = 0.3338$ ;  $\triangle$ ,  $x_2/x_3 = 1.0001$ ;  $\circ$ ,  $x_2/x_3 = 2.9989$ ; Curves:  $\cdots$ , calculated using the Liebermann-Fried model.

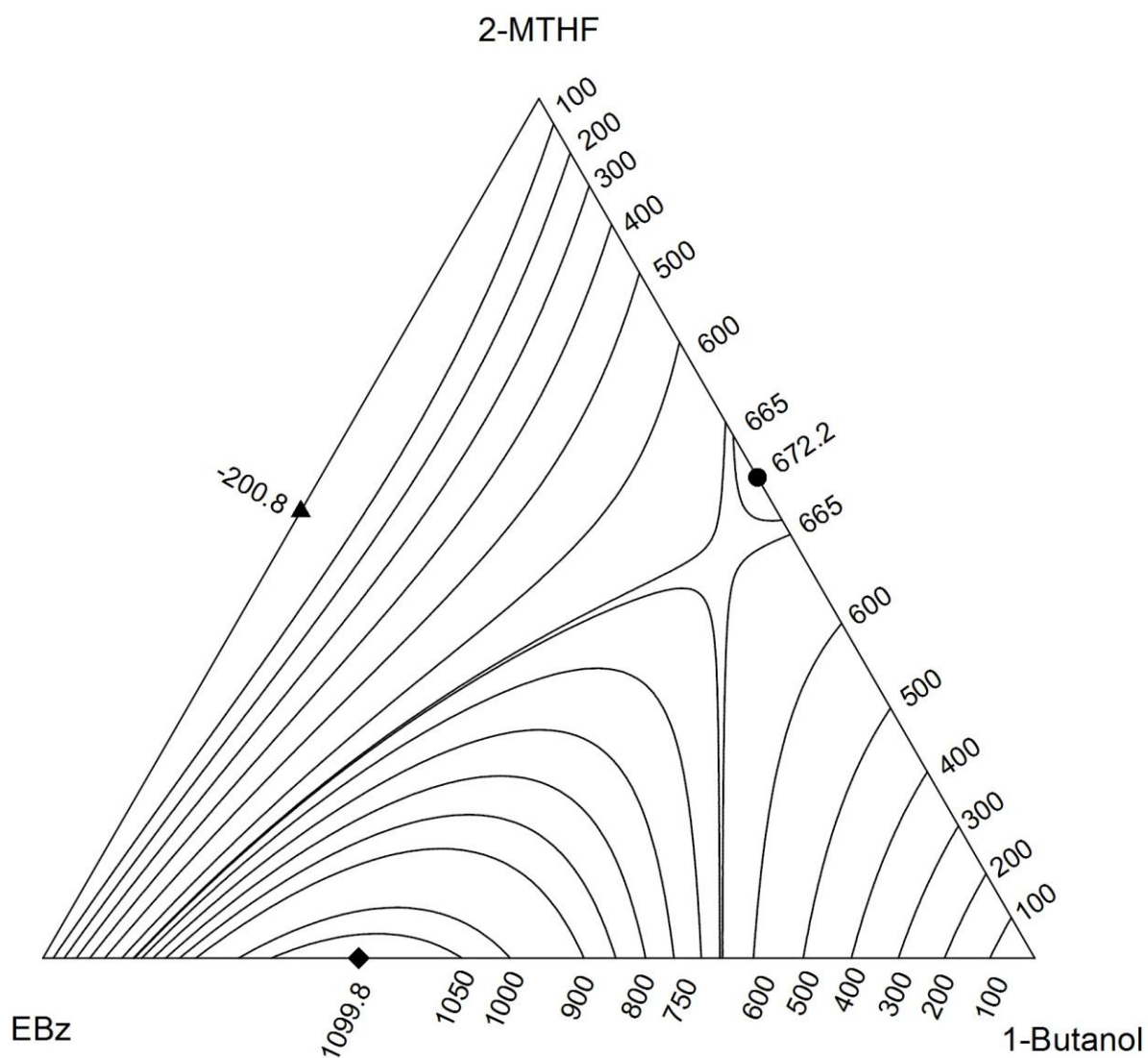


**Figure C2.14.** Constant enthalpy contours,  $H_{m,123}^E$  (J/mol) at 298.15K for the  $x_1$  1-Butanol +  $x_2$  2-MTHF +  $(1 - x_1 - x_2)$  EBz, calculated from the representation of the experimental results using the Liebermann-Fried model.

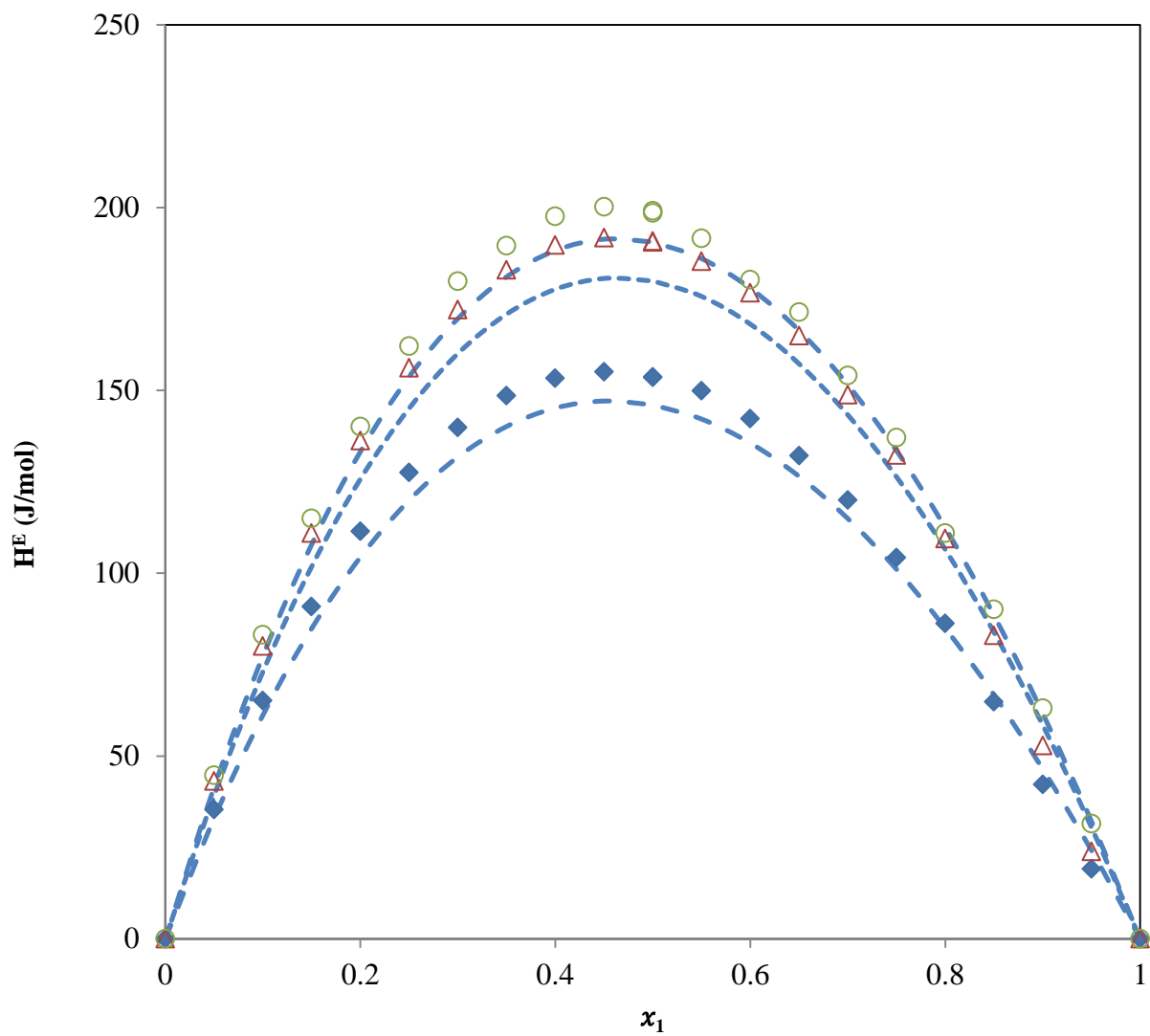


**Figure C2.15.** Excess molar enthalpies  $H_{m,1+23}^E$  for the ternary system  $x_1$  DNBE +  $x_2$  2-MTHF +  $(1 - x_1 - x_2)$  EBz at 298.15K. Experimental results:  $\blacklozenge$   $x_2/x_3 = 0.3338$ ;  $\triangle$ ,  $x_2/x_3 = 1.0001$ ;  $\circ$ ,  $x_2/x_3 = 2.9989$ ; Curves: ..... , calculated using the Liebermann-Fried model.

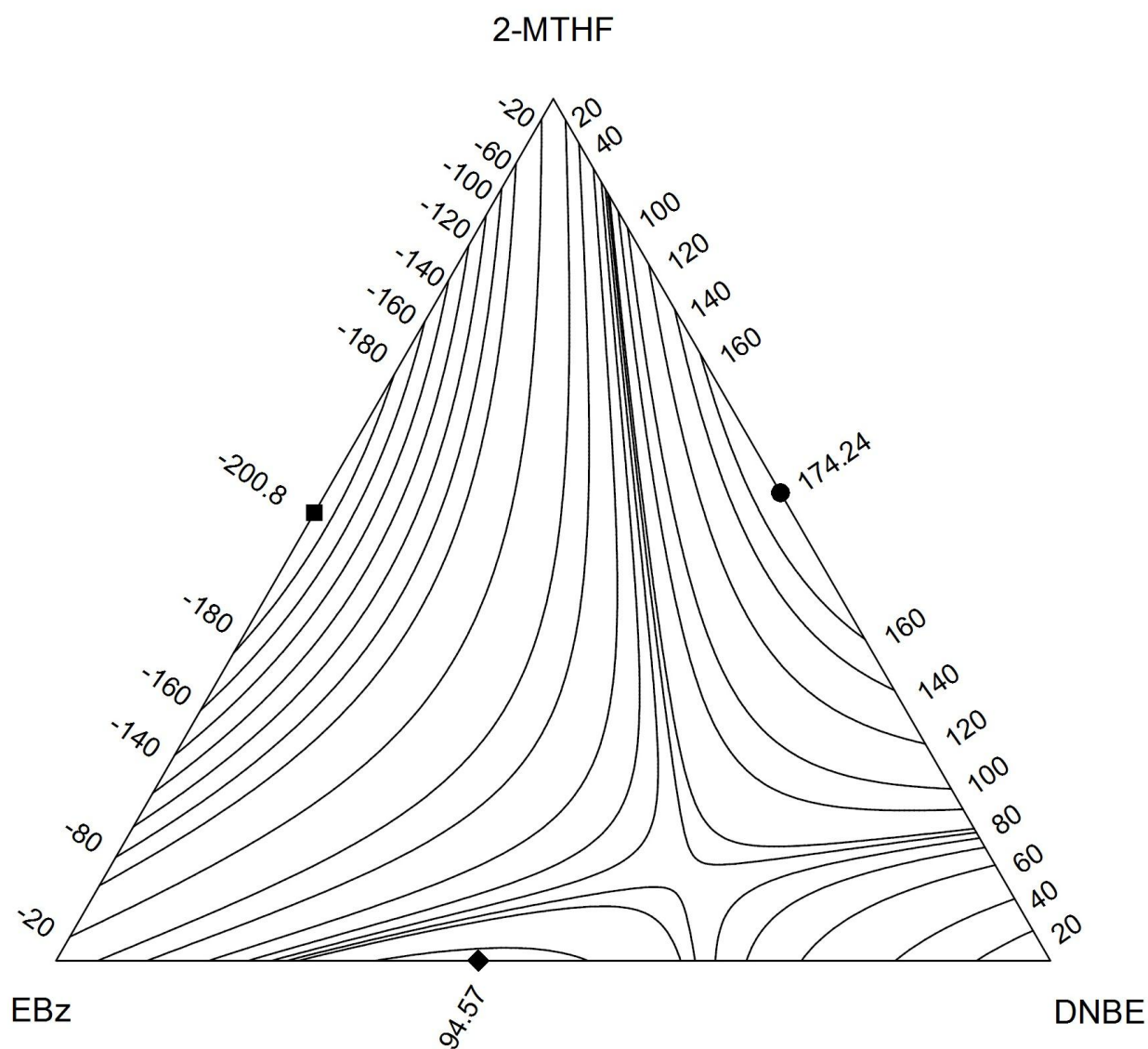


**Figure C2.16.** Constant enthalpy contours,  $H_{m,123}^E$  (J/mol) at 298.15K for the  $x_1$  DNBE +  $x_2$  2-MTHF +  $(1 - x_1 - x_2)$  EBz, calculated from the representation of the experimental results using the Liebermann-Fried model.

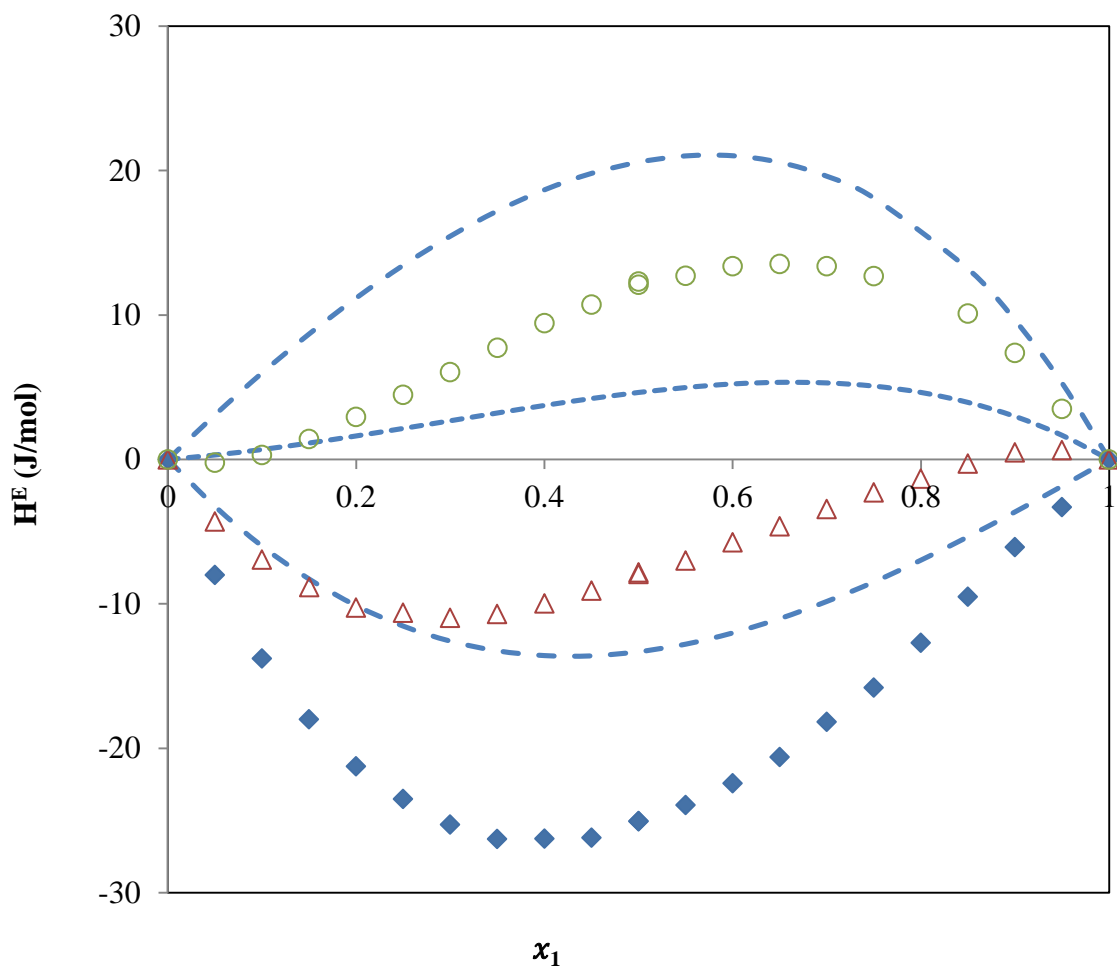


**Figure C2.17.** Excess molar enthalpies  $H_{m,1+23}^E$  for the ternary system  $x_1$  DNBE +  $x_2$  Mesitylene +  $(1 - x_1 - x_2)$  *p*-Xylene at 298.15K. Experimental results:  $\blacklozenge$   $x_2/x_3 = 0.3338$ ;  $\triangle$ ,  $x_2/x_3 = 1.0001$ ;  $\circ$ ,  $x_2/x_3 = 2.9989$ ; Curves: ..... , calculated using the Liebermann-Fried model.

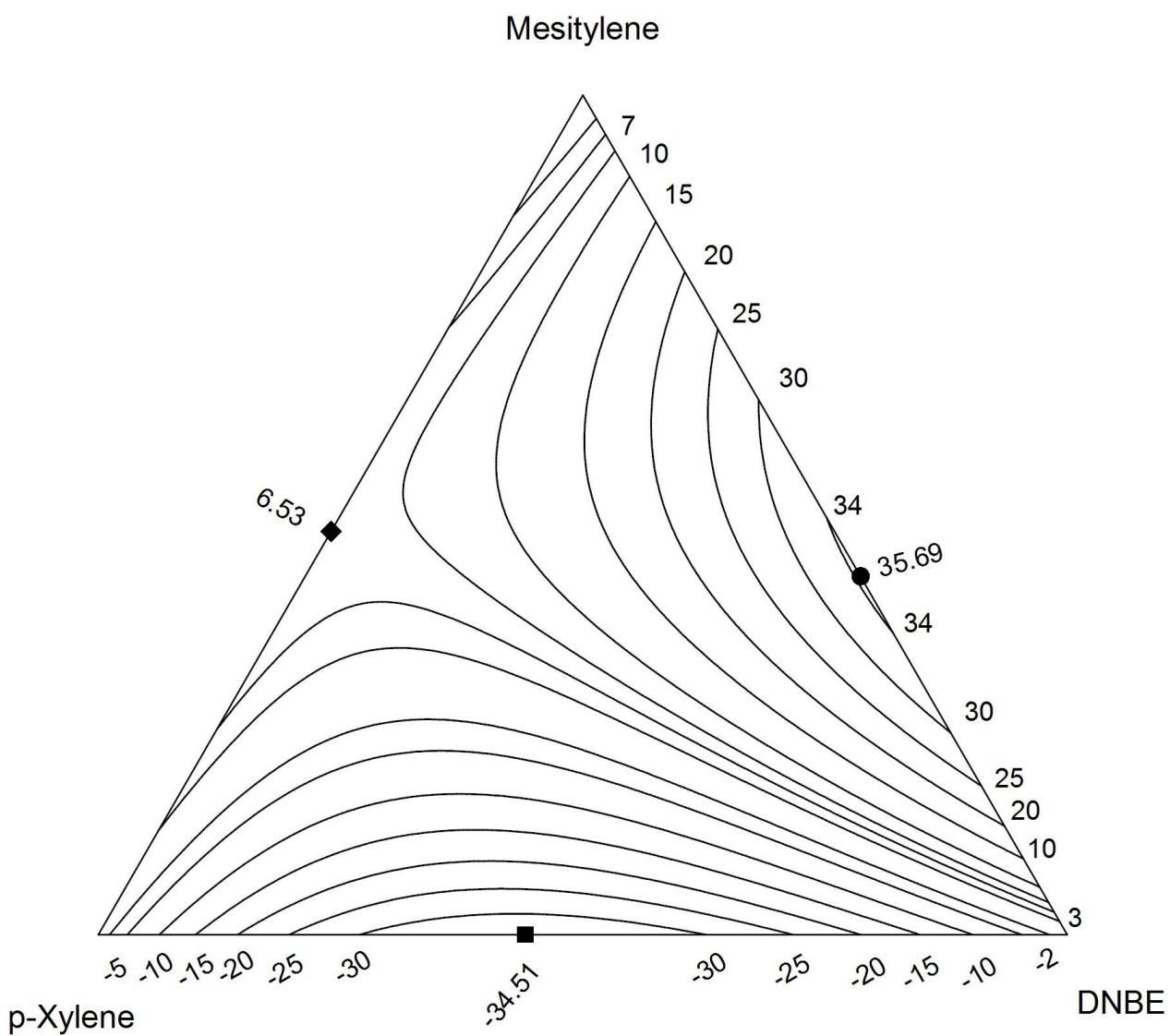


**Figure C2.18.** Constant enthalpy contours,  $H_{m,123}^E$  (J/mol) at 298.15K for the  $x_1$  1-Butanol +  $x_2$  Mesitylene +  $(1 - x_1 - x_2)$  *p*-Xylene, calculated from the representation of the experimental results using the Liebermann-Fried model.

## **APPENDIX D**

### **D1. Calibration and Mixing run procedure**

## **D.1 Calibration and Mixing run procedure**

The following steps should be carried out first before starting any mixing or calibration run,

- The water bath enclosing the calorimeter should be maintained at  $25 \pm 0.005^{\circ}\text{C}$  for at least 24 hours
- Both syringe A and syringe B are first cleaned with ethanol and then with acetone and finally purged with nitrogen for complete cleaning.
- The chemicals species A and species B should be dewatered with molecular sieves for at least 24 hours and then degassed by means of a vacuum pump.

(The molecular sieves used for dewatering must be baked in an oven at temperatures higher than  $100^{\circ}\text{C}$  for at least 24 hours)

### **Calibration run procedure**

Considering species A is calibrated in pump A

- 1) Syringe A is charged with species A and the flow control valve (figure D1.1) is connected to the syringe A
- 2) One end of the flow control valve is connected to the reservoir flask and the other end of the valve is connected to the Teflon tube tagged as pump A leading to the calorimeter

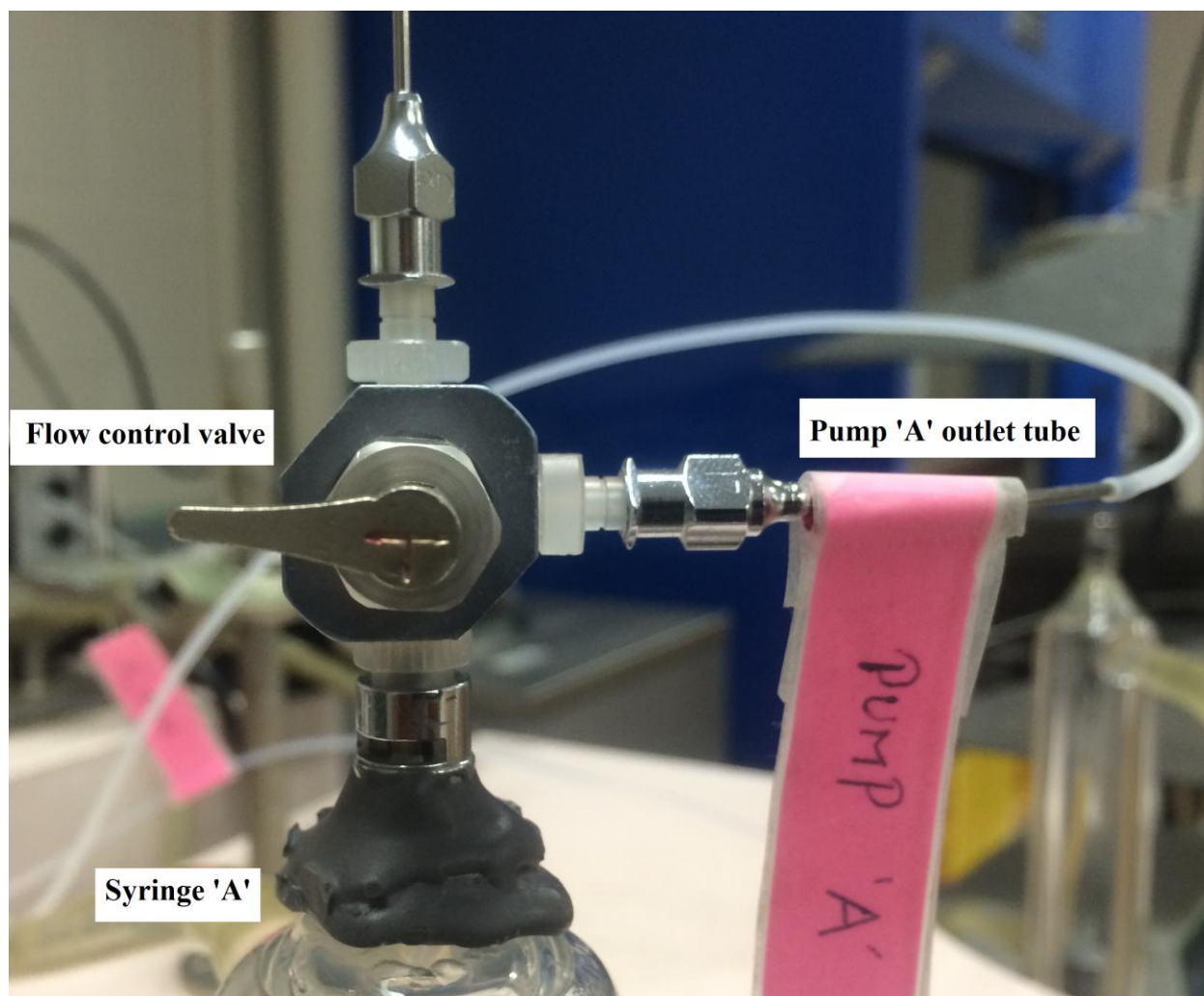


**Figure D1.1.** Flow control valve

3) The Teflon tube tagged as pump B (figure D1.2) is charged with species A with a 10- ml glass syringe and it is connected to the Teflon tube throughout the calibration run. The 10-ml glass syringe's plunger movement is restricted by applying a Swiss tape as shown in the figure D1.2

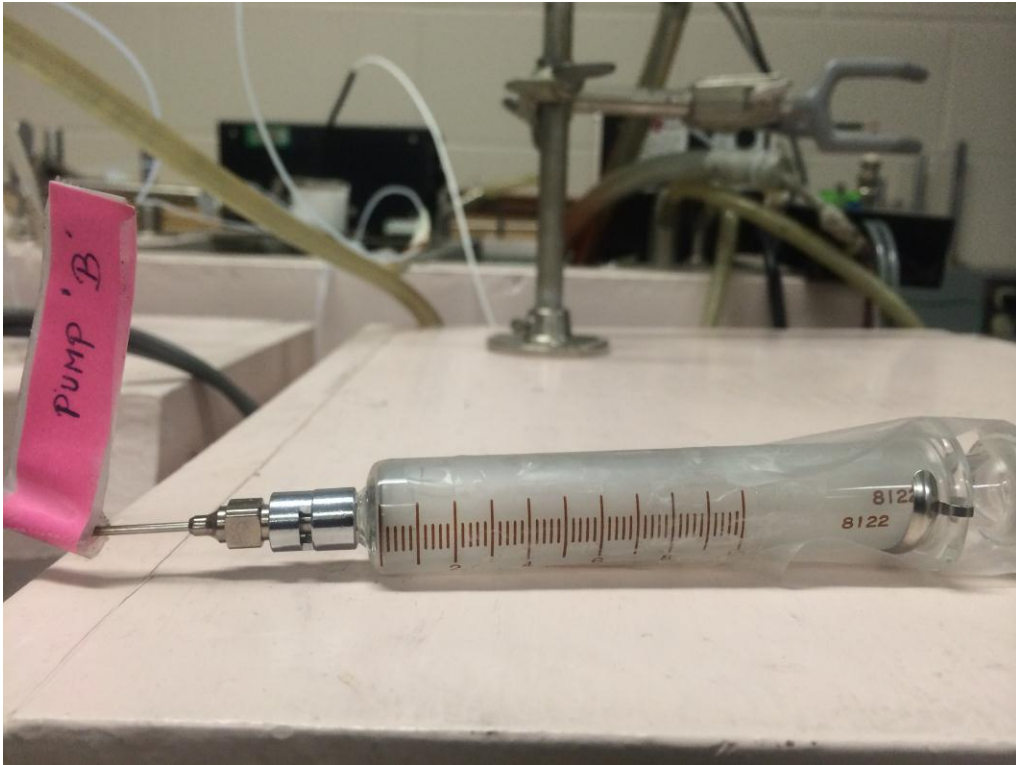


**Figure D1.2.** Glass syringe connected to pump B outlet tube

4) Before turning on the pump A controller, make sure that the flow control valve is in the 'T' position as shown in figure D1.1

(Do not run the motor when the flow control valve is in inverted 'T' position, i.e. '⊥' position).

5) When the motor is kept running with the flow control valve in the '⊥' position, pressure will build up inside the syringe's glass tube and eventually cause the glass tube to break.

6) After step 4, click the 'Set Baseline' button in the calorimeter software as shown in the figure D1.3. By doing this, the baseline voltage is set to near zero value.

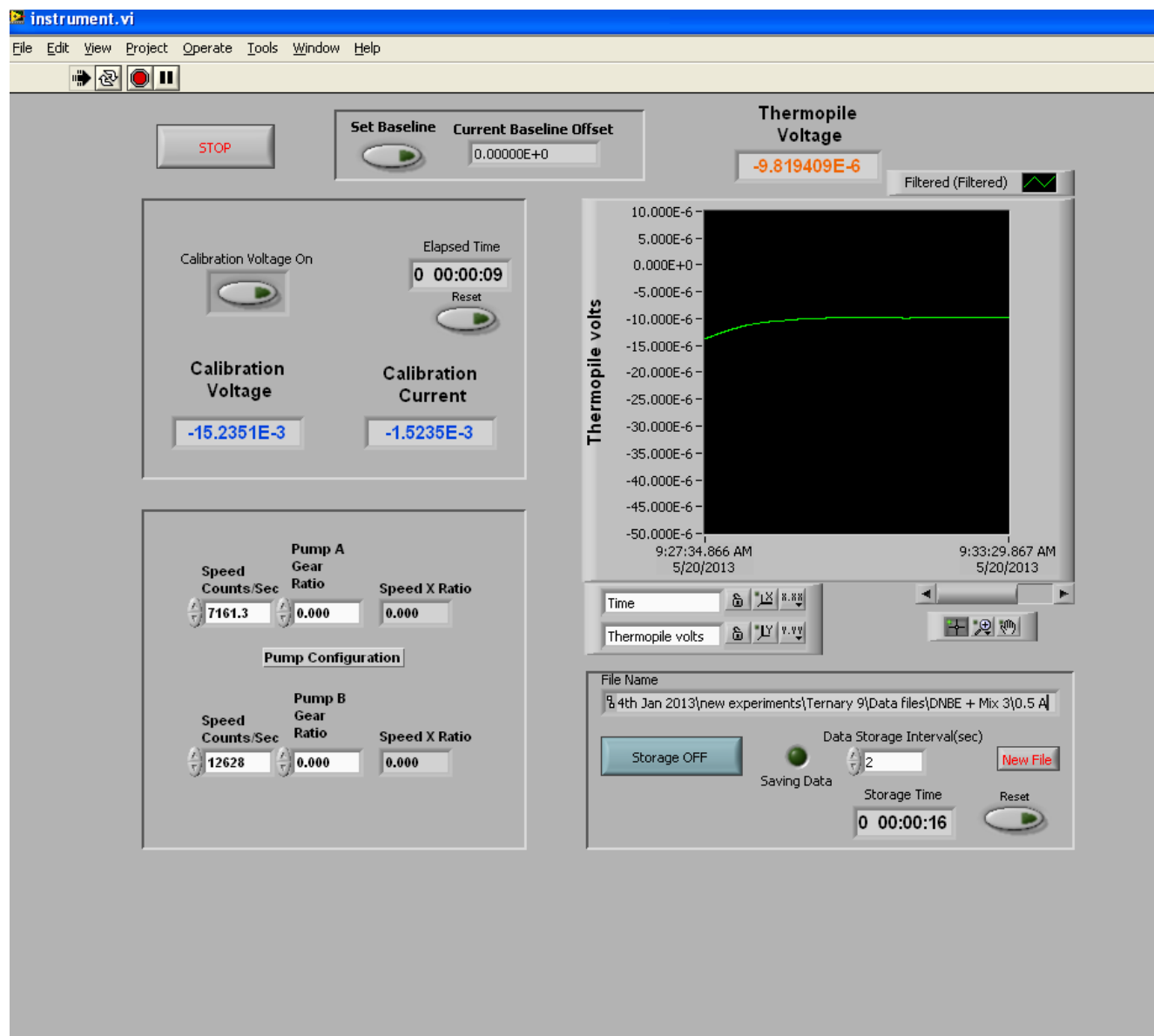


**Figure D1.3.** Calorimeter software

7) Turn on the pump A motor and set the speed at 10000 counts/sec and wait until the thermopile voltage become stable in the graph.

8) Once the thermopile voltage becomes stable, click the 'New File' button in the software (it will open a new window), after that create a file with a name '10000 without heating' and click 'OK'. After creating the file name, click the 'Storage' button in the software, this action will start recording the data (a green light flashes near the storage button when the data recording is on progress), record the data for five minutes and click the 'Storage' button again to stop recording the data.

9) Open the file '10000 without heating' using MS Excel and calculate the average of the thermopile voltage and note it in a data sheet.

10) After step 9, click the 'Calibration Voltage on' button in the software (A green light glows on the button, when it is turned on). This action will turn on the heating unit, causing the thermopile voltage to increase. The voltage becomes stable after 10 minutes (approximately)

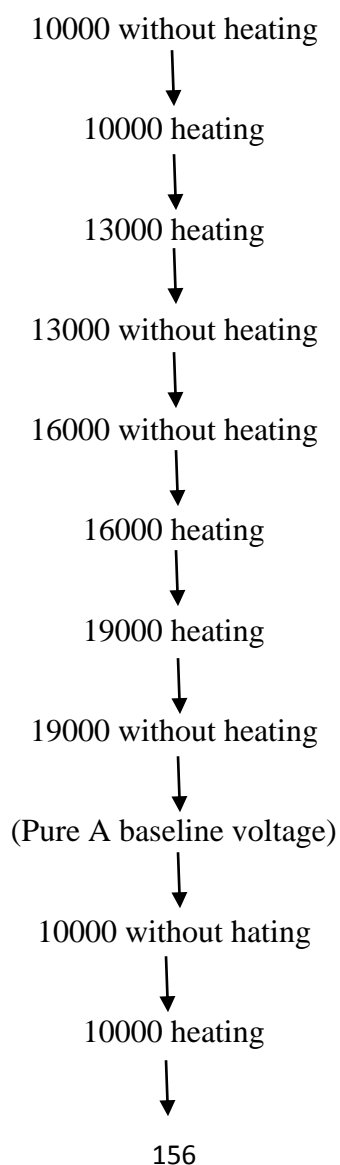
11) Once the thermopile voltage becomes stable, create a new file with the name '10000 heating' and record the data for five minutes. Calculate and note the average values of the thermopile voltage and current in a data sheet.

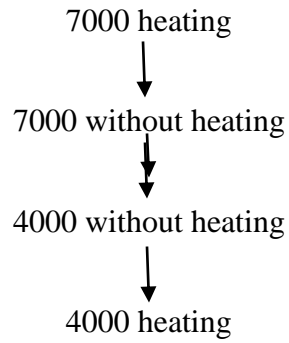
12) After step 11, increase the motor speed to 13000 counts/sec. Wait for the thermopile voltage to become stable (usually five minutes), meanwhile create a file with the name '13000 heating'. Once the voltage becomes stable, record the data for five minutes, calculate and note the average values of the thermopile voltage and current in a data sheet.

13) After step 12, click the 'Calibration Voltage On' button again to turn off the calibration voltage (The green light on the button stops glowing when the calibration voltage is turned off).

The thermopile voltage will become stable after 7-10 minutes. Once the thermopile voltage becomes stable, create a new file with the name '13000 without heating' and record the data for 5 minutes. From the recorded data, calculate and note the average value of thermopile voltage in a data sheet.

Then steps 7 to 13 should be repeated for different pump speeds (16000, 19000, 7000, 4000 counts/sec). Given below is the sequence of the calibration run.





The motor automatically stops once the piston reaches its maximum level. To continue the experiment further, the syringe should be recharged again with species A.

#### Recharging steps

- a) Turn off the pump A controller.
- b) Change the motor to reverse gear as shown in figure D1.4 (the gear switch is located at the front of the motor, reverse gear is engaged by pushing it downwards)

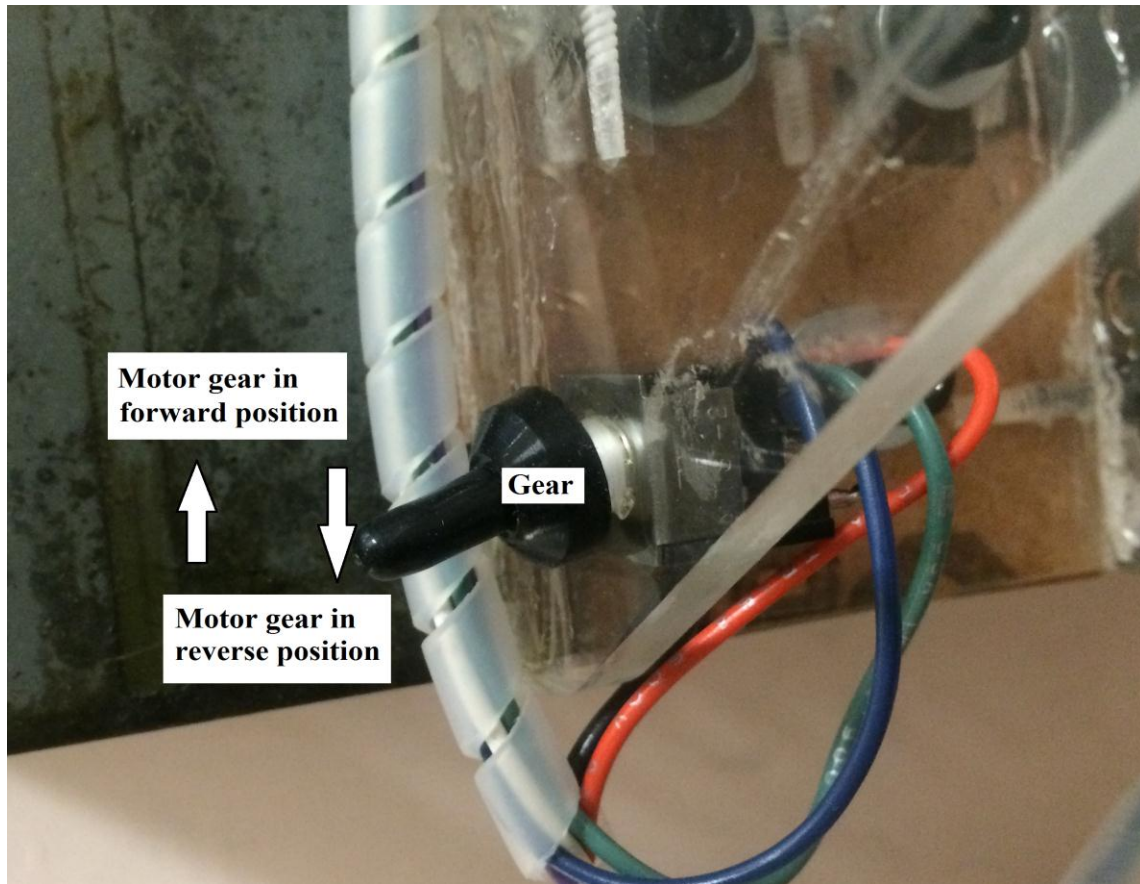


**Figure D1.4** Motor gear position

d) Set the flow control valve to '⊥' position

e) Open the reservoir stopper valve

f) Turn on the pump A controller and set the motor speed to 15000 counts/sec

The motor automatically turns off when the syringe is recharged. Once the motor is turned off, close the reservoir valve, turn the motor gear upwards, set the flow control valve to '⊥' position and continue the experiment.

The calibration procedure for the pump B is similar to that of pump A with few changes and they are

- i) Species B is charged in syringe B
- ii) Species B is filled in the Teflon tube marked as Pump A.

### **Mixing run procedure**

Mixing run should be carried out after finishing the calibration run for species A in pump A and species B in pump B respectively.

Before starting the mixing run 'motor speed table' should be generated. (An excel template is available in the lab computer to calculate the motor speed)

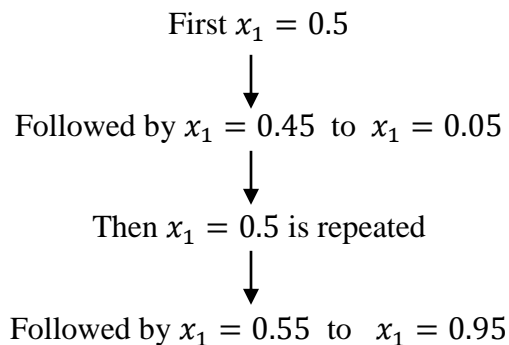
After creating the motor speed table, following steps should be followed

- 1) The flow control valves of syringe A and syringe B should be in 'T' position
- 2) The motor gears for both pump A and pump B should be in upward direction.
- 3) The pump controllers are turned on and the mixing run is carried out in the following order

The 1-Butanol (1) + *p*-Xylene (2) mixing run is taken as the basis for explaining the mixing run procedure.

Table D1.1 illustrates the 1-Butanol (1) + *p*-Xylene (2) mixing run. The mixing run has two parts, one that starts with equimolar molefraction  $x_1 = 0.5$  and ends with  $x_1 = 0.05$  and the

other part starts again with equimolar molefraction  $x_1 = 0.5$  and ends with  $x_1 = 0.95$ . Following flow chart illustrates the above explained steps.



- a) The mixing run is started with the pump A speed 8447.2 counts/sec and pump B speed 11346.9 counts/sec, which brings the mole fraction of the mixture  $x_1 = 0.50$ . After the start, proper mixing of the components takes place in 20 minutes, a stable thermopile voltage can be seen in the screen once the mixing takes place properly. (During the first 15 minutes of the mixing run, a continuous stream of air bubbles comes out of the exit tube and this occurrence of bubbles is normal for a mixing run)
- b) Once the thermopile voltage becomes stable, create a 'new file' with the name '0.5 A + 0.5 B' and record the data for five minutes. Here 'A' represents pump A fluid 1-Butanol and 'B' represents pump B fluid *p*-Xylene.
- c) Stop recording the data after five minutes, open the file where the data has been recorded, calculate the average value and record the average in a data sheet.
- d) Change the motor speed of pump A and B for the  $x_1 = 0.45$  molefraction, in this case 7491.7 counts/sec and 12298.9 counts/sec respectively.

e) Once the thermopile voltage becomes stable, create a new file with the name '0.45 A + 0.55 B' and record the data for five minutes. Calculate the average and note the average in a data sheet.

f) In the same method as explained above, the thermopile voltage for the composition ranging from  $x_1 = 0.40$  to  $x_1 = 0.05$  was recorded.

g) The upward arrow in the table indicates that the experiment is started with the run corresponding to the molefraction  $x_1 = 0.50$  and proceeded towards  $x_1 = 0.05$ . Then the mixing run is started again with molefraction  $x_1 = 0.50$  and proceeded towards  $x_1 = 0.95$  which is represented by the downward arrow.

**Table D1.1.** Motor speed settings for different molefraction of 1-Butanol + *p*-Xylene mixing run

<b>1-Butanol (1) + <i>p</i>-Xylene (2) mixing run</b>		
<b>Mole fraction (<math>X_1</math>)</b>	<b>Motor Speed (counts/sec)</b>	
	<b>Pump A 1-Butanol</b>	<b>Pump B <i>p</i>-Xylene</b>
<b>0.00</b>	0	19762.2
<b>0.05</b>	746.4	19019.6
<b>0.10</b>	1511.4	18257.3
<b>0.15</b>	2297.0	17474.6
<b>0.20</b>	3104.0	16670.6
<b>0.25</b>	3933.2	15844.4
<b>0.30</b>	4785.5	14995.2
<b>0.35</b>	5662.0	14121.9
<b>0.40</b>	6563.7	13223.5
<b>0.45</b>	7491.7	12298.9
<b>0.50</b>	<b>8447.2</b>	<b>11346.9</b>
<b>0.55</b>	9431.3	10366.4
<b>0.60</b>	10445.5	9355.9
<b>0.65</b>	11491.1	8314.2
<b>0.70</b>	12569.6	7239.7
<b>0.75</b>	13682.5	6130.8
<b>0.80</b>	14831.5	4986.0
<b>0.85</b>	16018.5	3803.3
<b>0.90</b>	17245.4	2581.0
<b>0.95</b>	18514.1	1316.9
<b>1.00</b>	19826.9	0.0

If bubbles come out of the exit tube during the mixing run, it will cause the thermopile voltage to fluctuate abnormally. The fluctuations can be seen in the graph on the screen. In that case, data recording should be stopped and disregarded for that particular run.

Once the air bubbles stops appearing at the exit tube, wait for a stable thermopile voltage and start recording the data again for that specific run.

(Bubble formation during the mixing run can be avoided by proper degassing of the pure component species)



manju nathan &lt;manjunath.43@gmail.com&gt;

---

## Permission request

3 messages

---

manju nathan <manjunath.43@gmail.com>  
To: Nazmul Hasan <hasan.nazmul@usask.ca>

Thu, Nov 14, 2013 at 5:28 PM

Dear Nazmul,

How are you and how is your job? I hope you are doing well out there!

I am writing my thesis now, since my research is continuation of your work, I want to use some of the materials from your dissertation and I am requesting your permission to use them in my thesis work.

The details of the materials which I want to use from your thesis are figure 3.1, 3.2, 3.3 and 3.4 from chapter 3.

Thank you

Regards,  
Manju.

---

Hasan, S M Nazmul <hasan.nazmul@usask.ca>  
To: manju nathan <manjunath.43@gmail.com>

Thu, Nov 14, 2013 at 5:55 PM

Hi Manju,

Congratulation on finishing your experiments. Yes, sure you can use those figures. How is everything going? How is Dr. Peng? Does he have any new student?

Good luck.

Regards,

Nazmul Hasan  
[Quoted text hidden]

---

manju nathan <manjunath.43@gmail.com>  
To: "Hasan, S M Nazmul" <hasan.nazmul@usask.ca>

Fri, Nov 15, 2013 at 11:03 AM

Thanks Nazmul,  
Dr. Peng is doing great, he is quite busy with his teaching and administration works, yes he took a new Ph.D student she is from Iran.  
and thanks for the wishes Nazmul :)

Manju.  
[Quoted text hidden]

--  
Manjunathan,  
M.Sc Student  
Dept.Of.Chemical Engineering,

4/17/2014

Gmail - Permission request

University Of Saskatchewan.